NOVA SCHOOL OF SCIENCE & TECHNOLOGY

DEPARTMENT OF PHYSICS

DIOGO SOARES MELO

Bachelor of Science in Biomedical Engineering

DESIGN, ASSEMBLY AND TEST OF A BIOREACTOR FOR THE ELECTRICAL STIMULATION OF NEURONAL CELLS

DISSERTATION SUBMITTED IN PARTIAL FULFILMENT OF THE REQUIREMENTS FOR THE DEGREE OF MASTER OF SCIENCE IN BIOMEDICAL ENGINEERING

MASTER IN BIOMEDICAL ENGINEERING

NOVA University Lisbon
March, 2022

NOVA SCHOOL OF SCIENCE & TECHNOLOGY

DEPARTMENT OF PHYSICS

DESIGN, ASSEMBLY AND TEST OF A BIOREACTOR FOR THE ELECTRICAL STIMULATION OF NEURONAL CELLS

DISSERTATION SUBMITTED IN PARTIAL FULFILMENT OF THE REQUIREMENTS FOR THE DEGREE OF MASTER OF SCIENCE IN BIOMEDICAL ENGINEERING

DIOGO SOARES MELO

Bachelor of Science in Biomedical Engineering

Adviser: Doctor Jorge Carvalho Silva
Associate Professor, NOVA University Lisbon

Co-adviser: Doctor Célia Maria Reis Henriques
Associate Professor, NOVA University Lisbon

MASTER IN BIOMEDICAL ENGINEERING

NOVA University Lisbon
March, 2022

Design, assembly and test of a bioreactor for the electrical stimulation of neuronal cells

This document was created with the (pdf/Xe/Lua)LaTeX processor and the NOVAthesis template (v6.7.0) [1].

To my late grandmother Maria Adelaide.

Acknowledgements

First and foremost, I would like to start by expressing my gratitude to my adviser Professor Dr. Jorge Carvalho Silva for all the help throughout this journey, the valuable discussions and shared ideas that culminated in the work hereby presented. To my co-adviser Professor Dr. Célia Henriques, I am grateful for all the lengthy and valuable discussions, suggestions, hours on the lab and shared knowledge. We ended up finding some pretty cells after all!

I would also like to leave a word of appreciation to all the members of this institution who have helped me complete this very important step in my academic life. A special thanks to Sr. Afonso Moutinho, for being a very attentive person and always trying to help in what was possible. Also, I would like to thank Sr. João Faustino, for the help in the production of the bioreactor, a key component of this dissertation.

To my laboratory colleagues, I would like to thank you for all the help throughout this last year. Asking for help was never a problem and I wish you all the best to your future endeavours. I would also like to leave a special note to Dr. Tânia Vieira. You are very knowledgeable and the funniest person I have had the pleasure to work with. But now I must go, I have an appointment at five.

To Dr. Nuno Amado, I deeply appreciate our conversations. You've helped me immensely at this stage of my life.

To all my friends, I cannot thank you enough for being with me throughout this phase. During these six years, you have made my days easier, and together, we created some of the best memories. From all the fun moments spend, be it at parties, lunch time, or sleeping at each other's floor, to the infinite study sessions, last minute revisions and motivation talks, your support was more than I could have asked for. For all that, and much more, I want to leave a special appreciation note to all the members from *Ohana de Biomédica* and *Só Choramos United* (William, why don't you have Whatsapp?). There are also those who have been with me for longer, supporting me from a distance, and who never denied a good old-fashioned walk at Ribeira. As such, a note of appreciation also goes to *Estarolas da ESRT*, and all my other friends from Porto. And to my lovely girlfriend, Mara. We are almost there! Thank you for your never-ending support, friendship, and

love. I hope you believe in yourself as much as you believe in me. You remind me that life is much more than work.

To my cousins, your support and love made Lisbon feel like home from day 1. I appreciate your trust and I am extremely grateful for being given the opportunity to enjoy these six challenging and memorable years.

To my grandmother Maria Adelaide, it has been very long, but the values I learned from you will never be forgotten. Ever since a little boy, I remember your love, and how proud you were of my curiosity and will to learn. You were the strongest person I've known and I hope I am making you proud.

Finally, to my family, Mãe, Pai and Manel, your love and support have always pushed me to endure the hardest times throughout my path so far. Beyond words of encouragement, your belief in my capabilities was always there when mine faulted. I am forever thankful for the life I have and for the efforts you make on a daily basis to make this possible. I will keep doing my best to make you proud. I love you all very much.

"Upward, not Northward." (A Square)

Abstract

Millions of people have suffered injury to their nervous system, which by its limited self-healing capacity, represents life-long complications, associated with loss of motor and sensory function. Though limited, this capacity is being extensively explored, and has been shown to increase through the use of electrical stimulation (ES). Therefore, this work was oriented towards the development of a setup for ES of neuronal cells, allowing the assessment of its potential in promoting neuronal regeneration.

An ES chamber was designed using the CAD software Fusion 360™ and produced by machining of a poly(methyl methacrylate) (PMMA) block. A fixation system for conductive scaffolds was included, using stainless steel electrodes, which fits the description for a direct coupling method found in the literature. Connection to a power supply or a function generator is possible, allowing for delivery of both direct current (DC) and alternating current (AC) to cells. In a different design, electrical insulation of the media was attempted, defectively.

The nature of this work supported the need for incorporating conductive polymers (CPs) in the scaffolds used for neuronal differentiation of cells in the stimulation chamber and so, poly(lactic acid) (PLA) aligned electruspun fibers were produced and coated with poly(3,4-ethylenedioxythiophene) (PEDOT) using vapor-phase polymerization (VPP). In this process, the polymerization takes place through the reaction of Iron(III) p-toluenesulfonate/Fe(III)Tosylate (FeTos) included in the scaffolds with 3,4-ethylenedioxythiophene (EDOT) on vapor phase. This fibers did not exhibit cytotoxicity and electrical characterization was attempted, using the bioreactor as a 2-point probe. Film casting using the same polymeric solutions failed, as an increase in the ratio of PLA to FeTos did not reduce film brittleness.

In vitro assays were conducted both with and without stimulation. SH-SY5Y extended neurites after only 2 days of exposure to retinoic acid (RA). Cells maintained some level of differentiation and neurite directionality with time, when cultured in the produced fibers. Importantly, an electrical field of 500 mV/cm was applied 1 h/day, for 9 days, without significant improvements on neuronal differentiation.

Keywords: Tissue engineering, Neuronal regeneration, Electrical stimulation, Bioreactor, SH-SY5Y cells, Electrospinnig, PEDOT

Resumo

Milhões de pessoas já sofreram lesões no seu sistema nervoso, o que, dada a sua capacidade limitada de regeneração, origina complicações a longo prazo, associadas à perda de função motora e sensorial. Embora limitada, esta capacidade tem sido amplamente explorada, e já se provou poder ser melhorada, com recurso a estimulação elétrica. Assim, este trabalho focou-se no desenvolvimento de um sistema para estimulação elétrica de células neuronais, permitindo avaliar o seu potencial para promover regeneração neuronal.

Desenhou-se um sistema para estimulação neuronal recorrendo ao software Fusion 360™ e fabricou-se o mesmo por maquinagem de um bloco de PMMA. A montagem inclui um sistema para fixação de *scaffolds* condutores, usando elétrodos de aço inoxidável, correspondendo a um sistema de acoplamento direto, segundo a literatura. É possível estabelecer contactos elétricos com uma fonte de tensão ou um gerador de funções, o que permite fornecer às células correntes diretas e alternadas. Houve uma tentativa, sem sucesso, para um novo *design* que permitisse isolamento elétrico do meio.

A natureza deste trabalho justificou a incorporação de polímeros condutores nos *scaffolds* usados para diferenciação neuronal de células no sistema de estimulação desenvolvido. Assim, foram eletrofiadas fibras alinhadas de PLA e, mais tarde, revestidas por PEDOT recorrendo a VPP. Neste processo, a polimerização ocorreu pela reação do FeTos, incluído nos *scaffolds*, com EDOT em fase de vapor. Foram feitas tentativas de produção de filmes, usando as mesmas soluções poliméricas, contudo verificou-se que o aumento da razão PLA:FeTos não reduziu a sua fragilidade.

Foram realizados testes *in vitro* com e sem estimulação. As células SH-SY5Y estenderam neurites, com apenas dois dias de exposição a meio contendo ácido retinóico. Quando semeadas nas fibras produzidas, estas células mantiveram um nível moderado de diferenciação neuronal ao longo do tempo, alinhando as suas extensões na direção das fibras. É de salientar que a exposição das células a um campo de 500 mV/cm aplicado 1 h/dia, por 9 dias, não resultou num aumento significativo de diferenciação neuronal.

Palavras-chave: Engenharia de Tecidos, Regeneração neuronal, Estimulação elétrica, Bioreator, Células SH-SY5Y, Eletrofiação, PEDOT

Contents

List of Figures xiii

List of Tables xvii

Glossary xviii

Abbreviations xx

1 Introduction 1
- 1.1 Nervous System . . . 1
  - 1.1.1 Regeneration of Nervous Tissue . . . 1
- 1.2 Context and Motivation . . . 3
  - 1.2.1 The Case for Electrical Stimulation . . . 4
  - 1.2.2 NEURiTES . . . 4
- 1.3 Dissertation Goals . . . 5
  - 1.3.1 Contribution to the Problem . . . 5
  - 1.3.2 Specific Goals . . . 5
- 1.4 Document Structure . . . 6

2 State of the Art 7
- 2.1 Bioelectricity . . . 7
- 2.2 Methods for Electrical Stimulation of Cells *In Vitro* . . . 8
  - 2.2.1 Direct Coupling . . . 9
  - 2.2.2 Capacitive Coupling . . . 11
  - 2.2.3 Inductive Coupling . . . 13
  - 2.2.4 Other Options . . . 14
- 2.3 Conductive Scaffolds . . . 16
  - 2.3.1 Polypyrrole . . . 17
  - 2.3.2 Polyaniline . . . 18
  - 2.3.3 Poly(3,4-ethylenedioxythiophene) . . . 19

2.4 Effects of Electrical Stimulation *In Vivo* 25

3 Materials and Methods **27**
3.1 Optimization of Differentiation Protocol 27
3.1.1 SH-SY5Y Proliferation and Subculture 28
3.1.2 SH-SY5Y Neuronal Differentiation 28
3.2 Design and Assembly of the Bioreactor 31
3.3 Fabrication of Conductive Scaffolds 35
3.3.1 Polymer Solutions 35
3.3.2 Film Casting 36
3.3.3 Spin Coating 37
3.3.4 Dip Coating 37
3.3.5 Electrospinning 37
3.3.6 Vapor-Phase Polymerization 38
3.3.7 Scanning Electron Miscroscopy 39
3.3.8 Electrical Characterization 40
3.4 Cytotoxicity Assay 40
3.5 SH-SY5Y Growth on Materials 41
3.6 Electrical Field Induced Medium Alterations 41
3.7 Electrical Stimulation of SH-SY5Y cells 41

4 Results and Discussion **44**
4.1 Optimization of Differentiation Protocol 44
4.2 Design and Assembly of the Bioreactor 52
4.2.1 Direct Coupling Setup 53
4.2.2 Attempt for an Electrically Insulated Setup 56
4.3 Fabrication of Conductive Scaffolds 58
4.3.1 Film Casting 59
4.3.2 Electrospinning 63
4.3.3 Electrical Characterization 64
4.4 Cytotoxicity Assay 67
4.5 SH-SY5Y Growth on Materials 67
4.6 Electrical Field Induced Medium Alterations 69
4.7 Electrical Stimulation Assay 74

5 Conclusions and Future Perspectives **76**
5.1 Optimization of Differentiation Protocol 76
5.2 Design and Assembly of the Bioreactor 77
5.3 Fabrication of Conductive Scaffolds 78
5.4 SH-SY5Y Growth on Materials 79
5.5 Electrical Field Induced Medium Alterations 79
5.6 Electrical Stimulation Assay 79

Bibliography **81**

Appendices

A Literature Review: SH-SY5Y neuronal differentiation **96**

B Protocols **101**
B.1 Cell Culture 101
B.1.1 SH-SY5Y Cell Thawing 101
B.1.2 SH-SY5Y Cell Trypsinization 101
B.1.3 SH-SY5Y Cell Subculture 102
B.1.4 Cryopreservation of SH-SY5Y Cells 102
B.1.5 Changing Cell Culture Medium 103
B.1.6 Cell Counting 103
B.1.7 Preparation of Retinoic Acid Stock Solutions 104
B.1.8 Resazurin Assay 104
B.1.9 Fluorescence Imaging 105
B.1.10 Culture Plate Layouts 105

C Fabrication of Conductive Scaffolds: Additional Content **108**
C.1 Spin Coating 108
C.2 Dip Coating 109
C.3 Electrospinning 109

List of Figures

1.1 Illustrated schematic displaying the set of histological events following trauma in the peripheral nerves. . . . 2
1.2 Illustrated schematic displaying the set of histological events following trauma in the central nervous system (CNS), specifically a contusive spinal cord injury. 3

2.1 Main types of ES that can be applied using a DC power supply or a function generator. . . . 8
2.2 Direct coupling scheme. . . . 9
2.3 Direct coupling stimulation systems found in the literature. . . . 11
2.4 Capacitive coupling scheme. . . . 12
2.5 Capacitive coupling stimulation systems found in the literature. . . . 13
2.6 Inductive coupling scheme. . . . 13
2.7 Inductive coupling stimulation systems found in the literature. . . . 15
2.8 Agar-salt bridge scheme. . . . 15
2.9 Agar-salt bridge stimulation systems found in the literature . . . 16
2.10 Influence of polypyrrole (PPy) and ES on neural differentiation of pheochromocytoma 12 (PC-12) cells. . . . 17
2.11 Influence of doping concentration of polyaniline (PANI) substrates on human mesenchymal stem cell (MSC) density and extension. . . . 18
2.12 Immunofluorescent staining of PC-12 cells with β-tubulin III (Tuj1) after 5 days of differentiation. . . . 19
2.13 Influence of brief ES applied immediately after surgery, 14 weeks after neuroma-in-continuity in rats. . . . 25

3.1 Example of a T25 cell culture flask used for SH-SY5Y cell proliferation. . . . 28
3.2 Example of 48-well plate used for neuronal differentiation of SH-SY5Y neuroblastoma cells. . . . 29
3.3 Diagram of the overall protocol followed for inducing neuronal differentiation of SH-SY5Y neuroblastoma cells. . . . 29
3.4 Final design of the chamber for ES of neuronal cells. . . . 32

3.5 Production of the chamber and lid of the ES setup. 33
3.6 Separate components necessary for complete assembly of the bioreactor. . 33
3.7 Devices used for applying distinct electrical fields to the cell culture chamber. 34
3.8 Assembly of the ES setup for preliminary testing. 34
3.9 Solution preparation scheme. 36
3.10 Film casting procedure scheme. 37
3.11 Spin coating setup. 37
3.12 Dip coating scheme. 38
3.13 Electrospinning setup scheme. 38
3.14 VPP scheme. 39
3.15 Producing conductive PLA/PEDOT fibers by performing VPP of EDOT. . . 39
3.16 Obtaining *IV* curves from the conductive scaffolds. 40
3.17 Diagram of the ES protocol followed for inducing neuronal differentiation of SH-SY5Y neuroblastoma cells. 43
3.18 Assembly of the bioreactor inside the incubator for the ES assay. 43

4.1 Inverted microscope image of undifferentiated SH-SY5Y cells in growth medium. 46
4.2 Inverted microscope images of SH-SY5Y cells cultured in Dulbecco's Modified Eagle Medium (DMEM) with 1% fetal bovine serum (FBS). 46
4.3 Inverted microscope images of SH-SY5Y cells cultured in DMEM with 1% and 0.5% dimethyl sulfoxide (DMSO). 47
4.4 RA-induced differentiation of SH-SY5Y cells cultured in DMEM, 1% FBS. . 48
4.5 Initial morphological changes resembling a differentiation state of SH-SY5Y cells after 2 days of exposure to RA. 49
4.6 Inverted microscope images of SH-SY5Y cells at day 7 of the differentiation protocol. 50
4.7 Inverted microscope images of SH-SY5Y cells seeded at a lower density . . 51
4.8 Comparison of the design and the prototype of the bioreactor produced. . 53
4.9 Multiple views of the design and the produced prototype of the bioreactor. 54
4.10 Dimensional drawing of the chamber and lid of the bioreactor made using Fusion 360™. 55
4.11 Errors and inaccuracies related to the production of the bioreactor. 56
4.12 New pieces used to isolate the culture medium from the electrodes. 57
4.13 Assembly of the bioreactor with electrically insulating PMMA spacers. . . 57
4.14 Determining the working volume for the bioreactor. 58
4.15 Films produced from PLA and PLA/FeTos solutions with a ratio of PLA to FeTos of 2:1. 59
4.16 VPP of films from group A. 60
4.17 Films produced from PLA and PLA/FeTos solutions with a ratio of PLA to FeTos of 2.5:1. 61

4.18 Films produced from PLA and PLA/FeTos solutions with a ratio of PLA to FeTos of 3:1. 61
4.19 Films produced from PLA and PLA/FeTos solutions with a ratio of PLA to FeTos of 12:1. 62
4.20 Films produced from PLA and PLA/FeTos solutions with a ratio of PLA to FeTos of 20:1. 63
4.21 Solutions prepared for the electrospinning process. 63
4.22 PLA/PEDOT scaffolds from VPP of aligned PLA fibers containing FeTos. . 64
4.23 scanning electron microscope (SEM) images of the PLA and PLA/PEDOT fibers produced. 64
4.24 Samples of electrospun PLA fibers, with and without PEDOT, for which *IV* curves were obtained. 65
4.25 *IV* graphs from the PLA electrospun fibers produced with and without PEDOT. 66
4.26 SH-SY5Y cell controls at the day of the resazurin assay. 68
4.27 Viability of SH-SY5Y cells when exposed to PLA and PLA/PEDOT extracts, in four different concentrations. 68
4.28 Fluorescence images of SH-SY5Y cell growth on the scaffolds at three different time points. 70
4.29 Visible alterations in water and low-serum DMEM from 1 h of continuous application of distinct voltage gradient between the electrodes. 72
4.30 Results from 1 h of biphasic voltage application between the electrodes, using water and low-serum DMEM. 73
4.31 Fluorescence image of the general view of SH-SY5Y cells subjected to the ES protocol, using the bioreactor. 74
4.32 Fluorescence images comparing SH-SY5Y growth and differentiation in aligned fibers of PLA/PEDOT, both with and without ES. 75

5.1 Dimensional drawing of a proposed 6-well stimulation system made using Fusion 360™. 78

A.1 SH-SY5Y cells in both an undifferentiated and a differentiated state. 96

B.1 Layout of the 48-well plate used for optimizing the differentiation protocol. 106
B.2 Layout of the 96-well plate used for the resazurin assay. 106
B.3 Layout of the 24-well plate used for assessing the growth of SH-S5Y5 cells on materials. 107

C.1 Fabrication of thin films from PLA/FeTos solutions using a spin coating technique. 108
C.2 Attempt for dip coating of a PLA film with a FeTos solution. 109

C.3 Basic microscopic images from the deposition of PLA/FeTos fibers on a coverslip. 109

List of Tables

2.1 Summary of neural tissue engineering (TE) studies *in vitro* using ES and CPs. 20
2.2 Summary of neural TE studies *in vivo* using ES and CPs. 26

3.1 Details from the polymer used for scaffold fabrication. 35
3.2 Reagents used for scaffold fabrication. 35

4.1 Results from 1 h of continuous electrical field application to water and low-serum DMEM using the bioreactor. 72
4.2 Results from 1 h of biphasic electrical field application to water and low-serum DMEM using the bioreactor. 73

A.1 Summary of the conditions used for culture and sub-culture of SH-SY5Y cells. 97
A.2 Summary of the conditions found to induce neuronal differentiation of SH-SY5Y cells. 99
A.3 Predominant phenotypic display of SH-SY5Y cells depending on the exposure to a certain differentiation agent/combination of agents. 100

Glossary

action potential	Elementary neural signal; determined by the precisely timed opening and closing of ion channels.
autologous nerve graft	Surgical procedure where a donor nerve is harvested from a healthy part of the body and sutured into an injured nerve to bridge the defect; also known as autograft.
biocompatibility	Ability of a material to perform with an appropriate host response in a specific application.
bioelectricity	Electric fields in the human body that modulate the behavior of cells and tissues.
biomaterial	Substance that has been engineered to take a form which, alone or as part of a complex system, is used to direct, by control of interactions with components of living systems, the course of any therapeutic or diagnostic procedure.
bioreactor	Any manufactured device or system that supports a biologically active environment.
conductive polymer	Polymer whose backbone displays loosely held electrons; conductive ability is dependent on doping, a process by which a neutral polymer becomes positively or negatively charged.
electrical field	Voltage difference per unit distance.
nervous system	Is divided in two parts, the central nervous system and the peripheral nervous system; its tissue is composed of two types of cells: neurons and glial cells.

neuron	Nerve cell that constitutes the basic unit of the nervous system; receives, integrates, propagates and transmits electrochemical signals based on changes in the membrane potential.
piezoelectricity	Electrical current that accumulates in materials upon application of mechanical stress.
schwann cell	Type of glial cell responsible for ensheathing axons in a layer of myelin and providing trophic support through the release of important neurotrophs.
Wallerian degeneration	Physiological process based on protease activity that leads to degeneration of a nerve's distal portion following peripheral nerve injury.

Abbreviations

AC	alternating current
araC	cytosine arabinoside
BBB	blood brain barrier
BDNF	brain-derived neurotrophic factor
BEC	biphasic electrical current
BNB	blood nerve barrier
cAMP	cyclic adenosine monophosphate
CHL	chloroform
CNS	central nervous system
CNT	carbon nanotube
CNTF	ciliary neurotrophic factor
CP	conductive polymer
DAPI	4',6-diamidino-2-phenylindole
DAQ	data acquisition
DBS	dodecylbenzenesulfonate
DC	direct current
DMEM	Dulbecco's Modified Eagle Medium
DMF	dimethylformamide
DMSO	dimethyl sulfoxide
ECM	extracellular matrix
EDOT	3,4-ethylenedioxythiophene
EDTA	ethylenediaminetetraacetic acid
EMEM	Eagle's Minimum Essential Medium
EMF	electromagnetic field

ES	electrical stimulation
EtOH	ethanol
FBS	fetal bovine serum
FCS	fetal calf serum
FdUr	5-fluoro-2'-deoxyuridine
FeTos	Iron(III) p-toluenesul–fonate/Fe(III)Tosylate
FIB	focused ion beam
GAD	glutamic acid decarboxylase
GO	graphene oxide
HA	hyaluronic acid
IGF-1	insulin-like growth factor 1
iPSC	induced pluripotent stem cell
ITO	indium tin oxide
MAP2	microtubule-associated protein 2
MEM	Minimal Essential Medium
MSC	mesenchymal stem cell
MW	molecular weight
NeuN	neuronal nucleous marker
NEURiTES	NEUral Regeneration with conducTivE Scaffolds
Nf-M	neurofilament medium polypeptide
NGC	nerve guidance conduit
NGF	nerve growth factor
NPC	neural progenitor cell
NSC	neural stem cell
PANI	polyaniline
PBS	phosphate buffered saline
PC-12	pheochromocytoma 12
PCB	printed circuit board
PCL	polycaprolactone
PEDOT	poly(3,4-ethylenedioxythiophene)
PEMFS	pulsed electromagnetic field stimulation
PEO	poly(ethylene oxide)
PET	poly(ethylene terephthalate)

PFA paraformaldehyde
PG polygelatin
PLA poly(lactic acid)
PLCL poly(l-lactic acid-co-ϵ-caprolactone)
PLGA poly(L-lactic-co-glycolic acid)
PMMA poly(methyl methacrylate)
PNI peripheral nerve injury
PNS peripheral nervous system
PPDO poly(p-dioxanone)
PPy polypyrrole
PSS polystyrene sulfonate
PVA polyvinyl alcohol
PVC polyvinyl chloride

RA retinoic acid
RC regenerated cellulose
rpm rotations per minute
RPMI Roswell Park Memorial Institute
RT-PCR reverse transcription polymerase chain reaction

SC Schwann cell
SCI spinal cord injury
SEM scanning electron microscope
SFM serum-free media
SYP synaptophysin

TE tissue engineering
TPA 12-O-tetradecanoylphorbol-13-acetate
Tuj1 β-tubulin III

Ur uridine

VEGF vascular endothelial growth factor
VOCC voltage operated calcium channel
VPP vapor-phase polymerization

WD wallerian degeneration

1 Introduction

This chapter starts by briefly presenting the nervous system. Then, it describes the context of the project in which this dissertation is integrated, as well as the motivation for this dissertation. An explanation of the goals that were aimed to achieve follows. Finally, the document structure is highlighted.

1.1 Nervous System

Damage to nervous tissue caused by trauma or a neurodegenerative disease represents a daily challenge for those suffering from such conditions. These are common clinical problems affecting both the CNS and the peripheral nervous system (PNS), which lead, in severe cases, to total loss of motor and sensory function, distal from the injury site. The clinical approaches aim at repairing the damaged tissue and restoring its function, varying according to the injury site, its type and severity [2].

1.1.1 Regeneration of Nervous Tissue

Lesions of the peripheral nerves can result in severed axons. Even though there is some potential for spontaneous axonal regrowth, it is typically limited to small gap injuries (under 3 cm) and may require surgical intervention. Development of new and improved treatments protocols constitutes an important field of research in neurosurgery. The regrowth process is mediated by cellular and molecular responses, namely by the activity of macrophages and Schwann cells (SCs) [3].

For larger gaps (greater than 2-4 cm), the physiological factors impairing functional recovery range from the lack of guidance/alignment cues to reconnect the proximal and the distal portions of the injured nerve to the degeneration of the distal stump through a process termed Wallerian degeneration, as shown in Figure 1.1. Furthermore, the nerve stumps are unable to rejoin without tension and for those cases, autologous nerve grafts are recognized as the gold-standard strategy [5], [6]. Nevertheless, this procedure has some significant drawbacks, such as donor site morbidity, limited tissue availability and

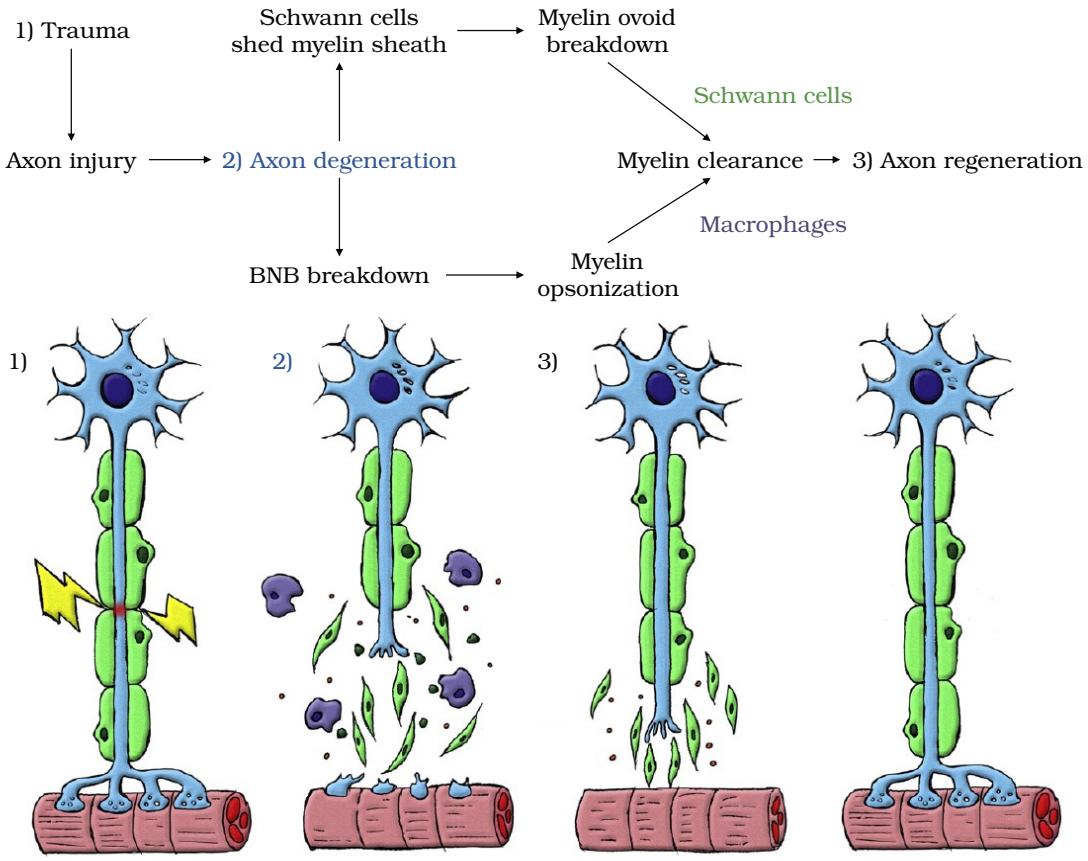

Figure 1.1: Illustrated schematic displaying the set of histological events following trauma in the peripheral nerves. WD in the PNS is characterized by axonal degeneration, which activates two lines of action. On the one hand, SCs shed myelin sheath into smaller ovoids. On the other hand, breakdown of the BNB allows for the influx of macrophages, responsible for opsonization of myelin debris. Ultimately, these series of events induce myelin clearance, which is paramount for axonal regeneration. Adapted from [3], [4].

neuroma formation [4]. Overall, current grafting solutions present limited functional recovery of patients and are only suitable for nerve gaps under 4 cm [6].

Despite the obstacles found in peripheral nerve injury (PNI) recovery, it is possible through regeneration and remyelination of axons [2]. Yet, CNS recovery poses challenges that are more complex, as WD is significantly slower when compared to what happens in the PNS. Thus, successful treatment options are considerably harder to develop. This limited regenerative capacity arises from a group of issues. Firstly, damage to the CNS compromises both the axons and the neuronal cell bodies, leading to immediate cell death. Besides that, blood supply becomes disrupted at the site of injury. Finally and more importantly, axonal regrowth is impaired by the formation of a glial scar due to local immune response, particularly in spinal cord injury (SCI) scenarios, as demonstrated in Figure 1.2 [3], [5].

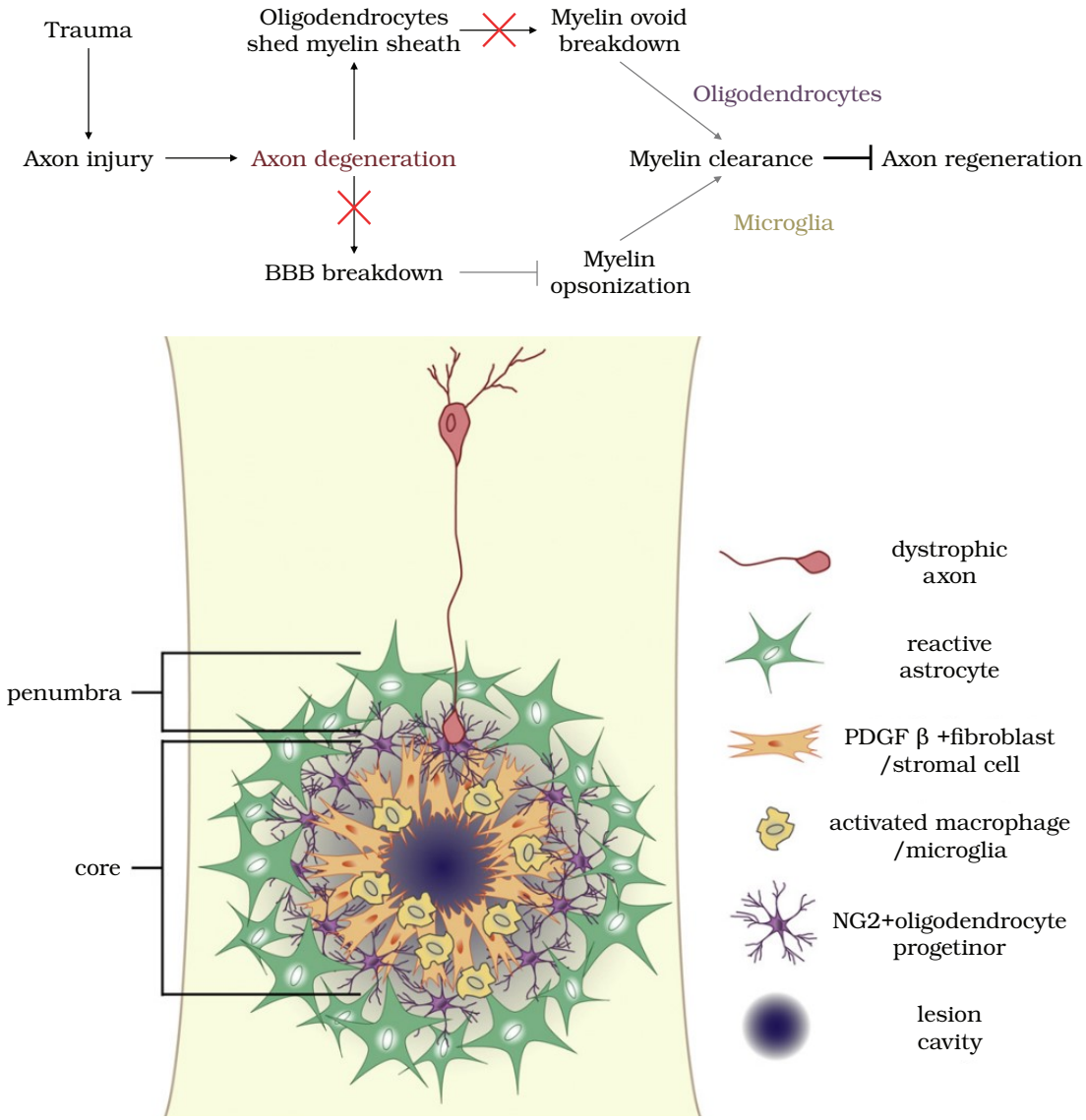

Figure 1.2: Illustrated schematic displaying the set of histological events following trauma in the CNS, specifically a contusive spinal cord injury. Following axon degeneration, oligodendrocytes shed myelin sheath but fail to clear the resulting myelin ovoids. Additionally, macrophage migration to the injury site is impeded by the incomplete disruption of the BBB post-injury, hindering opsonization of myelin debris and consequently, impeding axon regeneration. Adapted from [3], [7].

1.2 Context and Motivation

In this context, neural TE approaches emerged as highly promising to aid the repair and regeneration of nervous tissue, with studies being performed on several injuries including PNI, SCI and brain, retinal and cochlear injuries. Many attempts have been made, often involving the fabrication of polymers for scaffold-based approaches, with embedded cells and incorporation of biophysical (electrical) and biochemical (growth factors) cues or signals [8].

Some important conclusions have been drawn from such studies, establishing the background for this dissertation: nerve guidance conduits (NGCs) promote neural regeneration; aligned electrospun fibers constitute directional cues guiding neurite outgrowth; some scaffolds studied allow for cell transplantation; ES applied through a scaffold may activate intrinsic cellular pathways that support migration, differentiation and proliferation of diverse cell types [9].

1.2.1 The Case for Electrical Stimulation

The case for using ES in TE approaches is based on the importance of electrical phenomena taking place in living organisms, namely bioelectricity. In this regard, it is worth pointing out the intrinsic electrical nature of neurons, whose communication happens over electrochemical signals. Importantly, intercellular communication is dependent on electrochemical gradients of the neuronal cell membranes. These gradients emerge due to the activity of cell membrane ion pumps, which are also responsible for triggering action potentials. Action potentials are found in excitable cells, such as neurons and skeletal and cardiac muscle cells and can be induced through ES [10], [11].

Additionally, other biological functions, like muscle contraction and wound healing, are supported by bioelectricity [12], further justifying the increasing interest in the development of *in vitro* setups that mimic *in vivo* conditions with or without artificial biophysical cues, namely ES.

1.2.2 NEURiTES

In this scope, arose a project termed NEUral Regeneration with conducTivE Scaffolds (NEURiTES), project PTDC/CTM-COM/32606/2017, which optimizes scaffolds for neural TE applications. The main goal of the project is the optimization of electrospun scaffolds of aligned fibers to be used as substrates for the ES of cells, foreseeing the promotion of neural regeneration [13]. NEURiTES encompasses several stages, one of them being particularly important in the context of my dissertation. It regards the controlled application of distinct electrical stimuli to human cells seeded on electrospun conductive scaffolds mounted on a sterile *in vitro* environment.

Accordingly, a new device, hereupon called bioreactor, needs to be designed, assembled and tested for the delivery of both DC and AC in varied time intervals.

Summing up, the mechanisms by which external ES contributes to neural regeneration are still unclear. Therefore, the success of the aforementioned bioreactor will enable the pursuit of studies correlating ES parameters with cell morphology, proliferation and differentiation, aiming at the development of more efficient treatment options concerning neural TE.

1.3 Dissertation Goals

1.3.1 Contribution to the Problem

As previously mentioned, nervous tissue presents limited regenerative capacity, which can be improved resorting to ES. Research on this topic encompasses studies performed in a variety of cell types, using a wide range of methods and parameter combinations [9]. Although there have been promising results, ranging from enhancement of neurite outgrowth to faster functional recovery following injury, such strategies lack standardization and are typically performed in low throughput systems [14].

In this regard, the aim of this dissertation was the design, assembly and test of a setup, in other words a bioreactor, for the controlled application of ES using both DC and AC current for varied periods of time. The possibility of supporting different ES regimes on cells seeded on fibrous scaffolds will enable further investigation to take place on the mechanisms underlying neuronal differentiation of the cells used induced by ES, contributing to the field of nervous tissue regeneration.

1.3.2 Specific Goals

- **Optimization of differentiation protocol**

  Execute cell culture assays where cells are subject to distinct differentiation media. Assess cell morphology with the inverted microscope. Determine optimal differentiation conditions.

- **Design and assembly of the bioreactor**

  Choose materials that can be sterilized. Design a fixation system for the scaffolds and a chamber for the placement of cells. Include electrodes and electrical connectors, allowing for the controlled application of an electric field or current through the surface of the scaffold using both AC and DC current and a mechanism to measure them. Select an ES delivery method for satisfactory operation of the bioreactor. Following the design stage, produce and install the ES system.

- **Fabrication of conductive scaffolds for cell seeding**

  Along with the assembly of the bioreactor, produce fibrous conductive scaffolds, where neuronal cells can be seeded in order to perform the cellular tests. Coat the fabricated scaffolds with a conductive polymer.

- **Bioreactor testing**

  Culture neuronal cells on the nanofibrous scaffolds produced and fixed on the ES device. Define criteria for assessment of the effects of ES on neuronal differentiation and proliferation. Ultimately, evaluate the suitability of one or more designs chosen for neuronal cell culture under ES.

1.4 Document Structure

This document is composed by five chapters, organized as follows:

- Chapter 1: **Introduction**, presents the context of the project in which this dissertation is integrated, as well as its motivation and goals;
- Chapter 2: **State of the Art**, reports the results of the literature review performed on the topic of this dissertation;
- Chapter 3: **Materials and Methods**, details the materials necessary and methods performed for achieving each task;
- Chapter 4: **Results and Discussion**, exposes the main results of the work developed and discusses its value with respect to the general problem and specific tasks of this dissertation;
- Chapter 5: **Conclusions and Future Perspectives**, recapitulates the work developed, its contributions, and outlines suggestions of future work as well.

2

State of the Art

This chapter reports the results of the literature review performed on the topic of this dissertation. It starts by presenting bioelectricity as a beneficial biophysical cue for TE applications. Secondly, the principal methods of ES *in vitro* are described in detail, along with main results derived from such methods. Then, follows a review of the conductive scaffolds typically used for *in vitro* experiments with ES. Finally, it includes an overview of the effects of ES applied *in vivo*.

2.1 Bioelectricity

Electrical fields and currents are physical phenomena intrinsic to biological tissues and cells. These are tightly associated with a multitude of physiological events, namely action potentials, muscle contraction, hearing, and wound healing. The awareness developed on this type of endogenous phenomena, occurring at the cell membrane level, through ion pumps, channels and gap junctions, has been crucial when it comes to the design of novel TE approaches, since it drove this field of research towards both *in vivo* and *in vitro* experimentation with exogenous electrical fields [11], [12].

From this knowledge, a growing body of evidence emerged supporting the application of ES as a biophysical cue in TE, in particular for nerve [15], cardiac tissue [16] and skeletal muscle [17] engineering. Such interest in this type of stimuli derives from the excitable nature of the cells composing the mentioned tissues [18], as well as from the role of bioelectricity in the regulation of cell behavior, including proliferation, migration and orientation, differentiation, among other functions [12]. Moreover, ES has been successfully implemented in bone TE applications, a tissue whose cells present piezoelectricity and, however, are electrically non-excitable [11], [19].

Translating a new treatment into clinical practice is generally preceded by *in vitro* testing in order to predict possible outcomes more reliably and to reduce the need of animal resources. As such, *in vitro* research on this topic has been faced with two challenges of major relevance in the development of systems that allow for controlled application of ES as a biophysical cue for neural TE. These correspond to the design and development of

an adequate method of ES delivery to cells, as well as the fabrication and incorporation of suitable biomaterials that better mimic the natural flow of ions, and overall electrical characteristics of human neural tissue.

2.2 Methods for Electrical Stimulation of Cells *In Vitro*

The design and fabrication of setups appropriate for *in vitro* ES is paramount for both improving the current knowledge on the effects of endogenous electrical fields and currents on cells, in addition to paving the way for using exogenous ES as a possible treatment option in tissue engineering applications. Generally, these systems incorporate three major elements: a container for cell seeding (either typical cell culture plates, Petri dishes or personalized containers), a power supply or function generator and electrodes to connect the former two [11].

The outcome of ES in *in vitro* cell culture assays is highly dependent on the method of ES employed. Currently, there are three main methods for delivering ES: direct coupling, capacitive coupling and inductive coupling, each with its advantages and limitations. Combinations of more than one method are also being explored, as well as more sophisticated setups based on the three standard designs [9], [20].

Prior to describing the ES setups that have already been successfully implemented for TE applications, it is important to understand what parameters can be altered in the ES of cells (Figure 2.1). The most basic way to deliver ES to an *in vitro* cell culture consists in operating a power supply which provides a DC current. In this scenario, it is possible to control the overall duration of the ES, applied in a continuous or cyclic fashion, its amplitude of current (A) and magnitude of voltage (V). Another choice is using a function generator, which allows for the application of an AC current with distinct waveforms (be it sinusoidal, square, triangular, or sawtooth), monophasic or biphasic, with defined frequency (Hz) and in pulses of controlled width (ms), and frequency (Hz) [11], [20], [21].

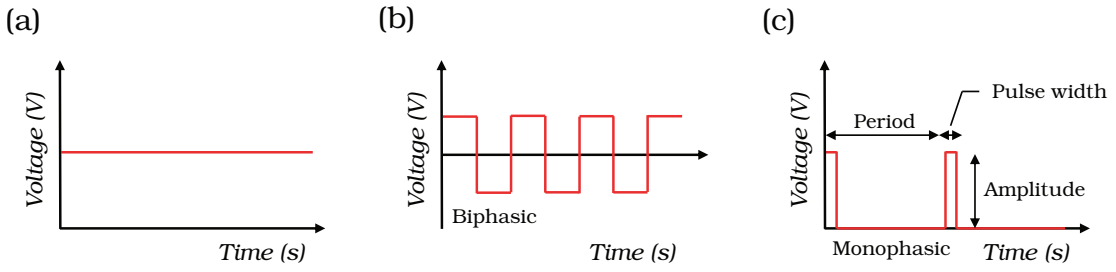

Figure 2.1: Main types of ES that can be applied using a DC power supply or a function generator: (a) Using a DC power supply it is possible to apply a constant voltage for different periods of time; (b) Using a function generator it is possible to implement more complex protocols, including monophasic and biphasic waves, different waveforms and; (c) pulses of varying width, frequency and amplitude. Adapted from [11].

2.2.1 Direct Coupling

The first method, direct coupling, is the most common and the simplest as well. It corresponds to a setup where the electrodes are in direct contact with the cell culture and connected to the scaffold (*in vitro* scenario) or is implanted into the patient or animal model (*in vivo* scenario). There are, however, some downsides to consider when using this method, specifically biocompatibility issues related to the electrodes, changes in pH and formation of unwanted byproducts in the culture medium [9]. A scheme of a direct coupling setup is provided in Figure 2.2.

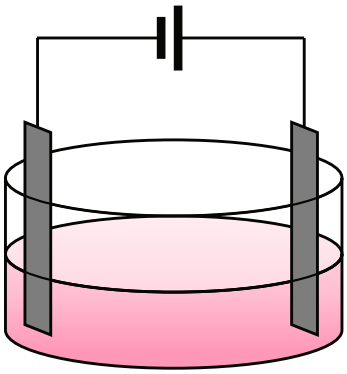

Figure 2.2: Direct coupling scheme. This setup shows two electrodes placed in direct contact with the culture medium and connected to a DC power supply via conductive wires. Based on [9], [20].

Langer et al. implemented an ES system using conductive PPy films attached to Plexiglass wells, and a biopotentiostat as the source of a constant voltage. The PPy film functioned as the anode and a gold wire, located along the length of the well but in the opposite end, was used as cathode. This setup allowed for the application of an electrical stimulus through the film to PC-12 cells (cultured on the film) with a constant potential of 100 mV (about 100 µA) for 2 hours, one day after cell seeding. Twenty-four hours after stimulation, cells exhibited longer neurite projections and therefore showed improved differentiation in comparison with the unstimulated control group. Furthermore, analogous results were observed in samples exposed to a constant current of 10 µA, delivered through electrical leads attached to opposite ends of the PPy film [15].

Based on the former example, an *in vitro* direct coupling setup was assembled by Ramakrisnha et al., using two electrodes and a DC power supply, for the stimulation of neural stem cells (NSCs). A silver and a platinum electrodes were placed in opposite ends of a PANI/polygelatin (PG) scaffold. NSCs seeded in PANI/PG nanofibrous scaffolds revealed improved proliferation and neurite outgrowth when subjected to an electrical field of 100 mV/mm for 1 hour, in contrast with samples exposed to a shorter duration of ES (15 and 30 minutes) and unstimulated samples [8].

This simple setup inspired the assembly of similar configurations in more recent studies. For instance, Golafshan et al. applied ES to PC-12 cells seeded onto graphene

embedded polyvinyl alcohol (PVA)/alginate fibrous scaffolds placed in standard 24-well cell culture plates. The electrodes (a silver electrode, used as anode and a platinum electrode, as cathode) were fixed in opposite ends of the samples and in direct contact with the medium. After exposing the samples to a constant voltage of 1 V for 1 hour, the effects of this protocol on cell proliferation were assessed, revealing greater proliferation of PC-12 cells cultured on both randomly oriented and aligned nanofiber scaffolds, comparing to samples without ES [22].

Furthermore, Babaie et al. differentiated rat MSCs into a neuronal cell line, by exploiting a synergy between conductive PVA/PEDOT electrospun scaffolds and ES. The group placed two 316-stainless steel electrodes, in contact with the conductive scaffolds, in each well of a 6-well plate. An electrical pulse generator was used to deliver 2 hours of 100 mV/mm of scaffolds to the seeded cells, through copper wires connected to the electrodes, for 3 days. Exposure to ES on the conductive scaffolds, along with the presence of neural differentiation factors resulted in increased expression of neural differentiation genes, such as nestin and Tuj1 by the MSCs, comparing to unstimulated cells [23].

Similarly, Chudickova et al. successfully differentiated MSCs using a combination of different differentiation factors, including polycaprolactone (PCL) electrospun scaffolds, growth factors and ES. The system developed to apply the ES consisted in two silver electrodes placed directly in a cell culture dish using Teflon clamps. The positive electrode received the output from a pulse generator, which was buffered using a voltage follower. The negative electrode was connected to a current-to-voltage amplifier, and the signals were then digitalized using a data acquisition device and stored in a computer. Cells were exposed to monophasic pulses, with a duration of 2.5 ms, a frequency of 4 Hz, an electrical field of 0.33 V/cm, for 5 min, in different days of a 9-day culture. The differentiation factors alone did not significantly influence the expression of neuron-specific markers but once combined in a more complex protocol, led to an increased expression of the markers neurofilament medium polypeptide (Nf-M), synaptophysin (SYP), and glutamic acid decarboxylase (GAD) [24].

Overall, despite its limitations, the simplicity in the concept of a direct coupling system has led to a variety of studies where neuronal cells showed improved proliferation and differentiation upon distinct protocols of exposure to ES. Moreover, these experiments support the idea that a more efficient *in vitro* protocol for neural differentiation of stem cells is to be found in the combination of differentiation-inducing agents, comprising the medium in which cells are kept during culture, the presence of a biocompatible scaffold and ES as a biophysical cue. The former conclusion highlights the need for a standardized and optimized setup, a bioreactor, where all the agents can be implemented in a synergy. Some examples of direct coupling stimulation systems found in the literature are shown in Figure 2.3.

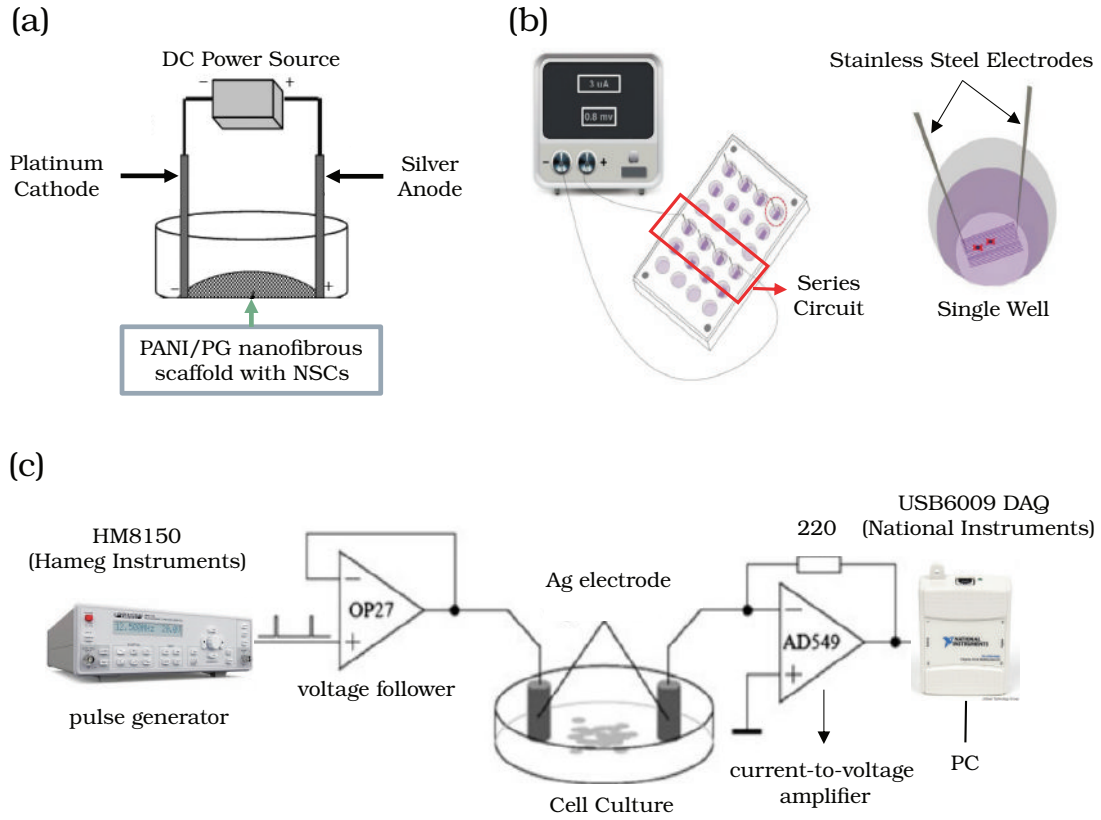

Figure 2.3: Direct coupling stimulation systems found in the literature: (a) In neural TE, direct coupling entails placing a pair of electrodes at opposite ends of a cell culture well or a biocompatible conductive scaffold, in direct contact with the culture medium. The system is powered by either a DC power source or a function generator; (b) Cell culture plates are usually utilized in order to perform stimulation of multiple replicates. In this case, the system is assembled as a series circuit, which ensures that each well is subjected to the same current; (c) Some systems have more sophisticated electronics, including voltage followers, current-to-voltage amplifiers and even DAQ systems. Adapted from [8], [24], [25].

2.2.2 Capacitive Coupling

The second method, capacitive coupling, is non-invasive and produces a uniform electromagnetic field (EMF) by placing two electrodes in parallel, with the scaffold and seeded cells in between. Therefore, it is biologically safer than direct coupling and provides cells with similar stimulation independently of their position within the culture. Furthermore, the presence of a conductive scaffold is not required in order to deliver uniform ES [9], [20]. A scheme of a capacitive coupling setup is provided in Figure 2.4.

A versatile setup based on the capacitive coupling principle was already used in neural TE. In one study, Chang et al. developed and tested a biphasic electrical current (BEC) stimulator chip capable of delivering continuous biphasic current pulses with a programmable choice of parameters for ES, namely amplitude (µA), pulse width (µs) and

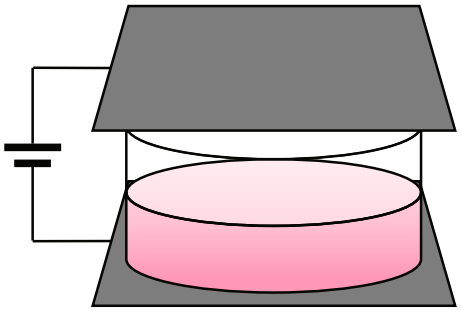

Figure 2.4: Capacitive coupling scheme. This setup shows two plates composed of a conductive material (e.g., gold, ITO) placed at opposite ends of the culture medium, providing cells with a uniform EMF. Based on [9], [20].

pulse rate (Hz). The custom made stimulator chip was attached to cell culture chambers, composed of Teflon jigs and ITO glasses, giving rise to a 6-well culture system on which fetal NSCs were cultured and electrically stimulated. ITO glass, the material composing the bottom and top of each cell culture chamber presents high electrical conductivity, serving as a capacitor in the described *in vitro* setup and was connected to the chip using printed circuit boards (PCBs). Importantly, the group assessed both proliferation and differentiation of NSCs when exposed to diverse stimulation protocols. Once subjected to a magnitude of 8 $\mu A/cm^2$ with 200 μs pulses at a frequency of 100 Hz for a total of 4 days, the number of NSCs was twice of controls. Finally, after 7 days of differentiation with 4 $\mu A/cm^2$ with 200 ms pulses at 100 Hz, cells showed a significant increase in expression of differentiation markers, namely Tuj1, neuronal nucleous marker (NeuN), and microtubule-associated protein 2 (MAP2) [26].

A similar construct had been used by Kim et al. for the sake of applying a BEC to osteoblasts. The system presented an analogous biphasic current stimulator chip, six Teflon®wells and two gold deposited glass plates per well, as electrodes, connected in a shunt configuration. Observations revealed a 31% increase in proliferation in osteoblasts exposed to 1.5 $\mu A/cm^2$, 3000 Hz, continuously for 2 days, compared to control. Interestingly, the same conditions applied for only 6 h/day produced no effect on proliferation rate. More importantly, cytokine synthesis and vascular endothelial growth factor (VEGF) induction were also assessed under the former ES protocols. While cytokine synthesis remained unaltered (1.5 $\mu A/cm^2$, 3000 Hz, continuously) or was inhibited (1.5 $\mu A/cm^2$, 3000 Hz, 6 h/day), there was a 2.8-fold induction of VEGF protein secretion with 2 days of stimulation and a 3.2-fold induction with 4 days of stimulation, in both the 6 h/day and the 24 h/day protocols, showing the potential of BEC for TE approaches demanding angiogenesis [27]. The above mentioned ES systems are presented in Figure 2.5.

Most of the existing literature on capacitive coupling ES systems focuses on bone TE applications [28]–[31]. Even though this is not the goal of the present dissertation, the majority of the setups found for *in vitro* ES can also be used or easily adapted for other purposes, namely neural TE, as long as the main pre-requisites are met: suitability for

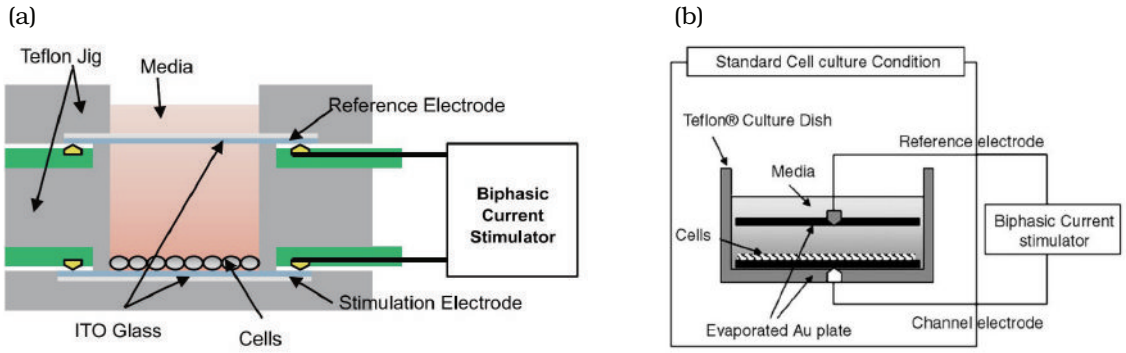

Figure 2.5: Capacitive coupling stimulation systems found in the literature: (a) Stimulation system used for culture and ES of NSCs using a custom made biphasic current stimulator chip, and ITO glass plates as electrodes. Adapted from [26]; (b) This simillar setup was used for stimulation of osteoblasts and presents gold deposited glass plates as electrodes. Adapted from [27].

cell culture and ability to deliver ES of some sort. This also stands for any other method of ES *in vitro*.

2.2.3 Inductive Coupling

Finally, inductive coupling typically consists in the placement of Helmholtz coils in pairs or a solenoid, around the cell culture, connected to an AC power source. Such display, based on Faraday's induction law, allows for the generation of a controllable uniform EMF throughout the culture, avoiding the use of electrodes (non-invasive application of the stimuli). This arrangement enables the delivery of pulsed stimulus, a technique also known as pulsed electromagnetic field stimulation (PEMFS). Some limitations associated with this method include time, space, and resource consumption [9], [20]. Another concern has been raised, namely that EMFs can foster tumor progression by promoting angiogenesis, however PEMFS is considered safe, since it does not act as mutagens [32]. A scheme of an inductive coupling setup is provided in Figure 2.6.

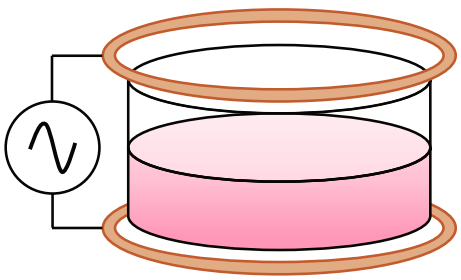

Figure 2.6: Inductive coupling scheme. This setup consists in placing the cell culture between Helmoltz coils or a solenoid connected to an AC power generator. The geometry of the system should be defined in order to deliver a uniform EMF to the cells. Based on [9], [20].

This technique has been explored for numerous applications, being considered a potential tool in the development of novel regenerative therapies. Areas of application range from bone [33] to cardiac [34] TE, since osteogenesis and cardiac cell differentiation have been observed, respectively, when exposing cells to distinct EMFs, typically at low frequency. Furthermore, the use of PEMFS has also been proven to modulate immune responses in studies involving macrophage cell cultures [35]. Importantly, there are some reports in the literature addressing the use of EMFs through inductive coupling systems in order to assess its influence on neuronal cell behavior, namely in proliferation, differentiation into a more mature and functional phenotype and neurogenesis [36]–[39].

Hei et al. conducted an *in vitro* study in which immortalized rat schwann cells were exposed to diverse PEMFS conditions. The setup used for the stimulation *in vitro* was composed of two Helmholtz coils of 30 cm diameter, placed 15 cm apart inside an incubator. The cells were maintained in culture for 7 days, while exposed to a magnetic field of intensity 1 mT in four distinct protocols combining frequency (Hz) and duration of exposure (h/day): 50 Hz or 150 Hz for 1 h/day or 12 h/day. It was shown that PEMFS led to increased cell proliferation, as well as the expression of S100 and brain-derived neurotrophic factor (BDNF) genes, particularly using 50 Hz as frequency, and an exposure time of 1 h/day compared with control [36].

In another study, Cheng et al. stimulated embryonic neural progenitor cells (NPCs) using extremely low-frequency EMFs generated by a solenoid. By using an AC power generator and an amplifier to power the solenoid, the group was able to deliver a 50 Hz field of intensity 0.4 mT, continuously, for different periods of time (4, 8, 16, 24 and 32 hours). Regarding cell proliferation, cells stimulated for 16 and 24 hours showed a marked increase compared with the control. Neural differentiation was assessed after exposure of the cells to 16 hours of extremely low-frequency EMFs (the time corresponding to the peak of proliferation) and 7 days. Even though 16 hours of exposure resulted in no significant improvement on differentiation, expression of Tuj1 by embryonic NPCs was increased from 7% to 12% when time of exposure corresponded to 7 days. Similar observations were made in NPCs cultured from ischemic mice brains [37].

These results support the interest in EMF as a non-invasive tool to modulate proliferation and differentiation of neuronal cells. Some examples of the inductive coupling systems used in the mentioned studies are presented in Figure 2.7.

2.2.4 Other Options

Other configurations are possible and have already been implemented in the context of neural TE. One famous example is using agar salt bridges as an alternative to direct stimulation. In this arrangement, a DC power supply is connected to Ag/AgCl electrodes immersed in a saline. The connection between the electrodes and the cell culture medium is established through agar-gelled salt bridges, which protects the cell culture from the dangerous byproducts of electrolysis [40], as shown in Figure 2.8.

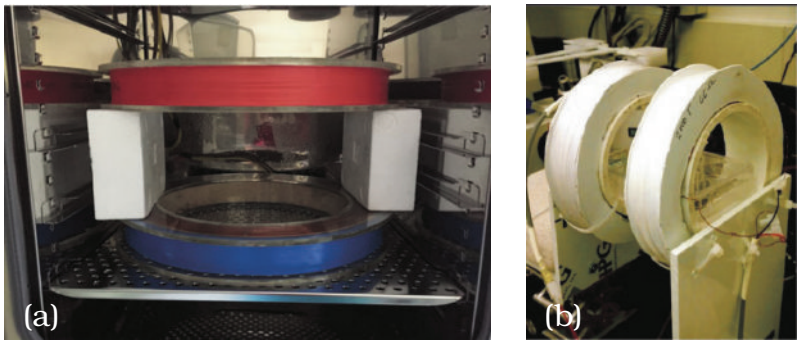

Figure 2.7: Inductive coupling stimulation systems found in the literature: (a) System of Helmoltz coils placed inside an incubator, used to apply a uniform EMF to rat SCs. Adapted from [36]; (b) Similar setup where a 6-well plate is supported inside Helmoltz coils. Only the four outer wells were considered to ensure a uniform EMF. Adapted from [35].

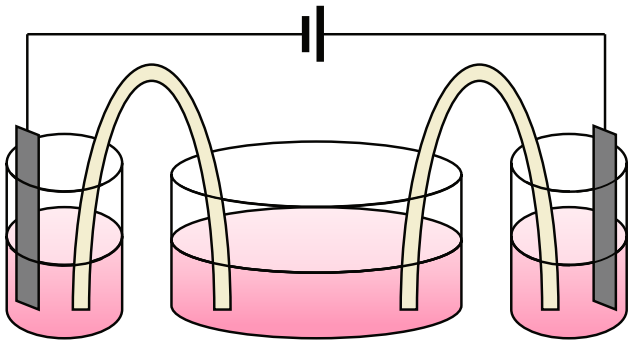

Figure 2.8: Agar-salt bridge scheme. This alternative to direct coupling consists in immersing the electrodes in separate containers containing a saline and connecting them to a DC power supply. The connection to the cell culture medium is established through agar-gelled salt bridges. Based on [41].

A setup using agar-salt bridges was described by Ariza et al. for the purpose of treating hippocampal NPCs with ES. Cells were seeded onto custom designed and machined polycarbonate chambers treated with poly-L-lysine and laminin-1. Glass tubes containing 1% agarose-gelled media with 5% FBS were used as a bridge between the mentioned chambers and Ag/AgCl electrodes immersed in media in two separate chambers. The Ag/AgCl electrodes were either connected to a 15 MHz waveform generator or an electrophoresis power supply, for an AC or a DC electrical field stimulation protocol, respectively. After cell seeding, two ES protocols were tested for 6 days: a 437 mV/mm DC electrical field (16-24 h/day) and a 46 mV/mm alternating electrical field (for the duration of the experiment). Immunocytochemistry assays revealed that the DC protocol was effective in promoting NPC differentiation and cell alignment. Surprisingly, the small alternating electrical field protocol produced no significant effects on cell differentiation, alignment nor proliferation [42].

Mobilizing NPCs to injured sites is critical in endogenous neurorepair, namely after

stroke. In this regard, galvanotaxis, the migration of undifferentiated NPCs towards the cathode in a direct stimulation system, gained attention and is being considered to possibly integrate new therapies in which cell recruitment is essential. Babona-Pilipos et al. explored this concept by delivering DC electrical fields (250 mV/mm) to NPCs through an *in vitro* system containing agar-salt bridges, observing cathodal migration in undifferentiated cells. This phenomenon did not occur in differentiated cells [43]. Even though galvanotaxis is possible, charge accumulation associated with DC electrical fields is not desirable for clinical applications. With this in mind, the group designed and performed a new study proving that charge balanced biphasic monopolar stimulation is a safer option that is also effective in inducing cathodic migration of undifferentiated NPCs. The same setup was used in both studies, including a custom galvanotaxis chamber and polyvinyl chloride (PVC) tubes filled with 1.5% agarose gel as a bridge between the chamber and two separate Petri dishes. Each dish included an Ag/AgCl electrode immersed in serum-free media (SFM) that was connected to an electrical stimulator [44]. The systems from the studies described are presented in Figure 2.9.

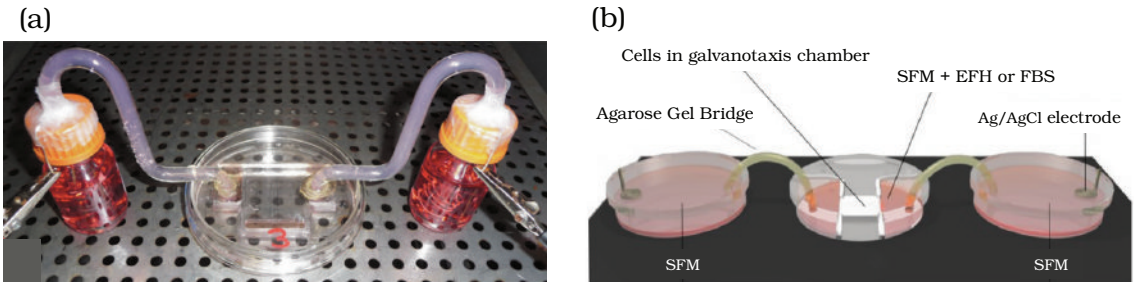

Figure 2.9: Agar-salt bridge stimulation systems found in the literature: (a) This system, on which NPC differentiation was achieved, contains custom made chambers connected to Ag/AgCl electrodes through glass tubes containing 1% agarose-gelled media; (b) Similar system used to study the role of different electrical fields on NPC galvanotaxis. Adapted from [42], [44].

2.3 Conductive Scaffolds

Another aspect to consider, along with the ES delivery method, is the choice of electrodes and scaffold material for cell seeding. In the domain of scaffold-based approaches for neural TE, CPs have been increasingly studied and represent a more efficient way of delivering ES. CPs are organic semiconductors that belong to the family of electroactive materials, along with electrets, piezoelectric and photovoltaic materials, possessing electrical and optical properties like those of metals, even though they are soft and extendable. Moreover, these polymers present tunable chemical/electrochemical properties and can be used to produce biocompatible, biodegradable and porous scaffolds [45]–[47].

Despite the numerous desired qualities, there are some obstacles to consider when using CPs, the primary one being the possibility of chronic inflammation due to their

inability to degrade, which limits *in vivo* applications and may require surgical removal. Additionally, CPs are mechanically brittle and present poor processability. On that account, CPs and biocompatible biodegradable polymers have been combined into composites. CPs can also be synthesized as hydrogels or nanofibers through electrospinning. So far, the most widely studied CPs have been PPy, PANI and PEDOT [40], [45], [47].

2.3.1 Polypyrrole

From the three polymers, PPy is the most studied and is already used as a cytocompatible biomaterial for neural TE scenarios, neural probes and NGCs [45]. Langer et al. showed that the electrically CP, oxidized PPy, is suitable for *in vitro* nerve cell culture and *in vivo* implantation, by observing a 90% increase in neurite length of PC-12 cells cultured on PPy scaffolds and subjected to ES compared to unstimulated cells. These results were obtained comparing neurite length in a culture subjected to a potential of 100 mV for 2 hours, and a culture without any ES, with same scaffold conditions [15].

In a similar study, Xu et al. fabricated a conductive composite based on PPy and PLA that was used as a NGC to bridge a rat sciatic nerve injury with results equivalent to using an autologous nerve graft, the gold standard procedure. *In vitro* tests were also performed by applying a potential of 100 mV for 2 hours to PC-12 cells seeded on the produced conduits. Results revealed more and longer neurites in the stimulated group compared to the unstimulated control cells. Another interesting observation, represented in Figure 2.10, is that, in the stimulated groups, the number of neurite-bearing cells and median neurite length increased with PPy composition [48].

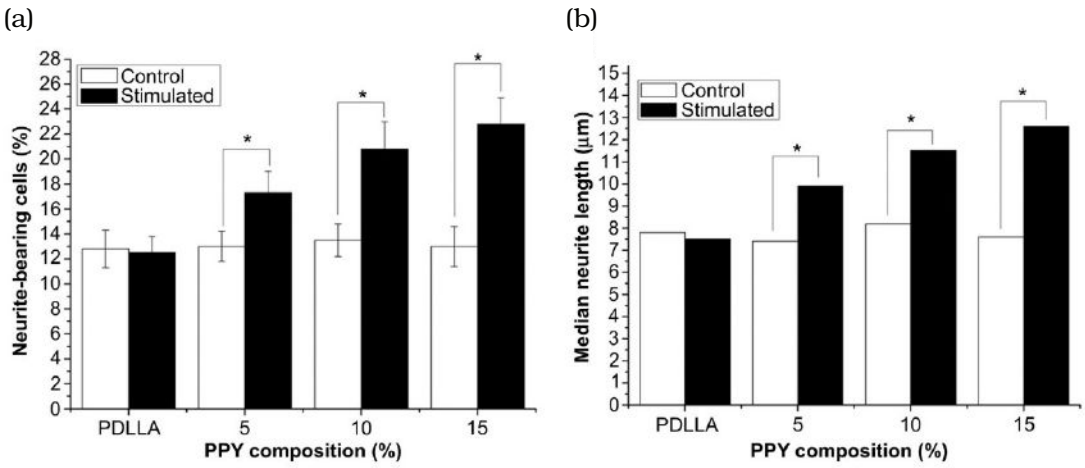

Figure 2.10: Influence of PPy and ES on neural differentiation of PC-12 cells: (a) Percentage of neurite-bearing PC-12 cells on PPy/PLA composite films with varying PPy composition; (b) Median neurite length on the same composite films. Adapted from [48].

2.3.2 Polyaniline

The second polymer, PANI, presents a good range of electrical conductivity and chemical stability at a low cost and has shown potential for neural TE applications in studies with and without ES of cells. However, in order to ensure adequate biological properties this polymer is commonly grafted with biocompatible and biodegradable polymers [49], [50].

Fan et al. evaluated the potential use of PANI for nerve regeneration without ES. The group developed conduits made of PANI and regenerated cellulose (RC), surgically introduced them in rats with defected sciatic nerves and found that PANI contributed to the regeneration process through the regulation of SC. At the functional level, the PANI/RC group exhibited better motor recovery, compared to the RC group. At the cellular and molecular level, the PANI/RC group also stood out, as a greater number of SCs and better axon regeneration with thicker myelin sheaths, together with pronounced levels of BDNF and ciliary neurotrophic factor (CNTF) were observed [51].

Considering ES, Thrivikraman et al. revealed that human MSCs, cultured in a PANI substrate, differentiated into neural-like cells when stimulated, intermittently, with an electrical field of 100 mV/cm. PANI substrates were prepared with different concentrations of dopant, as higher concentrations leads to an increase in conductivity. As shown in Figure 2.11, as conductivity increases, so does cell extension of human MSCs exposed to the same ES conditions. The contrary effect was observed for cell density, which decreased with dopant concentration [52].

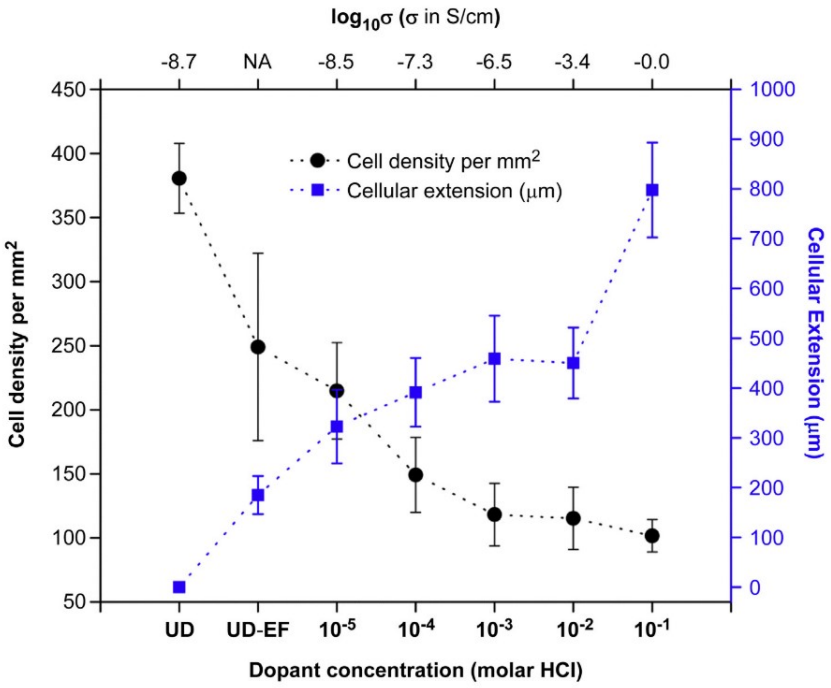

Figure 2.11: Variation of cell density and cellular extension of human MSCs with dopant concentration on PANI films, after 7 days of stimulation, 10 min/day, with 100 mV/mm. Adapted from [52].

2.3.3 Poly(3,4-ethylenedioxythiophene)

Lastly, PEDOT, constitutes the most popular polythiophene derivative and was shown to be more electrochemically stable comparing to the previously described CPs, PPy and PANI. Besides that, PEDOT has low intrinsic cytotoxicity, making it suitable for use as an electrode or scaffold component for ES in neural TE [45], [46].

Bolin et al. produced PEDOT coated eletrospun poly(ethylene terephthalate) (PET) nano-fibers deemed suitable for use as a substrate for cell attachment and proliferation. The PEDOT coating was achieved by VPP using FeTos as oxidant, turning the PET nano-fibers super-hydrophilic. SH-S5Y5 neuroblastoma cells were cultured on the coated nanofibers showing good adhesion and proliferation with actin cytoskeleton and neurite formation. Then, ES tests were carried out through the application of 3 V to the cultured cells using a DC power supply. This led to Ca^{2+} influx to the cells by activation of voltage operated calcium channels (VOCCs). Overall, this study showed the potential of PEDOT coated PET nano-fibers to be used as 3D electrodes for the ES of cultured cells [53].

In another study, Pires et al. introduced a cross-linked polymer mixture of PEDOT and polystyrene sulfonate (PSS) in their approach. It was shown that the application of a pulsed DC electrical field through such polymer mixture resulted in significant increase in differentiation of NSCs towards neurons and neurite elongation, compared to a scenario without ES [54]. More recently, Tsai et al. demonstrated that the chemical and topographical cues from aligned poly(ethylene oxide) (PEO)/PEDOT:PSS nanofibers were suitable for PC-12 cell adhesion and induced neurite elongation, in the direction of the fibers, without ES. Neuronal differentiation was assessed by the expression of the markers Nestin and Tuj1, which was higher in aligned rather than randomly oriented fibers (see Figure 2.12). The latter effect was further increased when cells were also exposed to ES, showing that a combined approach using a conductive substrate and ES is the most effective strategy for growth and differentiation of PC-12 [55].

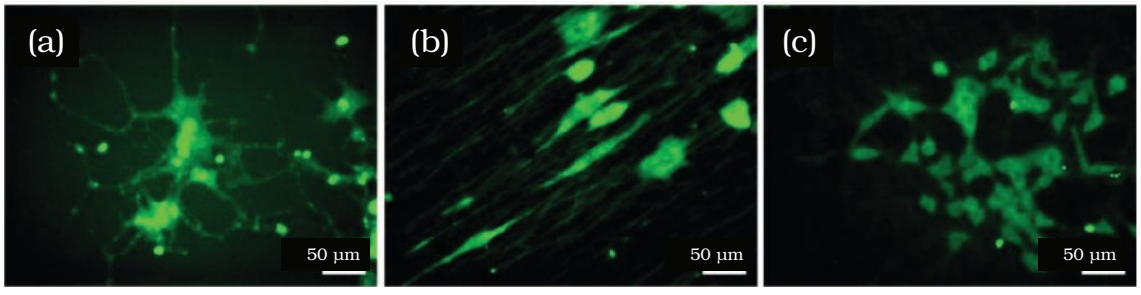

Figure 2.12: Immunofluorescent staining of PC-12 cells with Tuj1 (green) after 5 days of differentiation on: (a) a tissue culture plate; (b) aligned PEO/PEDOT:PSS nanofibers; (c) randomly oriented PEO/PEDOT:PSS nanofibers. Adapted from [55].

A summary concerning the neural TE studies *in vitro* that were described, as well as details from other important ones that were not mentioned can be found in Table 2.1.

Table 2.1: Summary of neural TE studies *in vitro* using ES and CPs.

Scaffolds	Electrodes	Cells	ES protocol	Results	Reference
PPy film	Anode: PPy film; cathode: Au wire	PC-12	DC: 100 mV, 2 h	90% increase in neurite length and enhanced cell spreading	[15]
PPy/PLA film	Unspecified	PC-12	DC: 100 mV, 2 h	More and longer neurites; number of neurite-bearing cells increases with PPy composition	[48]
RC/PPy	Anode: Pt nanoparticles; cathode: carbon nanotube (CNT)	Dorsal root ganglia cells	Self-powered system	Neurite outgrowth comparable to the effect of exogenous 50 mV/mm	[56]
PPy/chitosan membrane	Pt	SCs	DC: 100 mV/mm, 4 h	Increased neurotrophin secretion (nerve growth factor (NGF) and BDNF)	[57]
PLA/PPy fibers coated with extracellular matrix (ECM) components	Unspecified	PC-12	DC: 100 mV/cm, 2 h/day, 1,3 or 5 days	Increased cell adhesion rate, neurite-bearing cell rate, neurite extension and alignment rate	[58]
PPy/PCL nanofibers	Ag	PC-12	Monophasic pulses: rectangular wave, 40 mV, 30 min	Increased expression of neurofilament 200 and tubulin; not cytotoxic	[59]
PPy/poly(l-lactic acid-co-ϵ-caprolactone) (PLCL) nanofibers	Unspecified	PC-12	DC: 100 mV/cm, 4 h/day, 7 days	Significantly extended neurite outgrowth and increased cell proliferation	[60]
PANI/PG nanofibers	Anode: Ag; cathode: Pt	NSCs	DC: 100 mV/mm for 15, 30, and 60 min.	Enhanced cell proliferation and neurite outgrowth	[8]
PANI film	316L-stainless steel	human MSCs	DC: 100 mV/cm, 10 min/day, 7 days	Differentiation into neuronal-like cells; increased cell extension with dopant concentration	[52]

Table 2.1 continued from previous page

Scaffolds	Electrodes	Cells	ES protocol	Results	Reference
PVA/PEDOT	316-stainless steel	rat MSCs	DC: 100 mV/mm, 2 h/day, from day 10 to day 13	Increased expression of Tuj1, Nestin and Enolase	[23]
PET/PEDOT nanofibers	PET/PEDOT nanofibers	SH-SY5Y	DC: −3 V	Formation of an actin cytoskeleton and neurite outgrowth; activation of VOCCs	[53]
PEDOT:PSS	Au	NSCs	Monophasic pulses: 1 V/cm, 100 Hz	Differentiation in higher percentages of neurons and longer neurites; not cytotoxic	[54]
PEO/PEDOT:PSS	PEO/PEDOT:PSS	PC-12	Biphasic pulses: 100 mV/cm, 100 ms pulses, 5 Hz, 1 h/day, 5 days	Neurite extension along the fiber axis; increased expression of Nestin, Tuj1 and MAP2	[55]
PEDOT/PSS film	PEDOT/PSS film	human NPCs	Monophasic pulses: square-waves, 1 V, 100 Hz, 12 h/day, 8 days	Increased gene expression of Nestin and MAP2	[61]
PVA/alginate	Anode: Ag, cathode: Pt	PC-12	DC: 100 mV/mm for 60 min	Increased cell proliferation	[22]
poly(L-lactic-co-glycolic acid) (PLGA)/graphene oxide (GO)	Pt	NSCs	Monophasic pulses: square-waves, 100 mV, 100 Hz, 50% duty-cycle, 3 days	Increased proliferation and neurite elongation; promoted differentiation into neurons, inhibited differentiation into astrocytes	[62]
PCL	Ag	mouse MSCs	Monophasic pulses: 0.33 V/cm, 2.5 ms pulses, 4 Hz, 5 min, days 3-5 and 8	Increased expression of Nf-M, SYP, and GAD	[24]
Carbon nanofibers	Pt	mouse NSCs	Biphasic pulses: 100 µA, 100 µs pulses, 100 Hz, 24 h	Enhanced neural differentiation; upregulation of neural gene expression	[63]
CNT-multilayered film	Inert carbon	NSCs	Monophasic pulses: 1 mA, 20 Hz, 2 h/day, days 3-5	Increased expression of mature neuronal markers (Tuj1 and MAP2) and neurite outgrowth; higher concentration of BDNF; autophagy regulation	[64]

Table 2.1 continued from previous page

Scaffolds	Electrodes	Cells	ES protocol	Results	Reference
hyaluronic acid (HA)/CNT nanofibers	Cu	Chick embryo lumbar dorsal root ganglia cells	Biphasic pulses: charge balanced square-waves, 200 mV/mm, 25 ms pulses, 20 Hz, 50% duty-cycle, 30-60 min	Longer neurites and increased number of neurite bearing cells	[65]
poly(p-dioxanone) (PPDO)/CNT nanofiber yarns	Pt	rabit SCs	DC: 5-500 mV/mm, 1 h/day, 7 days	500 mV/mm leads to cell apoptosis; 5, 50 and 100 mV/mm leads to upregulation of SC-related gene expression	[66]
Carbon/laminin thin film	Carbon/laminin thin film	NSCs	Monophasic pulses: 1-10 µA/cm^2, 1 ms pulses, 10-15 pulses, spaced 1-10 s intervals	Films were deemed appropriate for differentiation and ES of NSCs	[67]
Iridium oxide film	Pt	PC-12	Biphasic pulses: 60 mV/mm, 100 µs pulses, 100 Hz, 6 h/day, 3 days	Very well aligned and extended neurites along the direction of ES	[68]
Silk fibroin nanofibers	Ti	conjuctiva MSCs	AC: 115 V/m, 100 Hz, 10 min/day, 7 days	Higher expression of Tuj1, MAP2 and Nestin; less cytotoxic than the same ES but at 0.1 Hz	[69]
-	Pt	NSCs	DC: 0.53 or 1.83 V/m, 10 min/day, 2 days	Mature neuron morphology and growth cone formation; expression of Tuj1 and NeuN	[70]
-	Pt/Ir	Spiral ganglion cells	Biphasic pulses: 0-2 mA, 10-400 µs pulses, 1 kHz, 24 h	Decreased to no cell survival; unaltered or shorter neurite length	[71]
-	ITO	Mouse retinal progenitor cells	Monophasic pulses: square-waves, 5 V, 1 ms pulses for every 100 ms, the first 3 s of every min, 3 days	Increased expression of Tuj1	[72]

Table 2.1 continued from previous page

Scaffolds	Electrodes	Cells	ES protocol	Results	Reference
-	Ag/AgCl	NPCs	DC: 115 V/m, 1.5 h	Directional migration in a calcium dependent manner; differentiation into neurons	[73]
-	ITO	PC-12	AC: 100 mV/mm, 100 Hz, 2 h	NGF-induced neurite outgrowth	[74]
-	ITO	fetal NSCs	Biphasic pulses: 8 µA/cm^2, 200 µs pulses, 100 Hz, 4 days	Twice the number of cells of control	[26]
			Biphasic pulses: 4 µA/cm^2, 200 ms pulses, 100 Hz, 7 days	Increase in expression of Tuj1, NeuN, and MAP2	
PPy:dodecylbenzenesulfonate (DBS) films	Working electrode: Au, mesh counter electrode: Pt, reference electrode: Ag/AgCl	human induced pluripotent stem cells (iPSCs)	Biphasic pulses: 0.1 µA/cm^2, 100 µs pulses, 8 h/day, 3 days followed by 0.25 µA/cm^2, 100 µs pulses, 8 h/2 days, 6 days	Downregulation of pluripotency markers; increased expression of endodermal, mesodermal and neuroectodermal markers	[75]
-	-	rat SCs	EMF: 1 mT, 50 Hz, 1 h/day, 7 days	Increased cell proliferation and expression of S100 and BDNF	[36]
-	-	embryonic and ischemic mice brain NPCs	EMF: 0.4 mT, 50 Hz, 16 and 24 hours	Increased cell proliferation	[37]
			EMF: 0.4 mT, 50 Hz, 7 days	Increased expression of Tuj1	
-	-	rat cerebral granule cells	EMF: 1 mT, 50 Hz, 10-60 minutes	Time dependent increase in voltage activated Na^{2+} channel currents	[38]
-	-	NPCs	EMF: 1 mT, 50 Hz, for up to 12 days	Differentiation toward the neuronal phenotype and active promotion of neurogenesis	[39]
-	Agar-salt bridge system with Ag/AgCl electrodes	NPCs	DC: 437 mV/mm, 16-24 h/day, 6 days	Increased expression of Tuj1 and cell alignment	[42]
-	Agar-salt bridge system with Ag/AgCl electrodes	NPCs	DC: 250 mV/mm, 2.5-8 h	Cathodic migration of undifferentiated cells	[43]

Table 2.1 continued from previous page

Scaffolds	Electrodes	Cells	ES protocol	Results	Reference
-	Agar-salt bridge system with Ag/AgCl electrodes	NPCs	Biphasic monopolar, charge balanced, cathodal amplitude: 3 mA (500 µs), anodal amplitude: 0.75 mA (3000 µs)	Cathodic migration of undifferentiated cells	[44]
-	Agar-salt bridge system with Ag/AgCl electrodes	NPCs	Monophasic pulses: 300 mV/cm, 50% duty-cycle, 100 Hz, 2 days	Presence of elongated processes and enhanced expression of Nestin; differentiation into astrocytes, neurons and oligodendrocytes	[76]
-	Agar-salt bridge system with Cu electrodes	*Xenopus laevis* neuronal cells	AC: rectangular waves, 80% duty-cycle, 1 kHz	Longer neurites; preferential cathodal growth	[77]
-	Agar-salt bridge system with Pt electrodes	SCs	DC: 50 mV/mm, 8 h	Sustained increase in neurite outgrowth; cell alignment parallel to the electrical field	[6]

2.4 Effects of Electrical Stimulation *In Vivo*

In vivo research has been employing ES and/or CPs with promising results regarding functional recovery in animal models of PNI and SCI. Mendonça et al. applied low intensity DC to a rat model of crush injury of the sciatic nerve, showing improved functional recovery in groups with ES, in contrast with unstimulated groups. The group also hypothesized that such results were due to three factors: delay of axonal degeneration; nerve sprouting stimulation; and faster remyelination [78].

More recently, Shapira et al. reported faster improvements in locomotor function in rodents with neuroma-in-continuity injury subjected to brief ES. Furthermore, as presented in Figure 2.13, there was a significant difference in the percentage of neural tissue after neuroma-in-continuity, favouring the group subjected to brief ES compared to the unstimulated group. It was also noted that the application of brief ES may have influenced the reinnervation of axons towards a predominantly motor rather than a sensory nerve [79]. In another study, functional ES considerably augmented cell birth in the lumbar spinal cord of rats with chronic SCI [80].

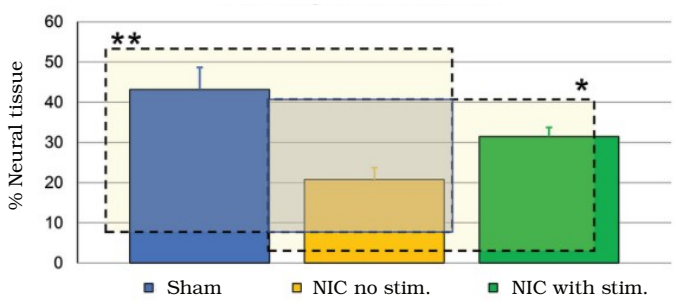

Figure 2.13: Influence of brief ES applied immediately after surgery, 14 weeks after neuroma-in-continuity in rats. This graphic represents the percentage of neural tissue in three groups: rats subjected to sham surgery, rats with neuroma-in-continuity with no ES post-surgery and rats with neuroma-in-continuity subjected to brief ES post-surgery. Adapted from [79].

Regarding neural TE, previous studies have been consistently displaying the beneficial effects of ES for both PNS and CNS regeneration following injury [20]. However, the mechanisms by which such stimulus induces a positive effect are still controversial and ideal settings for delivery of ES (stimulation parameters and setup and conductive scaffolds) are yet to be established, and standardized, supporting the need for further investigation.

A summary concerning the neural TE studies *in vivo* that were described, as well as details from other important ones that were not mentioned can be found in Table 2.2.

Table 2.2: Summary of neural TE studies *in vivo* using ES and CPs.

Scaffold	Electrodes	Animal Model	ES protocol	Results	Reference
PPy/PLA	-	Rat sciatic nerve injury	-	Performance similar to an autologous nerve graft, the current gold-standard, 3 and 6 months after surgery	[48]
PANI/RC hydrogel	-	Rat sciatic nerve injury	-	Larger axon diameter and thickness of myelin sheet; enhanced nerve regeneration	[51]
PCL nanofiber conduit filled with NSCs	Unspecified	Rat sciatic nerve injury	Monophasic pulses: 3 V, 100 µs pulses, 20 Hz, 1 h	Comparable to autologous nerve graft treatment 6 and 12 weeks after surgery and ES; enhanced locomotion, increased muscle weights, and increased myelinated axons	[81]
-	Stainless steel embedded in epoxi resin	Rat sciatic nerve crush injury	DC: 1 mA, for 3 weeks	Enhanced nerve regeneration; Intact nerve on the 21st postoperative day with ES; 23% higher nerve fiber density compared to normal	[78]
-	Unspecified	Rat neuroma-in-continuity injury	Monophasic pulses: 3 V, 0.1 ms pulses, 20 Hz, 1 h	Faster behavior and eletrophysiological recovery	[79]
-	Stainless steel	Rat SCI	Monophasic pulses: 3 V, 200 µs pulses, 20 Hz, three times daily, 1 hour, 1 s stimulation, 1 s rest	82-86% increase in cell birth in the lumbar spinal cord	[80]
-	-	Rat mental nerve crush injury	EMF: 50 Hz, 1 h/day, three week exposure	Higher count of axons, compared to other ES conditions; enhanced peripheral nerve regeneration	[36]

3

Materials and Methods

The present chapter sequentially details the materials necessary, and methods performed for achieving each task. Firstly, I describe the cell culture assays conducted to optimize the neural differentiation protocol. Secondly, the design and assembly of the bioreactor are detailed. Then, I expound on the fabrication methods utilized for obtaining a conductive surface, to be fixed on the bioreactor, and on which cells were seeded for the ES test. Finally, I explain how the main task of this dissertation was achieved, which concerned the ES assay performed for the sake of testing the bioreactor and improving the current knowledge on the role of ES in altering cell behaviour.

3.1 Optimization of Differentiation Protocol

Neuronal differentiation of cells can be achieved through several methods *in vitro*, including keeping cells in culture medium containing differentiation factors until they begin to express neuronal differentiation markers and display a morphology resembling that of neuronal cells [82]. In this regard, the composition of the differentiation medium and overall protocol were optimized in a standard 48-well cell culture plate.

All cultures were performed using cells from the SH-SY5Y cell line, a thrice-cloned sub-line of the neuroblastoma cell line SK-N-SH, derived from a bone marrow biopsy of a four-year-old human female [83], [84]. This cell line presents a set of characteristics favouring its extensive use as an *in vitro* neuron model for neuroscience studies over the use of primary neurons. Some advantages are the ability for large-scale expansion at a low cost, the avoidance of ethical concerns intrinsic to utilizing primary human neurons and the ability of expressing various human-specific genes that mark for neuronal differentiation, among others [82].

The literature review on the distinct medium compositions and protocols utilized for inducing neuronal differentiation was performed, given that a vast number of studies has already been conducted on this topic. The main results from the review can be found in Appendix A, and were essential in selecting the medium compositions and protocol details tested. The most abundantly used means for inducing differentiation of

SH-SY5Y neuroblastoma cells has been adding RA to the culture medium, a vitamin A derivative that is also responsible for inhibiting cell proliferation. This was the chosen differentiation agent for this task. Other less used agents include phorbol esters, dibutyryl cyclic adenosine monophosphate (cAMP), and growth factors [85]. It is also common to use a combined treatment with more than one agent, typically in separate days of the culture [86], [87].

Following, the details on the cultures performed, from the preparation of the cells to the specific protocols and conditions utilized for inducing and assessing SH-SY5Y neuronal differentiation are specified.

3.1.1 SH-SY5Y Proliferation and Subculture

The preparation of the cell cultures included thawing cell vials, stored at −80 °C, and culturing the thawed cells in T25 flasks (see Figure 3.1), following protocol B.1.1. To promote cell proliferation, SH-SY5Y cells were maintained in complete DMEM, i.e., DMEM low glucose with stable glutamine and sodium pyruvate (DMEM Low, Sigma Aldrich), supplemented with 10% v/v FBS (Invitrogen) and 1% v/v penicillin/streptomycin (Invitrogen) and incubated at 37 °C under 5% CO_2. Hereinafter, DMEM Low with 1% v/v penicillin/streptomycin is referred to as DMEM. Cells were passaged at approximately 90% confluency and medium was replaced every 48 hours, following the protocols B.1.3 and B.1.5, respectively. Cells were utilized at passages 27-33. All the described culture and subculture procedures were performed inside a biological safety cabinet (Labculture®Class II) for sterile work.

Figure 3.1: Example of a T25 cell culture flask used for SH-SY5Y cell proliferation.

3.1.2 SH-SY5Y Neuronal Differentiation

All the cultures performed for neuronal differentiation of SH-SY5Y cells followed the same general protocol (see Figure 3.3). Initially, cells were seeded at different densities in either a 24 or 48-well plate (see Figure 3.2) and kept in proliferative medium, consisting of DMEM with 10% v/v FBS and 1% v/v penicillin/streptomycin, for 24 hours prior to the onset of the induction of differentiation. The following procedure consisted in replacing the proliferative medium by a low-serum differentiation medium with RA

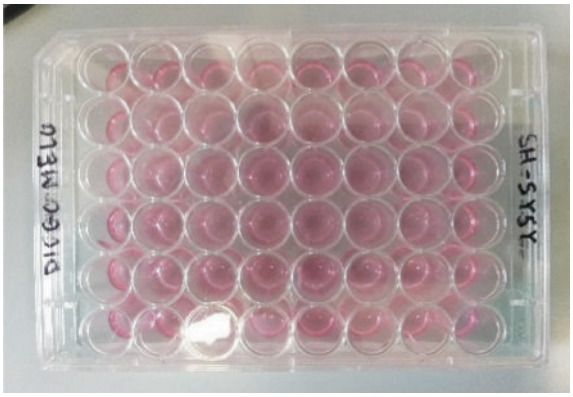

Figure 3.2: Example of 48-well plate used for neuronal differentiation of SH-SY5Y neuroblastoma cells.

(changed every 48 hours). Here, the goal was to let the cells adhere to the bottom of each well and then expose them to a variety of different medium compositions that led to both, a significant decrease in proliferation and induction of differentiation of cells to a more mature neuronal phenotype by exhibiting extensive neurite outgrowth. The evolution of cell morphology was recorded by using an inverted microscope (Eclipse Ti-S, Nikon) to photograph the cultures before each medium change, for future assessment. The cell cultures were kept at 37 °C and 5% CO_2 conditions.

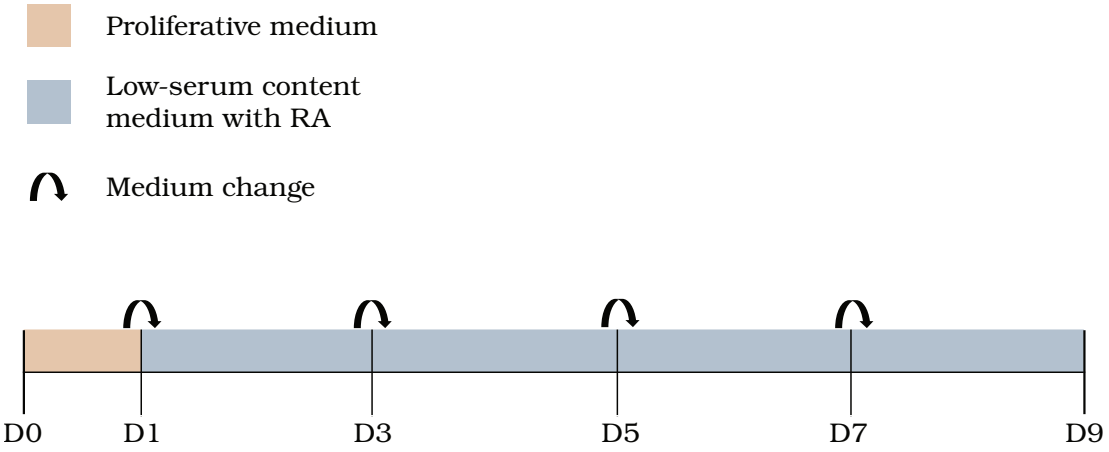

Figure 3.3: Diagram of the overall protocol followed for inducing neuronal differentiation of SH-SY5Y neuroblastoma cells.

In accordance with what was found in the literature review, the protocols tested consisted in a combination of DMEM with RA in different concentrations and a low-serum content. Other protocol specifications were also defined, including initial cell density, time of exposure to initial proliferation medium, frequency in which differentiation medium was changed, v/v % of DMSO in DMEM and the total time of exposure to the differentiation medium. Next, I explain the reasoning behind the chosen parameters.

As previously mentioned, RA was the chosen differentiation agent used in this task.

In the literature, this agent was found to be commonly used at a concentration of 10 µM in the culture medium [82]. However, some studies have reported effective differentiation with RA at a concentration of 5 µM and so, both concentrations were considered [88].

The other aspect related to inducing differentiation is reducing the serum content of the medium. The v/v % FBS should be low enough so that proliferation is decreased favouring differentiation, however it shouldn't be so low that it leads to significant cell death. Accordingly, three values were selected: 5% v/v FBS, 3% v/v FBS [89] and 1% v/v FBS [90] in DMEM.

Regarding initial cell density, values between 1×10^3 and 1×10^5 cells/cm^2 were successfully used in neuronal differentiation of SH-SY5Y cells [82], [91]. Accordingly, the chosen values for the final cell culture assay were 2×10^3 and 1×10^3 cells/cm^2. All the medium compositions enumerated bellow were tested with an initial cell density of 2×10^3 cells/cm^2, in cells seeded in both the bottom of the wells and onto coverslips placed in the wells. This allowed characterizing cell behaviour in two distinct surfaces, one of plastic and another of glass. Two to three replicates of each condition were used for this initial cell density. Furthermore, three replicates were made (with and without coverslip) from conditions 1 and 4, detailed below, with a lower initial cell density of 1×10^3 cells/cm^2.

As previously stated, the differentiation media was refreshed every 48 hours, following protocol B.1.5. The literature on this subject varies, with changing frequency ranging from once a day to once every three days [85], [88], [92].

The preparation of the differentiation medium consisted in adding both an FBS and a RA solution to DMEM, and was performed right before use, since RA in solution is susceptible to oxidative damage with light, air and temperature [93]. The preparation of RA stock solutions encompassed the dissolution of a RA powder in DMSO, as described in protocol B.1.7. This solvent, typically used to solubilize drug molecules, is used in cytotoxicity assays at a concentration in culture medium over 10% v/v to establish positive controls (by causing cell death). For usage in biological assays, it is recommended to keep DMSO under 1% v/v [94]. Therefore, all the media compositions tested for inducing differentiation were prepared at a concentration of 0.5% v/v of DMSO in DMEM. Furthermore, a control group with only DMEM, serum and DMSO at 1% v/v was considered to check for solvent toxicity.

Finally, the total duration of the culture was not defined previously to its onset. The latter was divided in: time of exposure to the proliferative medium (which was 24 hours, as previously mentioned) and time of exposure to the differentiation medium. To get the maximum information possible regarding the morphological evolution of the SH-SY5Y cells with time, the culture was only stopped once differentiation was considered not to be effective or cell death became significant. In this case, it meant a total time of exposure to the differentiation medium of 8 days.

Summing up, the medium compositions tested for inducing neuronal differentiation consisted in DMEM low glucose with stable glutamine, sodium pyruvate and penicillin/streptomycin, with the following supplements (relative concentrations are in v/v):

1. 5% FBS, 10 µM RA;
2. 3% FBS, 10 µM RA;
3. 1% FBS, 10 µM RA;
4. 5% FBS, 5 µM RA;
5. 3% FBS, 5 µM RA;
6. 1% FBS, 5 µM RA.

The composition of the control media consisted in DMEM low glucose with stable glutamine, sodium pyruvate and penicillin/streptomycin, with the following supplements:

7. 5% FBS;
8. 3% FBS;
9. 1% FBS;
10. 5% FBS, 0.5% DMSO;
11. 3% FBS, 0.5% DMSO;
12. 1% FBS, 0.5% DMSO;
13. 5% FBS, 1% DMSO;
14. 3% FBS, 1% DMSO;
15. 1% FBS, 1% DMSO.

The layout of the 48-well plate used for optimizing the differentiation protocol is displayed in Figure B.1.

3.2 Design and Assembly of the Bioreactor

The process of designing a bioreactor should consider several factors, from its ability to perform the desired function to its usability. The two mentioned points are not trivial and can be divided in more aspects such as the choice of materials given the nature of the studies to be performed, the overall dimensions of the setup and its ease of assembly for the scientists that will be conducting research with the bioreactor.

In this case, the goal was to create a chamber with a fixation system for conductive scaffolds on which cells could be seeded. Furthermore, the system should contain electrodes and electrical connectors to support the application of distinct electrical fields along the surface of the scaffold. With this in mind, a literature review was performed on the current setups for ES of neuronal cells and other types of cells and, after discussing the advantages and drawbacks of each design, several attempts were made until the final design of the new setup, which is presented in Figure 3.4, was deemed appropriate for production.

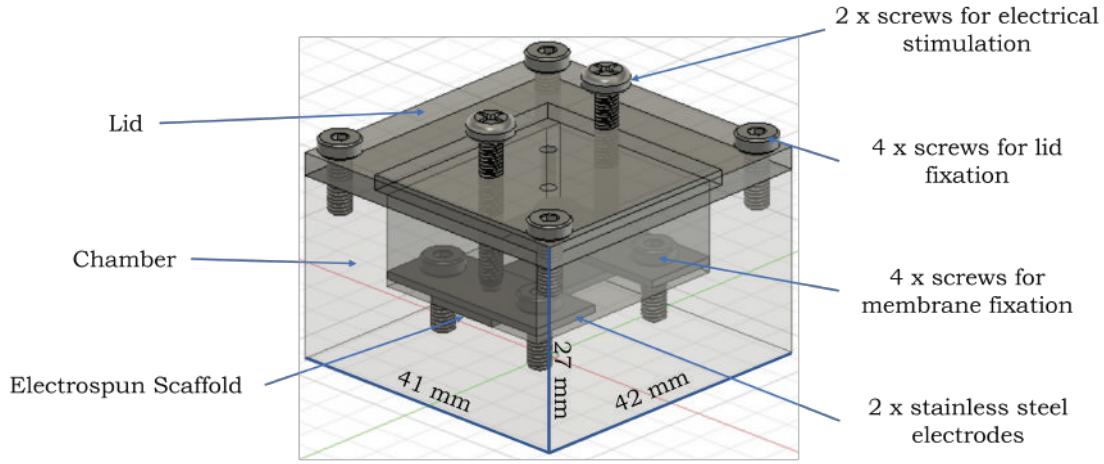

Figure 3.4: Final design of the chamber for ES of neuronal cells. This design was executed using the software Autodesk®Fusion 360^{TM} and was the one chosen for production.

Firstly, the design of the chamber was executed using the software Autodesk®Fusion 360^{TM}, a cloud-based 3D modelling, CAD, CAM, CAE and PCB platform for product design and manufacturing [95]. Then, after the design was approved, both the chamber and the lid were produced by machining of a PMMA block using a milling machine and a mechanical lathe, as presented in Figure 3.5. PMMA is a biocompatible thermoplastic and thus, is suitable for cell culture [96]. This design includes two electrodes made from stainless-steel plates, necessary for fixation of the conductive scaffold, where the cells should be seeded. Moreover, a variety of screws is needed for assembling the chamber, namely four M3 × 12 mm screws for lid fixation, two M2 × 8 mm screws for fixing each electrode to the bottom of the chamber, and finally two M2 × 20 mm screws, screwed in the chamber lid, working as an electrical bridge between the inside and outside of the chamber, as they directly contact the electrodes, when the setup is fully assembled. All the screws are also stainless-steel, a biocompatible and sterilizable metallic material already used in the context of cell culture [23], [97]. Finally, the chamber lid also includes a hole (4.5 mm diameter) meant for fitting a syringe filter. This filter is necessary for securing gas exchanges and, consequently exposing the interior of the chamber, including the cells, to a 5% CO_2 atmosphere, while the chamber is in the incubator. All the components mentioned, necessary for complete assembly of the bioreactor, are shown in Figure 3.6.

Figure 3.5: Production of the chamber and lid of the ES setup: (a) Milling machine and mechanical lathe; (b) Machining of a PMMA block.

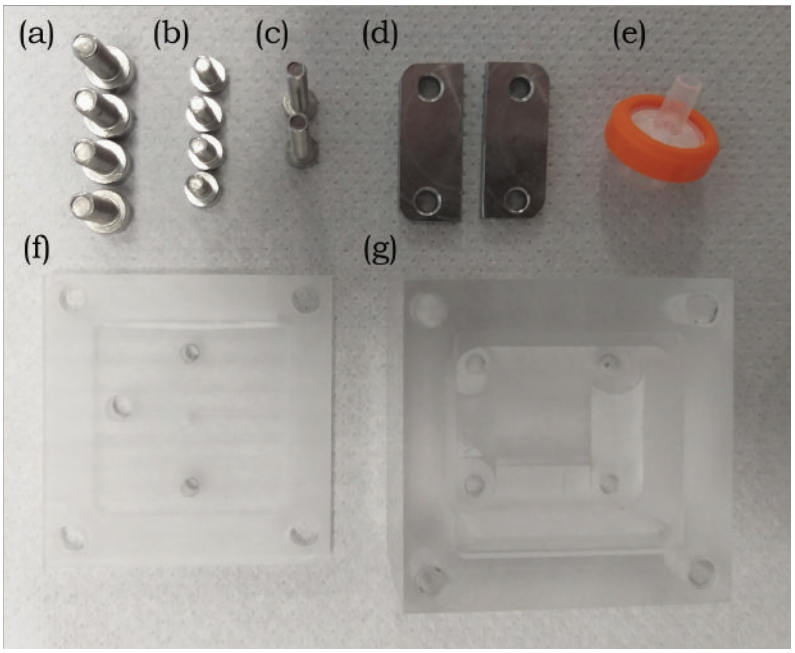

Figure 3.6: Separate components necessary for complete assembly of the bioreactor: (a) Four M3 screws for fixation of the lid to the chamber; (b) Four M2 screws for fixation of the two electrodes to the bottom of the chamber; (c) Two M2 screws working as electrical connectors between the inside and outside of the chamber; (d) Two stainless steel electrodes; (e) Syringe filter for gas exchanges; (f) PMMA chamber lid; (g) PMMA cell culture chamber.

There are two main ways for delivering the ES to the cell culture chamber that was produced: a DC power supply or a function generator. The two models used for this dissertation are displayed in Figure 3.7. One way of assembling the setup consists in connecting the two electrodes of either the DC power supply or the function generator to the two screws of the cell chamber lid using crocodile wires. The described way of assembling the bioreactor was used for preliminary testing of its adequacy to the functions to be performed and is depicted in Figure 3.8.

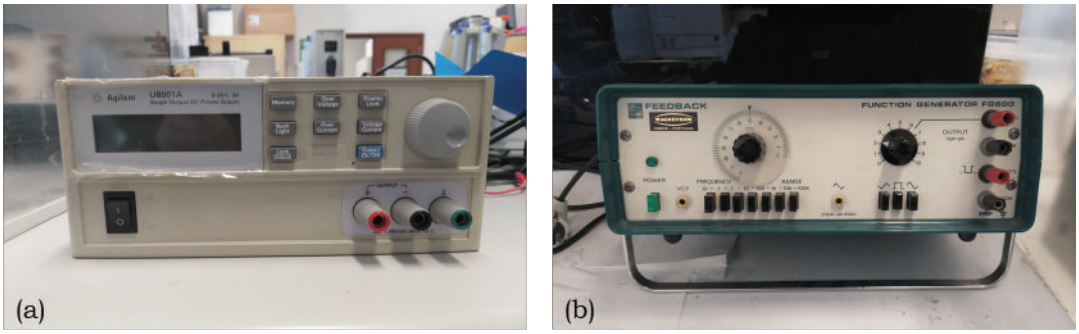

Figure 3.7: Devices used for applying distinct electrical fields to the cell culture chamber: (a) Agilent U8001A Single Output DC Power Supply; (b) Feedback FG601 Function Generator.

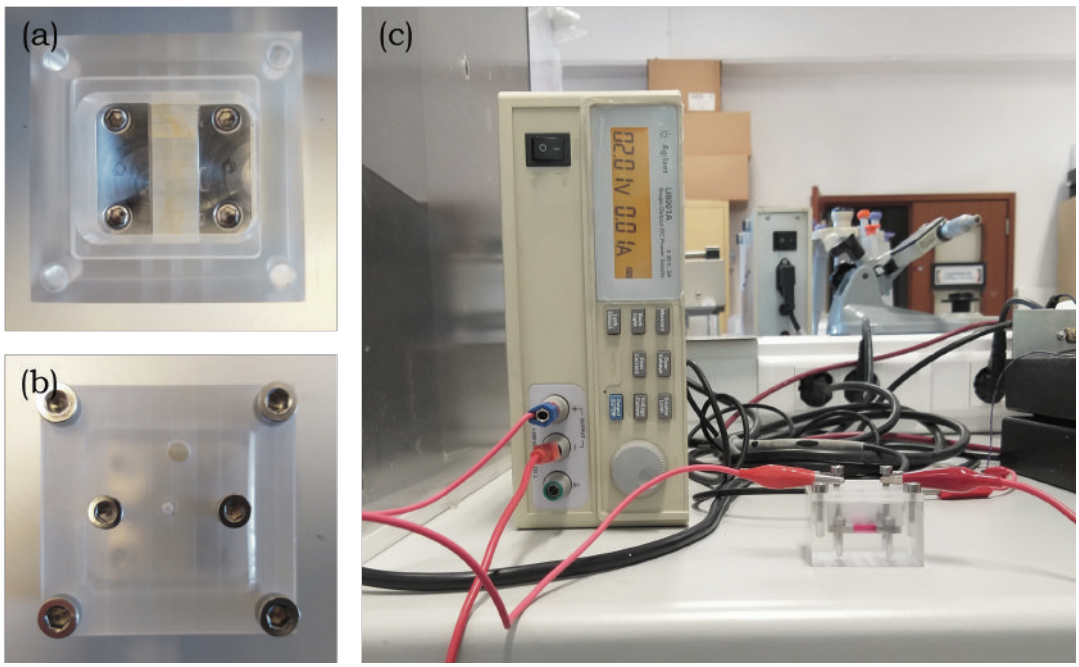

Figure 3.8: Assembly of the ES setup for preliminary testing: (a) PMMA chamber with two stainless steel electrodes, screwed to the bottom of the chamber; (b) Lid and chamber assembled using four M3 screws (one in each corner). It also includes two M2 screws, screwed until touching the electrodes at the bottom of the chamber; (c) A DC power supply is connected to the cell culture chamber using cables with crocodile connectors.

3.3 Fabrication of Conductive Scaffolds

During this stage, the focus consisted in fabricating a conductive biocompatible surface on which cells could be seeded for the ES assays. The approach adopted for this step consisted in producing PEDOT coated scaffolds by VPP. The process of VPP itself was the last to be performed and is detailed in section 3.3.6. Firstly, several fabrication methods were tested in order to produce a scaffold suitable to be submitted to VPP, namely film casting, spin coating, dip coating and electrospinning. These methods, as well as the preparation of polymeric solutions is detailed bellow.

Details from the main polymer used for this task, as well as a list, concerning the reagents that were used, can be found in Tables 3.1 and 3.2, respectively.

The general line of thought to produce a suitable scaffold entailed preparing a polymeric solution to which an oxidant solution could be incorporated, either by mixing the two solutions or by other method applied after processing the polymeric solution. All the steps concerning polymeric and/or oxidant solution preparation were performed inside of a fume hood.

Table 3.1: Details from the polymer used for scaffold fabrication.

Polymer	**molecular weight (MW) (kDa)**	**Supplier**
PLA L175	209	Corbion

Table 3.2: Reagents used for scaffold fabrication.

Reagent	**Suplier**
Chloroform (CHL) >99%	Carlo Erba Reagents
N,N - Dimethylformamide (DMF) >99.9%	Carlo Erba Reagents
Ethanol (EtOH)	LabChem

3.3.1 Polymer Solutions

The main polymer used in this task was PLA L175, a biocompatible homopolymer with a high melting point (necessary for the VPP) [98]. PLA solutions were prepared in four different wt/wt percentages, using CHL as polymer solvent: 6%, 8%, 10% and 12%. Solutions were subjected to constant magnetic stirring overnight before use.

FeTos (ChemCruz) powder was used as oxidant and was prepared using DMF and EtOH as solvent. Once joined, the dissolution process was aided with a spatula until complete dissolution. The solutions were then stored at −4 °C until use.

PLA/FeTos solutions were then prepared by mixing the previously described solutions. After transferring the desired amount of oxidant solution to the PLA solutions,

the mixture was left under constant magnetic stirring until use (ideally, until complete homogenization). A variety of PLA:FeTos (wt:wt) ratios were prepared, including 2:1, 2.5:1, 3:1, 6:1, 12:1 and 20:1. A scheme of the steps described is shown in Figure 3.9.

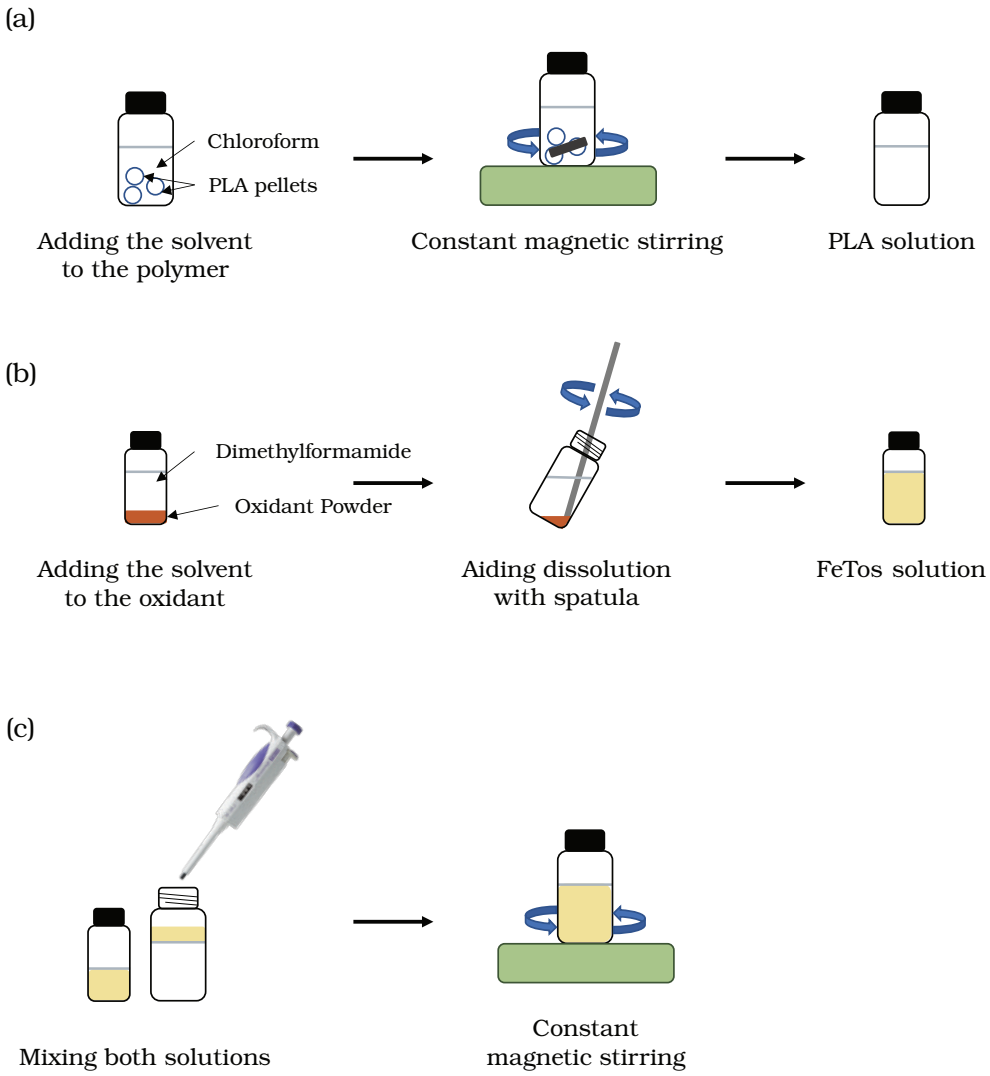

Figure 3.9: Solution preparation scheme: (a) Preparation of a PLA solution; (b) Preparation of a FeTos solution; (c) Preparation of a PLA/FeTos solution.

3.3.2 Film Casting

Film casting was performed by pouring a polymeric solution onto a surface and allowing the solvent to evaporate obtaining a detachable film. Solutions were poured onto acetate sheets or glass Petri dishes and left to dry overnight before attempting their detachment from the surfaces. Once detached, the films were stored in a desiccator, inside identified plastic Petri dishes with lid, until subjected to VPP. A scheme illustrating the film casting method is shown in Figure 3.10.

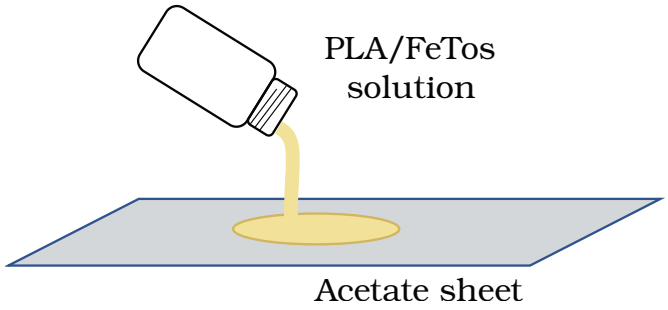

Figure 3.10: Film casting procedure scheme. PLA/FeTos films are being fabricated by pouring the polymeric solution onto an acetate sheet allowing the solvent to evaporate.

3.3.3 Spin Coating

Thin film fabrication was also attempted by spin coating of PLA/FeTos solutions (prepared as described in section 3.3.1) onto acetate sheets and glass coverslips. This technique was performed at 2000 rotations per minute (rpm) for 120 seconds. The apparatus used for this experiments is displayed in Figure 3.11.

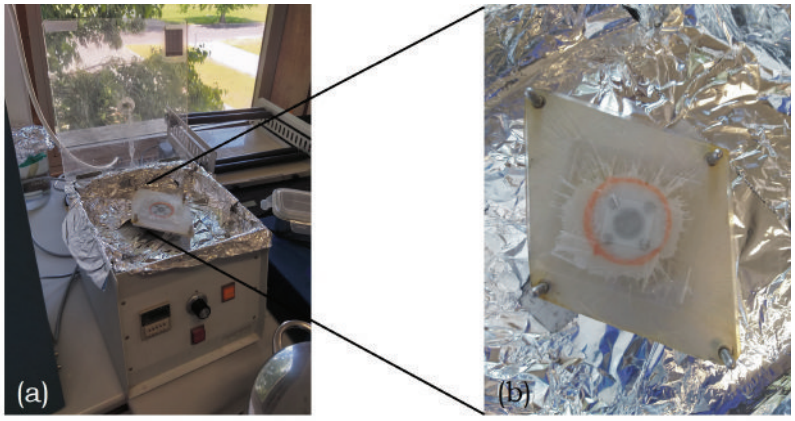

Figure 3.11: Spin coating setup: (a) Spin coater lined with aluminum foil; (b) PLA film spin coated onto a glass coverslip fixed with tape to the rotatory chuck.

3.3.4 Dip Coating

Dip coating was applied by immersing a PLA film into a glass Petri dish containing a wt/wt 40% FeTos solution prepared in EtOH. Then, the sample was removed and left to drain in plastic Petri dishes until dry. This process was performed inside of a fume hood. A scheme of the dip coating process is shown in Figure 3.12.

3.3.5 Electrospinning

The electrospinning technique was used to produce PLA/FeTos scaffolds with aligned nanofibers. The needle tip and the grounded collector were placed at 15 cm from each

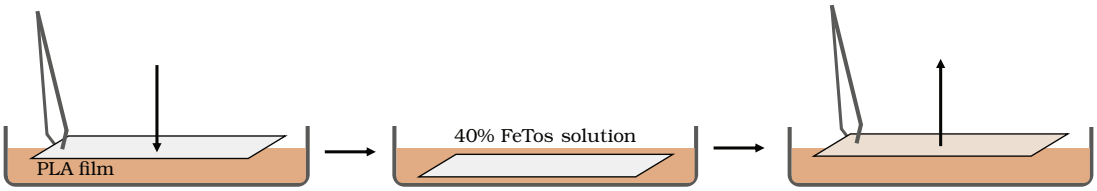

Figure 3.12: Dip coating scheme.

other. A 21G metallic needle was used, and the rate of extrusion was set to 0.5 mL/h, with an applied voltage of 18 kV applied to the needle. The collector consisted in a rotatory mandrel that was set at 3000 rpm to induce fiber alignment. Both room temperature (°C) and relative humidity (%) were registered. The setup used for this task is illustrated in Figure 3.13.

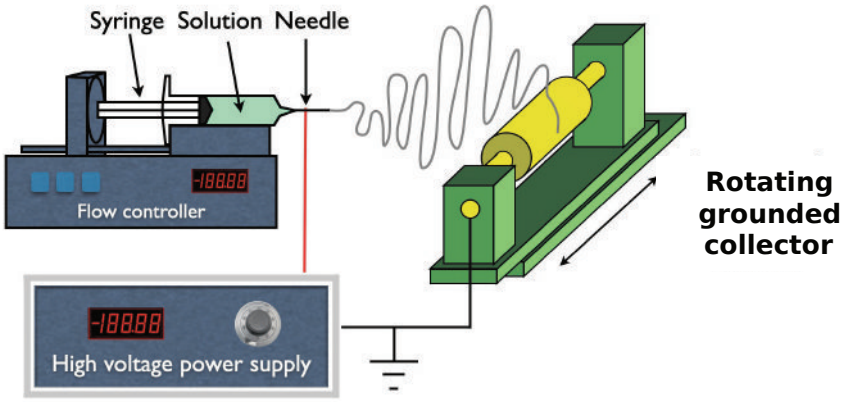

Figure 3.13: Electrospinning setup scheme.

3.3.6 Vapor-Phase Polymerization

There are three main ways of achieving polymerization of CPs: wet chemical oxidation, electrochemical polymerization and VPP. The chosen method for polymerizing EDOT into the pre-made samples was VPP, a technique that consists in exposing an oxidant containing substrate to a monomer in vapor form, allowing polymerization to occur at the oxidant/monomer interface [99]. A scheme of the VPP process is shown in Figure 3.14. The polymerization reaction is described in detail elsewhere [100].

The samples used in this step consisted in PLA electrospun nanofibers and films containing FeTos. Samples from nanofibers, fixed on aluminum foil, were cut the size of the interior of the chamber lid, while films were cut in 3 cm × 1 cm samples using standard scissors or a surgical blade. For each VPP assay, the samples were gently fixed to the chamber lid using tape. Secondly, the lid containing the samples was assembled to a chamber containing an open flask of an EDOT (Acros Organics, 99%) solution. Finally,

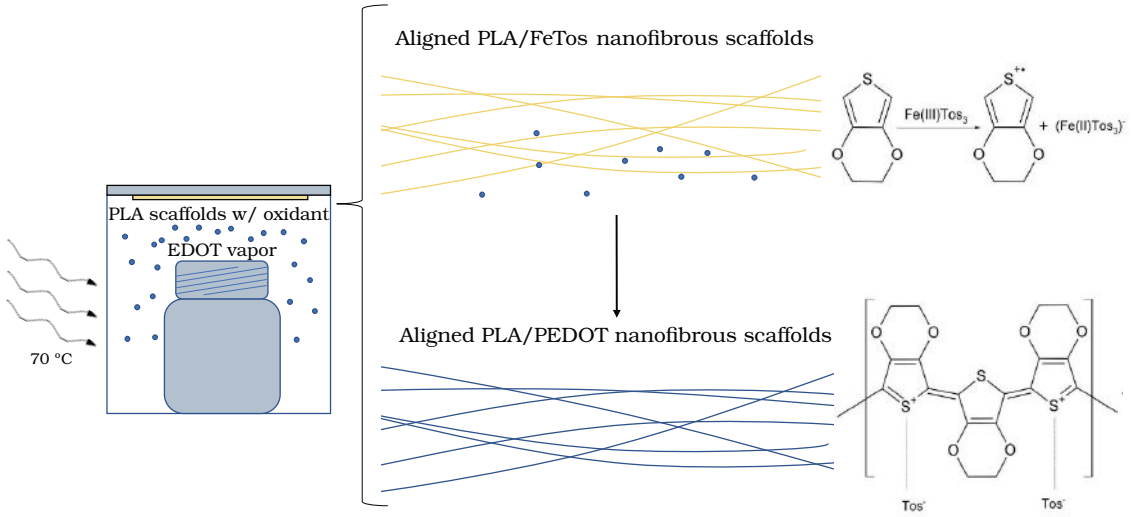

Figure 3.14: VPP chamber scheme. At the monomer/oxidant interface, the EDOT monomers are oxidized by Fe(III), allowing the polymerization reaction to take place. At the end, PLA fibers coated with conductive PEDOT were obtained by this process.

depending on the samples used, VPP was carried out for 2 h, 4 h or 6 h, at 50 or 70 °C. The typical setup used for this task is displayed in Figure 3.15.

After the process was completed, the chamber lid containing the fixed samples was opened inside of a fume hood and the samples were immersed, twice, in a 96% EtOH solution for 20 min. EtOH is a solvent for FeTos, allowing the removal of the unreacted oxidant left in the samples. Finally, the samples were left to dry at the fume hood overnight.

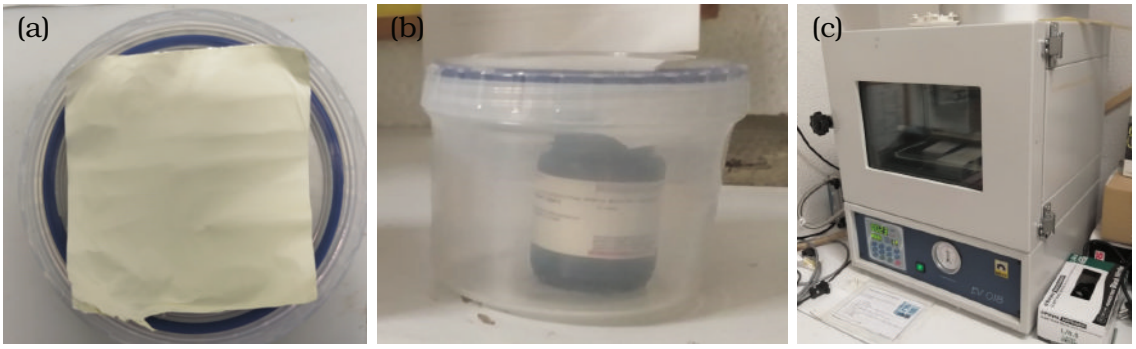

Figure 3.15: Producing conductive PLA/PEDOT fibers by performing VPP of EDOT: (a) PLA/FeTos aligned electrospun fibers fixed with tape at the chamber lid; (b) VPP chamber containing an open flask of an EDOT solution; (c) Oven.

3.3.7 Scanning Electron Miscroscopy

SEM images were obtained using a SEM-focused ion beam (FIB) Zeiss Auriga CrossBeam Workstation and a Hitachi TM 330Plus Tabletop. Samples were coated with a thin layer of iridium, preceding image acquisition.

3.3.8 Electrical Characterization

IV curves were obtained for all the electrospun scaffolds by measuring the current, *I* flowing through the samples fixed in the bioreactor, when applying a voltage, *V* ranging from −1 V to 1 V with 0.1 V steps. The samples were cut with a surface area of 3 cm x 1 cm and so that when mounted in the bioreactor the voltage gradient was set along the preferential direction of fiber alignment (larger side).

The setup used, shown in Figure 3.16, is analogous to a 2-point probe system which allowed obtaining *IV* curves for each sample using a Keithley 6487 Picoammeter/Voltage Source. This device was connected to the bioreactor, in a similar fashion to what is presented in Figure 3.8, and to a computer running a custom made software which produced the *IV* curves. Three measurements were performed in three replicates per material.

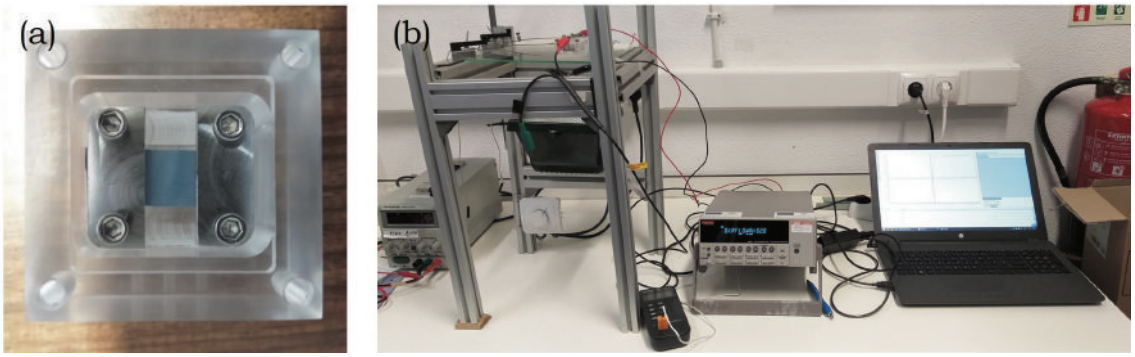

Figure 3.16: Obtaining *IV* curves from the conductive scaffolds: (a) PLA/PEDOT sample fixed with two stainless steel electrodes to the bottom of the bioreactor, establishing two electrical contacts with the sample; (b) Keithley 6487 Picoammeter/Voltage source connected to the bioreactor containing the samples and to a computer.

3.4 Cytotoxicity Assay

This assay was performed in order to assess possible cytotoxic effects of the produced scaffolds on a culture of SH-SY5Y cells. The procedure consisted in applying the extract method, according to the specifications of International Standard ISO 10993-5. The first step, extract preparation, consisted in sterilizing pre-weighted samples of each scaffold in EtOH 70% v/v for 20 min and letting the samples dry overnight in the sterile environment of the biological safety cabinet. Secondly, the sterilized samples were immersed in growth medium (DMEM + 10% v/v FBS + 1% v/v penicillin/streptomycin), at a concentration of 15 mg/mL and incubated for 48 h inside an incubator at 37 °C. SH-SY5Y cells were cultured on a 96-well plate at 2×10^4 cells/cm^2. After 24 h of incubation, growth medium was replaced by the medium conditioned by the extracts, prepared in four different concentrations: initial concentration and three dilutions of a factor of 2, as depicted on the layout of Figure B.2. Lastly, after 48 more hours of incubation, cell viability was assessed by performing a resazurin assay, as detailed in protocol B.1.8. The resazurin

assay had three control groups: a live-cell group (C-), with cells kept in culture media; a dead-cell group, with cells exposed to 16% v/v DMSO in culture media (C+); and the media control (CM), composed only of culture media.

3.5 SH-SY5Y Growth on Materials

This task was performed to assess how SH-SY5Y cells behave when cultured on the produced materials while exposed to RA. Cells were cultured on samples of two different types of electrospun nanofibers placed in custom-made *teflons* inserts, with a culture area of 0.5 cm^2 and using a working volume of 200 µL, following the 24-well plate layout displayed on Figure B.3. At first, cells were seeded at 4×10^3 cells/cm^2 with DMEM + 10% v/v FBS + 1% v/v penicillin/streptomycin and incubated for 24 h. Subsequently, cells were exposed to DMEM + 3% v/v FBS + 1% v/v penicillin/streptomycin + 10 µM RA, with medium being changed every 48 h. Cells were fixed at three different times, namely 5, 9 and 13 days after cell seeding, which corresponds to 4, 8 and 12 days of exposure to the low-serum DMEM with 10 µM RA, allowing for a temporal evaluation of cell behavior on the materials. Fixation and staining for fluorescence imaging of the samples was performed as described in protocols B.1.9.1 and B.1.9.2, respectively. The control for this experiment consisted in cells cultured on coverslips placed in the *teflons* inserts, cells cultured on the bottom of the wells and cells cultured on a coverslip placed at the bottom of the wells. Two samples of each condition were made.

3.6 Electrical Field Induced Medium Alterations

Before subjecting the cells to an electrical field, it was necessary to consider possible alterations that may occur in the culture medium upon the application of such field.

As such, as a means to study the occurrence of undesired electrochemical reactions, and thenceforth establish a safe ES protocol to perform on SH-SY5Y cells, the bioreactor was filled with 500 µL of either water or low-serum DMEM and assembled as shown in Figure 3.8 c). Once properly assembled, the approach consisted in applying the chosen voltage condition for 1 h and registering if any visible alterations occurred.

3.7 Electrical Stimulation of SH-SY5Y cells

As widely present in the literature review, it has been shown that a more efficient way to induce neuronal differentiation of cells is to be found in the combination of multiple differentiation factors, including differentiation agents incorporated in the medium in which cells are kept, conductive biomaterials where cells can be seeded, and the exposure of cells to several forms of ES, among others.

Accordingly, the task at hand corresponded to the exposure of cells to a combination of conditions that were previously optimized for neuronal differentiation, and was only performed once the following conditions were met:

1. Choosing the most effective differentiation medium composition from the ones tested;
2. Obtaining a biocompatible conductive scaffold, suitable to be fixed on the bioreactor;
3. Testing the usability and electrical contacts of the bioreactor assembled with the conductive scaffold;
4. Choosing an ES protocol to test, considering both the parameters found from the literature review and the ones tested in Section 3.6.

For this purpose, a 9 day cell culture was performed on the bioreactor. After fixing a PLA/PEDOT scaffold with aligned nanofibers on the bottom of the bioreactor, as shown in Figure 3.16 (a), SH-SY5Y neuroblastoma cells, at passage 28, were seeded at a density of 4×10^3 cells/cm^2 using DMEM + 10% v/v FBS + 1% v/v penicillin/streptomycin.

After 24 h, medium was changed to DMEM + 3% v/v FBS + 1% v/v penicillin/strepto–mycin + 10 µM RA, to which cells were exposed for 8 days, with medium being changed every 48 h. Simultaneously, cells were subjected to an ES protocol consisting in the application of 500 mV/cm, 1 h/day for 9 days.

Finally, at the last day of culture, cells were fixed following protocol B.1.9.1. Staining for fluorescence imaging was performed as described in protocol B.1.9.2. Following, the images obtained were edited using the image processing software ImageJ [101]. Cells were kept in a humidified 5% CO_2, 37 °C incubator. Only one replicate was run. An overview of the protocol followed is illustrated in Figure 3.17.

The assembly of the whole ES setup consisted in placing the power generator on top of the incubator, the bioreactor inside it, and connecting both through wires with crocodile connectors passed by a hole, containing a removable cover, on the back of the incubator. Once the wires were passed through that hole, it was covered again, in order to maintain the desired atmosphere of 5% CO_2 and 37 °C. Before connecting the crocodile connectors, corresponding to the positive and negative electrodes to the lid of the bioreactor, the lid screws were gently tightened. This assembly is represented in Figure 3.18.

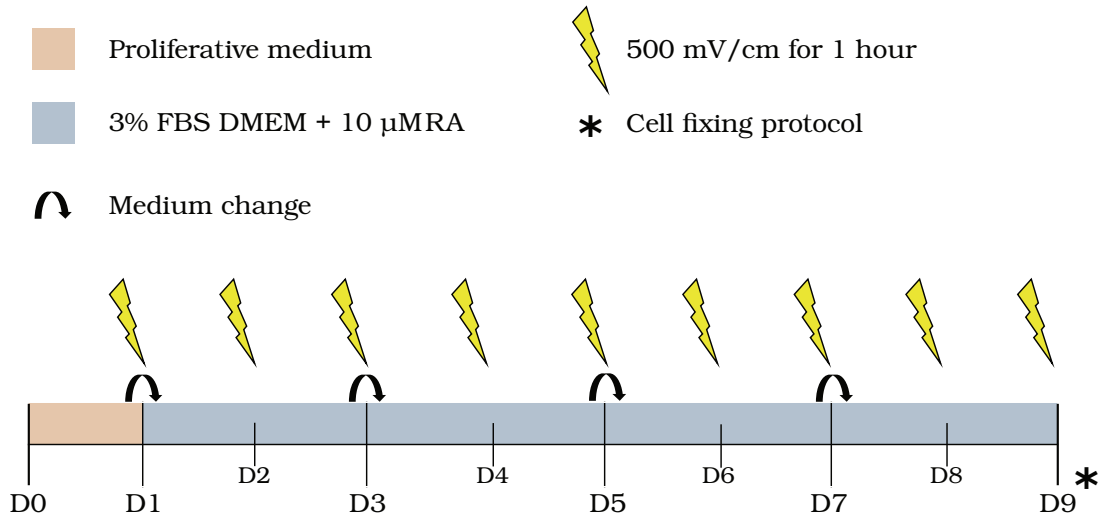

Figure 3.17: Diagram of the ES protocol followed for inducing neuronal differentiation of SH-SY5Y neuroblastoma cells.

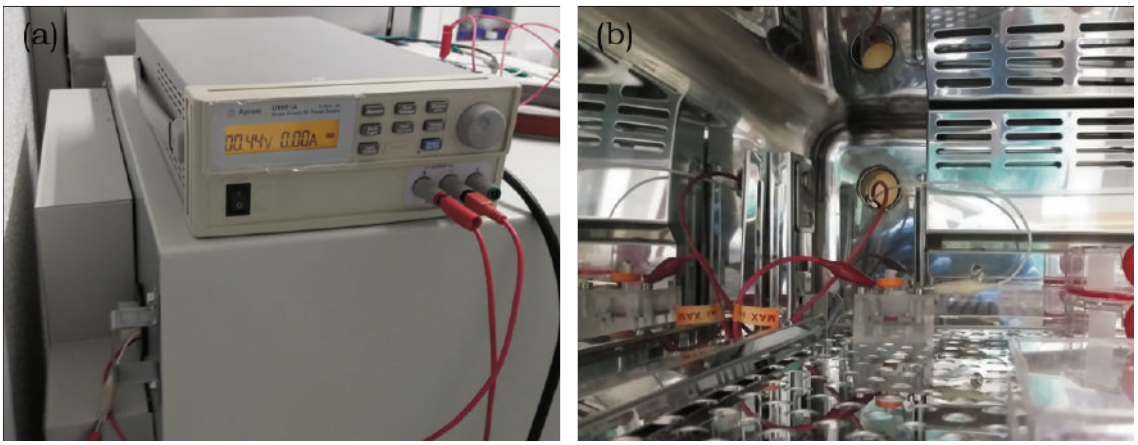

Figure 3.18: Assembly of the bioreactor inside the incubator for the ES assay: (a) Power supply placed on top of the incubator. The positive and negative electrodes were passed through the hole at the back, which was then covered with a silicone stopper; (b) Inside the incubator, the electrical connection is established with the bioreactor using wires with crocodile connectors.

4

Results and Discussion

This chapter encompasses the main results derived from the experimental tasks performed throughout this dissertation, as well as a thorough discussion, from which key conclusions were derived.

4.1 Optimization of Differentiation Protocol

Neuronal differentiation of SH-SY5Y neuroblastoma cells is, typically, assessed in three main ways: morphological analysis by observing and photographing the evolution of cells using and inverted microscope [102]; quantification of the length and number of neurite projections with the aid of image processing software [64]; and evaluation of genetic expression of neuronal markers by reverse transcription polymerase chain reaction (RT-PCR) or Western blot analysis [61], [92].

In this assay, whose goal was to determine which media composition containing RA would favour a more marked neuronal differentiation, only morphological analysis was performed. In this respect, in order to properly describe the visible differences, present throughout the culture, it is important be acquainted with the main morphological differences between undifferentiated and differentiated SH-SY5Y cells. On the one hand, undifferentiated cells are characterized by their high proliferation rate, tendency to form clusters and by unpolarized cell bodies with few small extensions. On the other hand, differentiated SH-SY5Y cells have more elongated and pyramidal shaped cell bodies, more and longer neurite projections, resembling axons or dendrites. Furthermore, they present significantly lower proliferation rates and tend not to form clusters. Medium manipulation, namely through addition of RA has proven its efficacy in differentiating this population of cells into cells of a more mature neuronal phenotype [82].

From day 1, following the diagram of Figure 3.3, it is clear that there was a high concentration of cells in the centre of each well, forming a main cluster. This had already been observed and theorized to be related to higher initial cell densities, however, lowering initial cell density in preliminary tests did not completely stop this effect. Another

possible reason for this is associated with the unavoidable movement necessary to transfer the cell culture plate from the biological safety cabinet to the inverted microscope or the incubator, which could be creating a small swirl effect in the culture medium, enough to aggregate the dispersed cells in the centre, immediately after the seeding process. Interestingly, many cells were found to adhere and grow close to the wall of the wells, independently of the initial cell density, which is also problematic for establishing a specific density for study. In those regions, cells were very hard to focus, contrast was poor, and consequently, said occurrence was not recorded. Even though it is still possible to assess cell morphology 24 hours after cell seeding, the described phenomenon hinders a proper assessment of cell morphology as cells proliferate and further aggregate, making it notably difficult to distinguish cell shapes and extensions.

At day 1, cells exhibited the described and expected signs of an undifferentiated morphology, as depicted in Figure 4.1. Following up on the previous paragraph, the first aspect that stands out is the presence of one big cluster of cells located at the centre of the well, with some spots where cells seem to be growing on top of each other forming clumps. Furthermore, some small neurite projections are already visible, mainly outside the centre of the cluster. The shape of the cell bodies varies and can be either more round and less elongated in the interior of the cluster, and tends to be more elongated, or pyramidal-shaped as the distance from the centre increases.

Cells cultured in control media containing only FBS at 5%, 3% and 1% v/v in DMEM exhibited significant proliferation on day 3. Already, some cell death was visible, detectable as detached round small circles appeared over the major cell cluster. As the culture progressed, it was evident that the number of cells was decreasing, as proliferation rate decreased due to lower FBS concentration and cell death occurred. This effect was similar with 3% and 5% of FBS, yet was more significant in the 1% FBS group, as expected. Overcrowding of the centre region of the well might have caused the cell death, which was enhanced due to the decreased concentration of FBS. The described alterations were expected, as a decrease in FBS concentration meant that cells were exposed to less supplement, hindering their growth. At day 9, cell shape was not significantly altered for groups with 3% and 5% of FBS compared to cells from day 1. Moreover, as previously mentioned, given that most cells were part of a large cluster, cell morphology was not easily characterizable. Cells of the 1% FBS group were more equally distributed and spaced at day 9, which allowed assessing cell morphology, as presented in Figure 4.2. These cells still exhibited very few and short neurite projections, as well as varied cell shapes. Some much smaller clusters were still present, where cells were more rounded and a lot of evenly distributed pyramidal-shape, as well as few more elongated cells were visible. Overall, these results show that reducing the serum content of the cell culture medium was not enough to induce neuronal differentiation and cell viability was more significantly affected in the 1% FBS control group.

Using DMSO at 1% v/v in culture medium led to considerable cell death, independently of the concentration of FBS. However, this effect was more carved at 1% v/v FBS

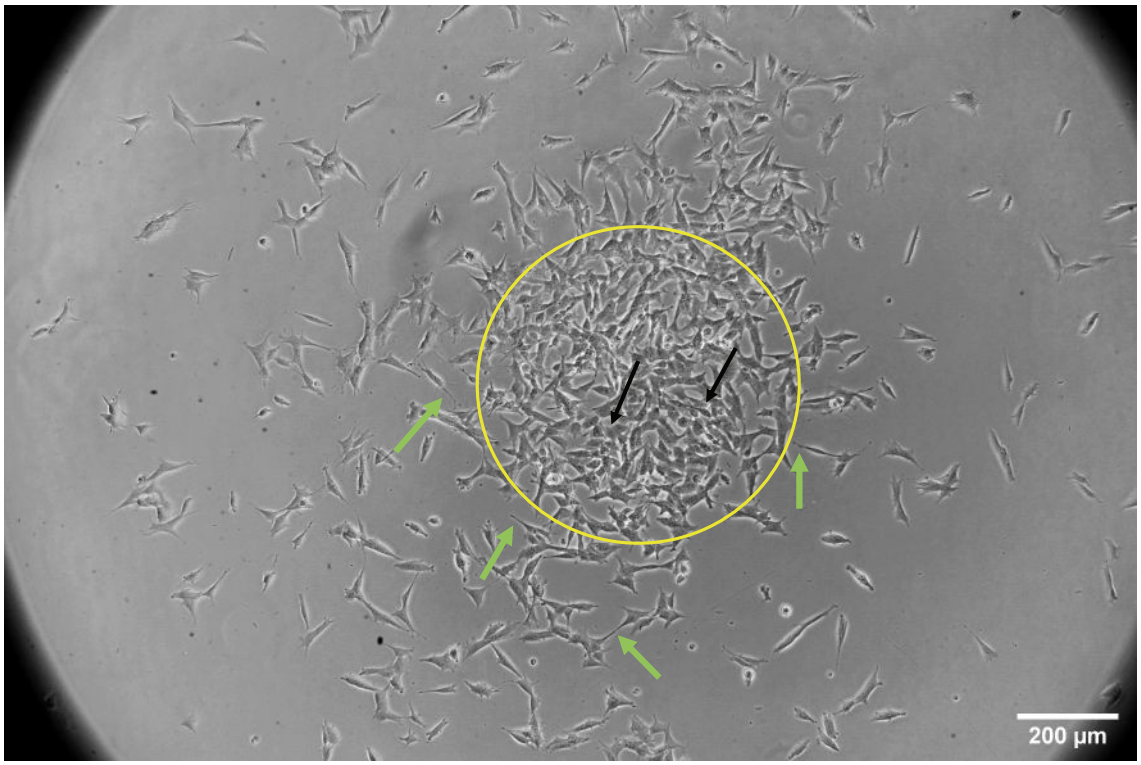

Figure 4.1: Inverted microscope image of SH-SY5Y cells in growth medium. This photo was taken on day 1 of the differentiation assay and shows undifferentiated cells, agglomerated in the centre of the well (yellow circle). At this stage, cells present small projections (green arrows) and can form clumps, growing superimposed to each other (black arrows).

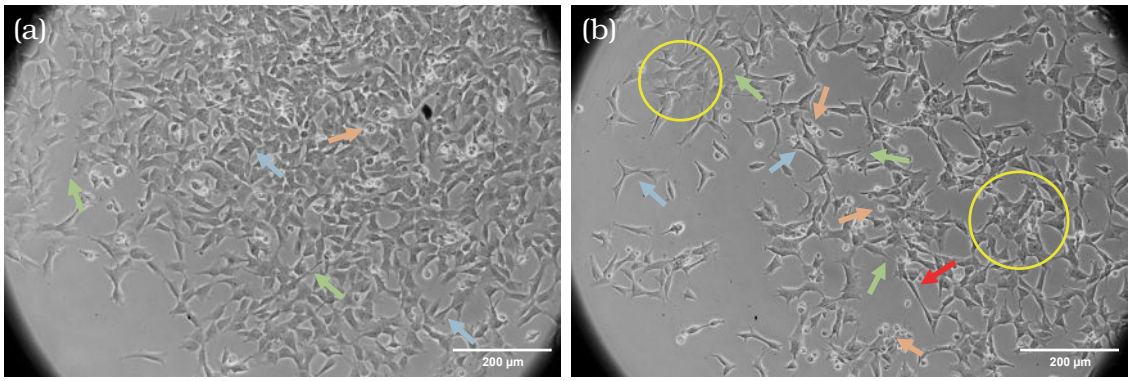

Figure 4.2: Inverted microscope images of SH-SY5Y cells: (a) after 2 days of culture in DMEM with 1% FBS; (b) after 8 days of culture in DMEM with 1% FBS. At this time, it was easier to identify small clusters of cells (yellow circles), pyramidal-shaped (blue arrows) and elongated cell bodies (red arrow), some of which presented short projections (green arrows). There are also visible dead cells (orange arrows).

and from day 7 on. These results had been observed in preliminary studies, which led us to establish that RA should be added to the culture medium achieving a final concentration of 0.5% DMSO, in an attempt to minimize its toxic effect.

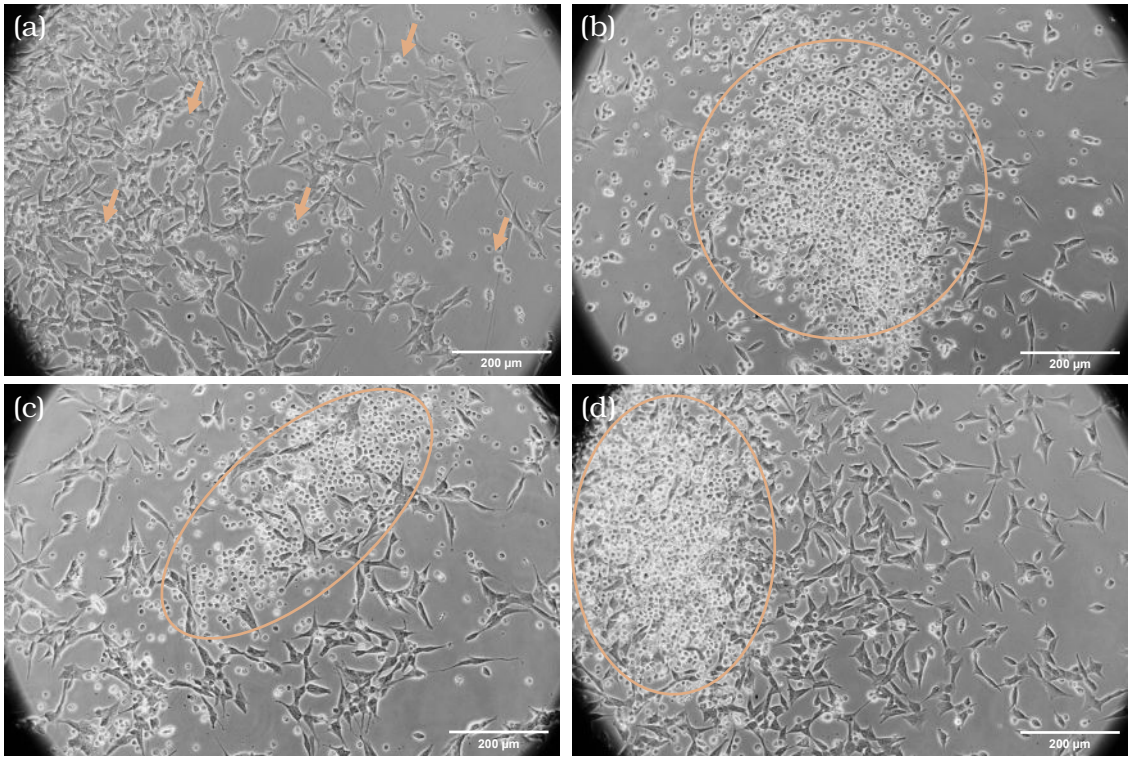

Figure 4.3: Inverted microscope images of SH-SY5Y cells: (a) after 8 days of culture in DMEM with 1% DMSO and 5% FBS; (b) after 8 days of culture in DMEM with 1% DMSO and 1% FBS; (c) after 8 days of culture in DMEM with 0.5% DMSO and 5% FBS; (d) after 8 days of culture in DMEM with 0.5% DMSO and 1% FBS. The orange arrows, circles and oval shapes indicate regions with dead cells.

Regarding cell differentiation, one clear conclusion is that, along with control groups, differentiation groups with 1% FBS and RA are not a viable option for differentiation of SH-SY5Y cells. These groups presented, both at 5 µM and 10 µM of RA, almost complete cell death by day 5, with the exception of some cells remaining on the groups where a glass coverslip was placed at bottom of the well. Cells were found under the coverslip, even at day 9, the last day of culture, and with some morphological indications of differentiation, namely very elongated cell bodies with extended projections compared to day 1. The mentioned results can be consulted in Figure 4.4 (a) and (b). At day 3, cell morphology suffered some visible changes that can be attributed to the role of RA, in that cells presented more and longer neurites and, overall, pyramidal and more elongated cell bodies, resembling a more mature neuronal morphology. Also, there are some spots where contact between extensions is visible, in a similar fashion to what occurs in sinapse formation. Some cell death was already visible by this time. In Figure 4.4 (c) it is possible to identify the mentioned alterations in cells, which were similar for both 10 µM and 5 µM

of RA.

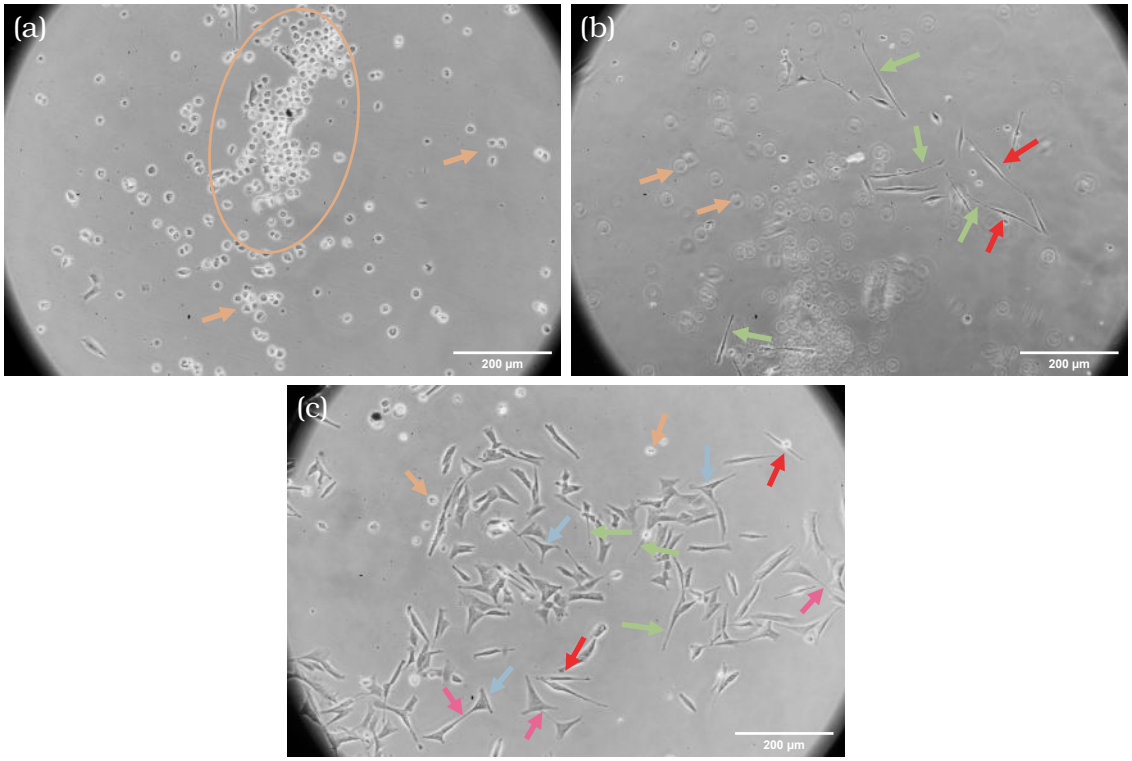

Figure 4.4: RA-induced differentiation of SH-SY5Y cells cultured in DMEM, 1% FBS: (a) Dead SH-SY5Y cells, after 4 days of exposure to DMEM with 1% FBS and 10 µM of RA; (b) Some elongated cells with extended neurites under a coverslip, after 8 days of exposure to DMEM with 1% FBS and 5 µM of RA; (c) Cells show initial signs of a more neuron-like morphology, after 2 days of exposure to DMEM with 1% FBS and 5 µM of RA. This figure shows dead cells (orange oval shape and arrows) and cells with pyramidal (blue arrows), as well as elongated bodies (red arrows) and extended neurites (green arrows). Also present are some points of contact between close cells through their extensions (pink arrows).

Moving on to the conditions that seem to have manifested a higher differentiation state, maintaining some level of cell viability, there are several findings worth mentioning. By comparing the images representing the morphological evolution of SH-SY5Y cells in conditions 1, 2, 4 and 5 detailed on subchapter 3.1.2 for the duration of the culture, it was found that after only 2 days of exposure to RA, cells began to exhibit signs of differentiation. Firstly, unlike the distribution found on groups without RA, where cells would cluster and mainly proliferate in the centre, cells grown with RA displayed a more evenly spaced distribution, and the absence of a big centered cluster. Some small clusters were still present, however not hindering the morphological assessment. In this regard, cell bodies were much less round and more clearly pyramidal-like. Most of the pyramidal-like cells presented neurite extensions, in which, one of the extensions was particularly longer than the others on the same cell, resembling an axon. The latter description was

visible in all four conditions, yet more perceptible in groups with 3% FBS and 10 µM of RA, as shown in Figure 4.5. By this time, cell viability was high compared to the following days of culture.

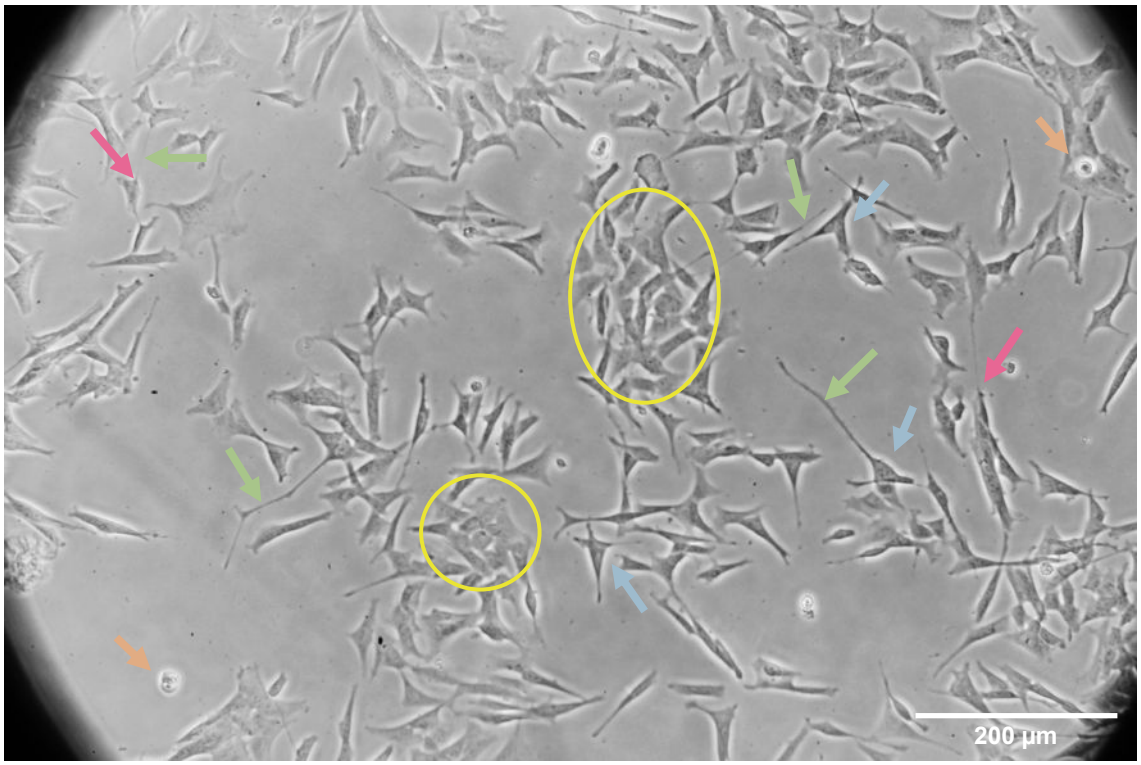

Figure 4.5: Initial morphological changes resembling a differentiation state of SH-SY5Y cells after 2 days of exposure to 10 µM of RA in DMEM with 3% FBS. Some small cell clusters are present (yellow circle and oval shapes) and cells display a less round and more pyramidal-like body (blue arrows). Cells developed long neurites (green arrows), some of which establishing a connection (pink arrows) with nearby cells. Cell death (orange arrows) is not relevant compared to controls.

Still in regards to conditions 1, 2, 4 and 5 of subchapter 3.1.2, day 5 showed no significant improvements on the differentiation process. By day 7 of exposure to RA there were two main alterations in the culture profile. Regarding cell death, it became more pronounced, particularly in groups with 3% FBS, and both concentrations of RA. The other observation concerns the existence of a small number of cells of a distinct morphology. Along with the morphologies described so far, some of the cells were characterized by a rounded cell body with a high number of neurite projections, but of a short length. The number of neurite projections is also a marker of differentiation, along with neurite length, as previously stated, which might have been a positive indicator of some differentiation still taking place. However, only a small number of cells presented said morphology, whose neurites didn't significantly increase in length until the end of the culture. One possible explanation for this phenotype is that, due to cell death, clusters became less prevalent, which could allow, on the one hand, the observation of hiding projections or,

on the other hand, the growth itself of new projections in multiple directions, by rounded cells, whose sides had been previously blocked by neighbouring cells inside of a cluster. This effect is captured in Figure 4.6 (a).

Day 7 was also characterized by a significant cell growth on groups with 5% FBS and 10 µM of RA. As proliferation still occurred, as expected comparing to groups with less serum content, cell clusters became an issue for distinguishing cell morphology and might have influenced the differentiation process as well, in that there was limited or no space for cells to extend their neurites. Importantly, according to what had been observed in previous days of culture, neurites grew longer in regions where cells were more spaced and less clusters were visible.

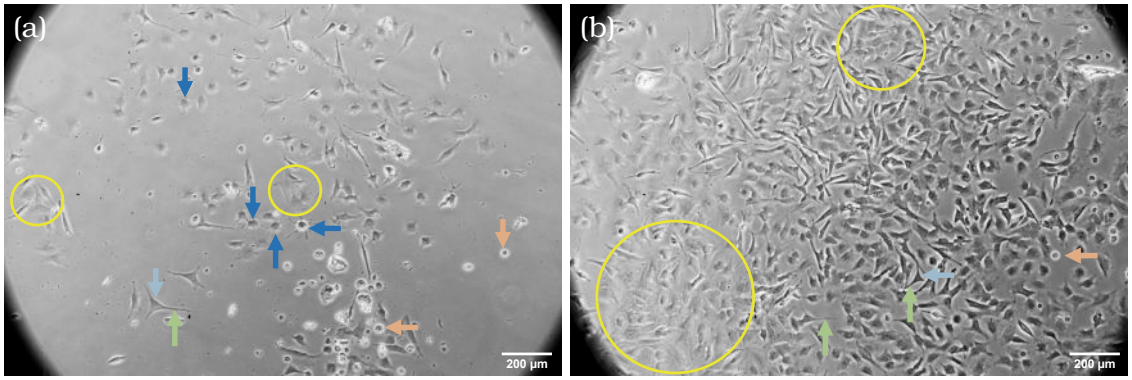

Figure 4.6: Inverted microscope images of SH-SY5Y cells: (a) after 6 days of culture in DMEM with 5% FBS and 5 µM of RA; (b) after 6 days of culture in DMEM with 5% FBS and 10 µM of RA. This figure shows cell clusters (yellow circles), pyramidal shaped cell bodies (light blue arrows) with projections (green arrows), dead cells (orange arrows), and some rounded cells with short projections in multiple directions (dark blue arrows).

At the last day of culture, although there were some differentiated cells with a pyramidal shaped body and more extended projections in groups with 3 and 5% FBS, most cells were round and did not exhibit many morphological signs of differentiation into a neuronal state. As such, and also due to the decrease in cell viability compared to control groups, the culture was not maintained further.

Altogether, cells appear to have reached a maximum state of neuronal differentiation as soon as day 2 of exposure to RA, yet were not able to maintain such state or further grow into a more mature neuronal phenotype, although still subjected to low-serum DMEM with RA. This observation is independent of the FBS and RA concentrations, with the exception of 1% FBS groups, in which cell death prevailed.

In an attempt to better visualize and distinguish cell morphology, some groups were prepared with an initial cell density of 1×10^3 cells/cm^2, half that of the groups discussed so far. Only conditions 1 and 5 of subchapter 3.1.2 were tested at this density, since they were found to be the best conditions for neuronal differentiation in preliminary tests of a similar nature.

Using this smaller density posed an expected risk, as beyond the presence of DMSO, SH-SY5Y cell death is increased and growth rate is reduced if cells are plated too sparsely, according to Datta et al. [82]. In fact, for both conditions (5% v/v FBS with 10 µM RA and 3% v/v FBS with 5 µM RA), growth rate was considered very low, since very few cells were visible throughout the culture, when compared to the previously discussed results for twice the cell density. Moreover, the initial cell density itself appeared less than the desired 1×10^3 cells/cm^2. This may be due to experimental errors in the cell seeding process and to the fact that cells were found to be growing close to the walls of the wells, hindering an even distribution, as already mentioned. Nevertheless, the reduced number of cells observed as the culture advanced was most likely due to the joint effect of cell death and the reduced growth rate, as reported in the literature.

Regarding differentiation, cells presented a similar behaviour compared to groups of a higher initial cell density exposed to the same medium. Some indications of early differentiation were visible in both low density groups following two days of exposure to RA, including more polarized and pyramidal cell bodies exhibiting some projections, as shown in Figure 4.7 (a). In the following days, the same signs of differentiation were still visible although with less cells found per well and undifferentiated cells still present in both groups. Occasionally, and towards the end of the culture, few cells presented one or more longer neuritic extensions, comparing to other cells of the same well and to previous days. At day 9, some cells with longer projections were found under a coverslip in 3% FBS + 5 µM RA medium conditions. These extensions established points of contact with other cells, as visible in Figure 4.7 (b). Importantly, as progressively less cells were found, it was challenging to extrapolate on a general description of their morphology and behaviour, leaving only the possibility of characterizing individual cells, which it not ideal and can give a false impression of the effects of each medium composition on SH-SY5Y cell behaviour.

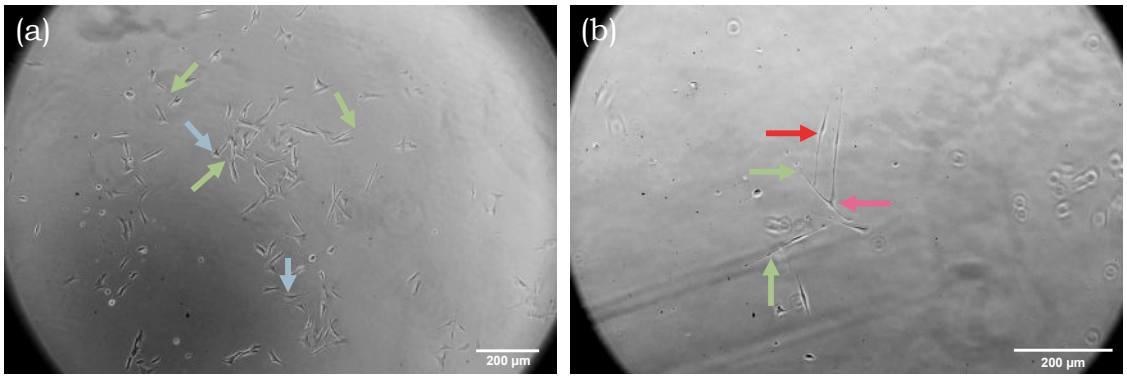

Figure 4.7: Inverted microscope images of SH-SY5Y cells: (a) after 2 days of culture in DMEM with 3% FBS and 5 µM of RA; (b) found under a coverslip, after 8 days of culture in DMEM with 3% FBS and 5 µM of RA. This figure shows elongated (red arrow) and pyramidal shaped cell bodies (light blue arrows) with projections (green arrows). Some longer projections were found to establish points of contact with other cells (pink arrows).

Overall, the differentiation protocol needs further optimization. Despite achieving a moderate level of neuronal differentiation, primarily early in the culture, none of the tested conditions led to a clear, evenly distributed, and sustained differentiation of SH-SY5Y cells maintaining high viability. Even though results were similar for groups with 3% and 5% FBS with RA, the condition that led to the presence of more extended neurites in a relatively distributed manner was the group with 3% FBS + 10 µM RA. Thus, despite the cell death in the last days of the culture, this was the condition chosen for testing the growth of cells on the produced materials, as well as for the ES assay. The difficulty in obtaining better differentiated neuronal cells may be due to several factors, some of which have already been explored. This may be related to the distribution of cells in the well, either forming clusters, preventing neurite extensions to freely form, or in contrast, to the low cell density in some groups, which increased cell death and left a low number of cells to grow. Furthermore, the main cause that should be investigated is the medium composition itself, since there are reports of similar protocols producing better results, namely exposing cells to 3% FBS + 10 µM RA medium for 7 days [89]. In last instance, possible errors performed during medium preparation should be investigated. Another important characteristic to consider is the passage of the cells used. This experiment was performed with cells from passage 30, which is considered a high passage. Simões et al. successfully differentiated SH-SY5Y cells by exposing them to 1% FBS + 10 µM RA medium for 3 days, but only used cells from passage 23 or below [90]. Moreover, it has been described that, with increasing passage numbers, SH-SY5Y cells tend to lose their neuronal characteristics [91]. By these standards, the high cell passage in which cells were used, probably, negatively affected the differentiation capability of the cells. Meanwhile, it has been reported that using RA alone is not sufficient to induce the formation of a mature neuronal phenotype and morphology in stem cells [23]. This was an important aspect in this dissertation, advocating for the attempt of multi-factor approaches, namely exposing cells to RA, CPs and ES, simultaneously. These attempts are described in following sections.

4.2 Design and Assembly of the Bioreactor

After performing a thorough review on current methods used for ES of various types of cells, with a special focus on neuronal cells, the advantages and drawbacks of each setup were discussed, which resulted in the selection of several aspects that were taken into account in the design of the new bioreactor. This design was set to include a cell culture chamber with a fixation system for the conductive scaffolds produced, and a system for establishing electrical contacts between the inside and outside of the chamber. From now on, I will refer to the chamber created for cell culture and stimulation as bioreactor, even though other elements are necessary for delivering ES.

4.2.1 Direct Coupling Setup

The design on which the production of the first prototype was based, as well as a perspective view of the prototype itself are presented in Figure 4.8, for a side-by-side comparison of results. Furthermore, the top (with and without lid), front and side views of both the design and the prototype are displayed in Figure 4.9. Regarding the method used for ES, this prototype is considered a direct coupling system, as electrodes will be in direct contact with the cell culture medium. Some problems concerning direct coupling-related medium alterations during ES were observed and will be further discussed in section 4.6.

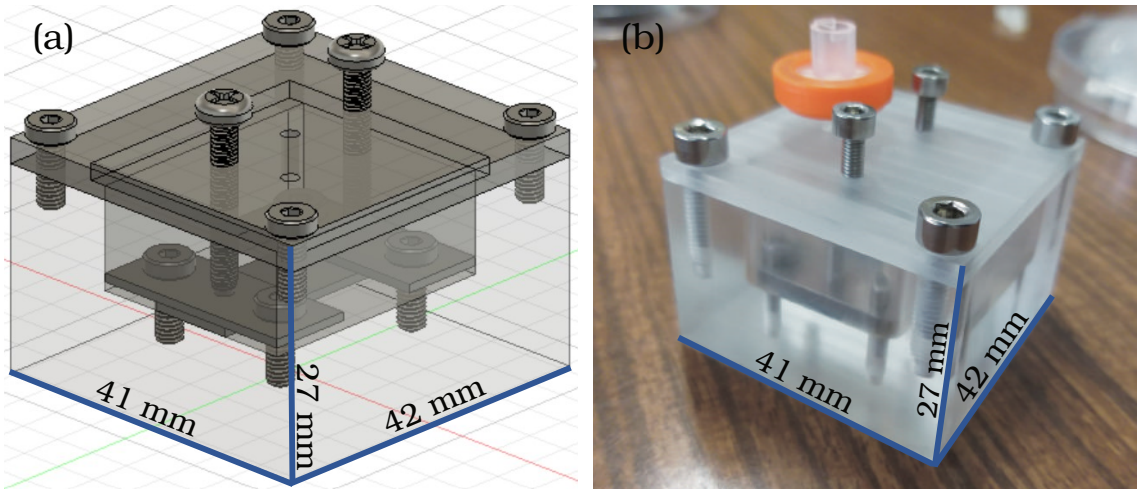

Figure 4.8: Comparison of the design and the prototype of the bioreactor produced: (a) Ortographic view of the design developed using the software Autodesk Fusion 360^{TM}; (b) Perspective view of the prototype produced when fully assembled.

As a first prototype, this design was developed anticipating that it is unlikely to achieve an optimal function and usability on the first attempt, and the need for further adjustments was probably going to emerge from the tests performed. Accordingly, the bioreactor produced consists in a single personalized well, with the capability of being connected to an external current or voltage provider. As there is only one well available, cultures with ES can only be performed one sample at a time, which can be very time consuming. However, it was necessary to ensure proper function, before considering a multi-well design.

In respect to the semblance of the bioreactor to the design, the production of the first prototype was successful, in that it closely resembles the design developed using the software Fusion360^{TM} from Autodesk. All dimensions of the prototype are in accordance to what was defined and can be consulted in Figure 4.10. However, there are some inaccuracies worth mentioning, related to the fabrication process. Firstly, the machining of the PMMA block was not effective in building sharp edges in the internal chamber walls. Instead, they were produced slightly rounded, which ends up only being an aesthetic error, not compromising its main function, delivering ES to cells fixed in a conductive

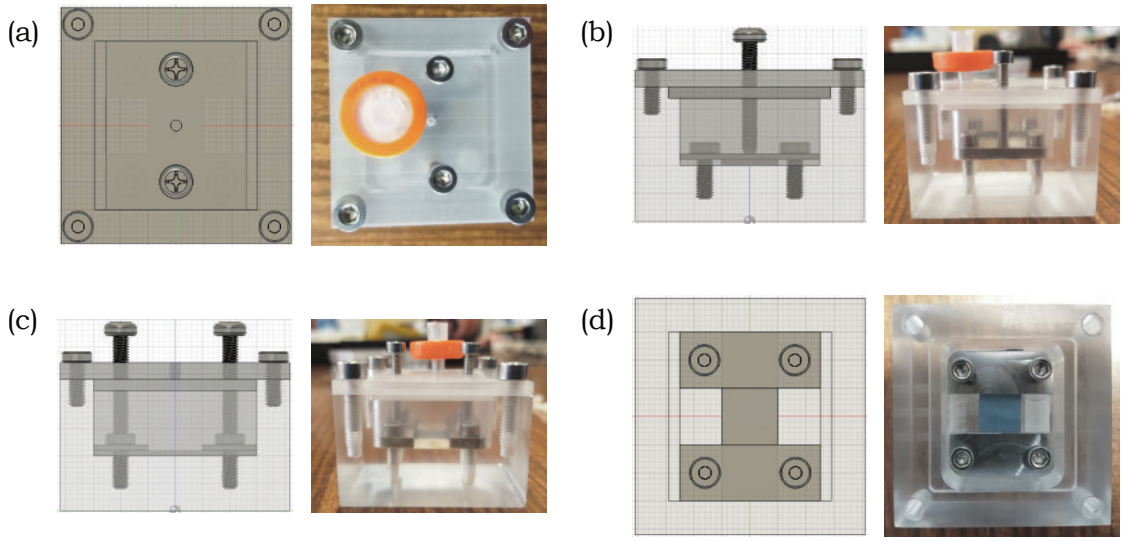

Figure 4.9: Side-by-side comparison of the top (with (a) and without (d) lid), front (b) and side (c) views from the design of the bioreactor and the prototype produced.

scaffold. Secondly, the electrodes were designed so that a 1 cm gap was left between electrodes, facilitating the calculation of the electrical field established between them. Yet, once screwed to the bottom of the chamber, this gap is only 0.88 cm wide. This can be easily corrected by reducing the width of the stainless steel plates, until the gap matches 1 cm. Moreover, two edges in each electrode were rounded for fitting purposes. Finally, the lid was incorrectly designed to contain a hole for the syringe filter exactly between the two M2 screws, not taking into consideration the size of the filter itself, which ended up not fitting. To correct this, a new hole, with a 4.5 mm diameter, was made deviated from the screws, and the original one was covered using an 8% PLA solution. The inaccuracies mentioned are highlighted in red in Figure 4.11.

Concerning the assembly and usability of this first prototype, once assembled, the bioreactor has a low weight and height profile, fitting easily in a standard cell culture incubator. Assembling a sample is a relatively simple and quick process, and starts by cutting the material to be fixed at the bottom of the chamber in 3 cm × 1 cm samples. Secondly, the material is placed on the chamber and is fixed at the ends leaving an area of culture in the sample of 1 cm × 0.88 cm, which was ideally designed to be 1 cm × 1 cm. Importantly, using this approach to assemble the sample leads to a total culture area of 2.5 cm × 0.88 cm. As such, during the cell culture assays, there are two 7.5 cm × 0.88 cm areas uncovered by the conductive sample. This is not an ideal solution, since approximations will need to be made in establishing the initial cell density at the sample, and from a resource consumption point of view, since a part of the cell suspension is wasted. It is also important not to excessively screw the plates, which can pressure the sample to the point of damage. The lid should be fixed watertight to the chamber and the syringe filter should be pressed to fit the hole at the lid. Some attempts were made using an Arduino Uno as the voltage or current provider, however this option was left to be explored as

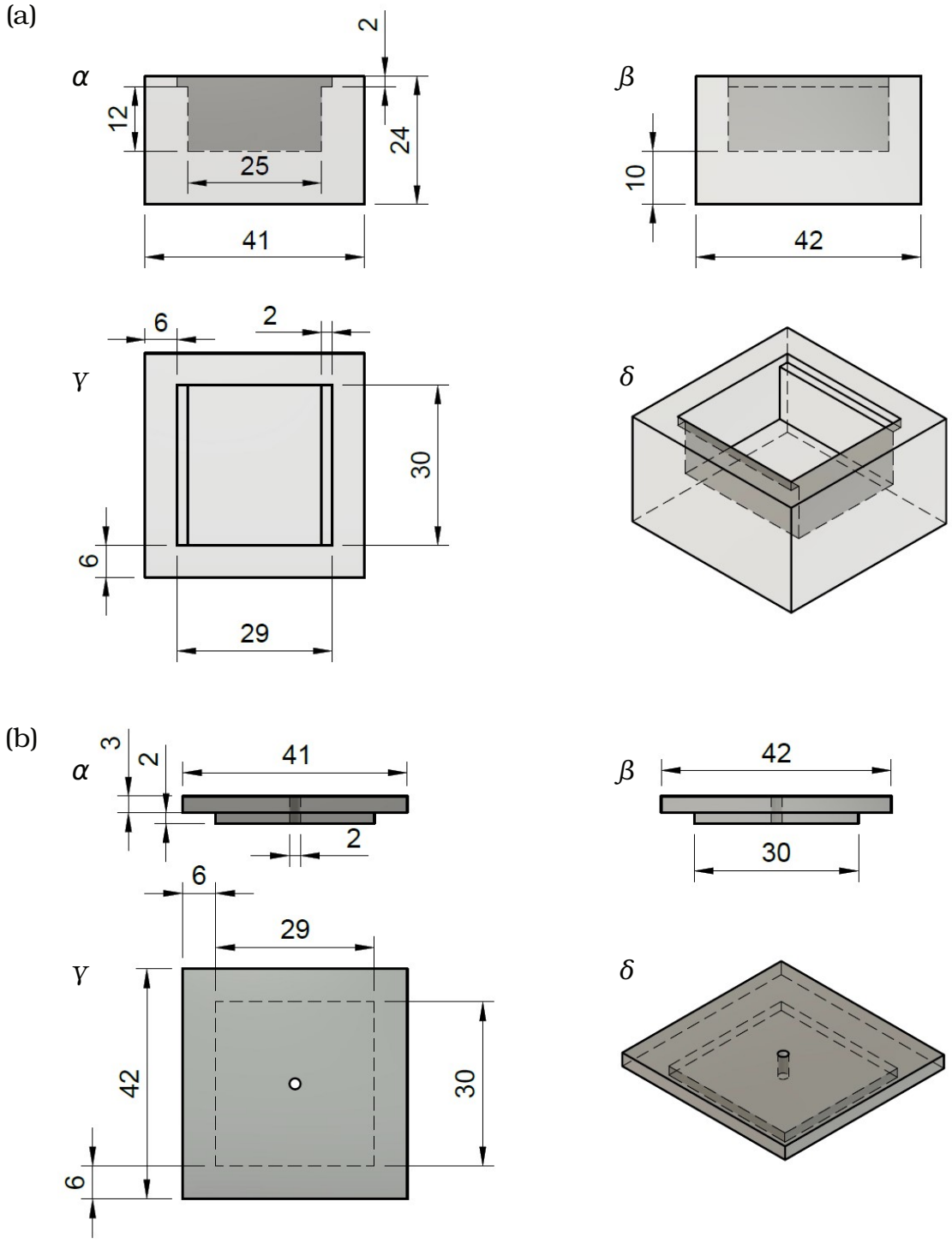

Figure 4.10: Dimensional drawing of the front (α), side (β), top (γ) and orthometric (δ) views of the (a) bioreactor chamber and its (b) lid. All dimensions are in mm.

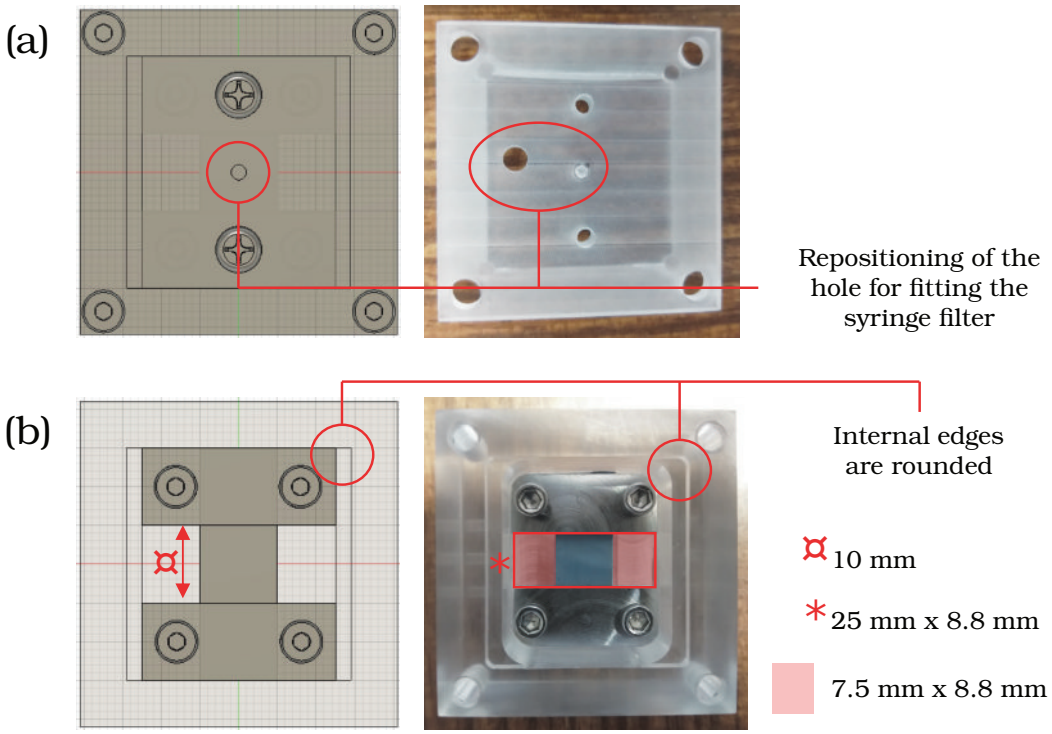

Figure 4.11: Errors and inaccuracies related to the production of the bioreactor: (a) Lid; (b) Internal edges and electrode spacing.

future work, and is further discussed in section 5.

4.2.2 Attempt for an Electrically Insulated Setup

In an effort to improve the versatility of the bioreactor in terms of the range of electrical fields it can safely provide to cells, a different design was though out. The goal was to achieve a configuration where the electrodes could be in contact with the conductive scaffold but not with the culture media, avoiding the occurrence of water electrolysis, electrode corrosion, and consequent exposure of cells to a medium with an altered pH and containing toxic compounds. This setup consisted in using the same apparatus, but with extra internal pieces, allowing for a distinct way of fixing the scaffold to the chamber. So, to avoid the contact between the electrodes and the culture medium, the following alterations were made:

1. Two 19 mm x 9 mm x 4 mm PMMA blocks were added to work as electrical insulating spacers (Figure 4.12 (a));

2. The stainless steel screws used for fixation of the electrodes to the bottom of the chamber were substituted for M2 x 14 mm nylon screws, also for the sake ensuring electrical isolation (Figure 4.12 (b));

3. Two extra stainless steel plates were used to establish the contacts with the conductive scaffold (Figure 4.12 (c)).

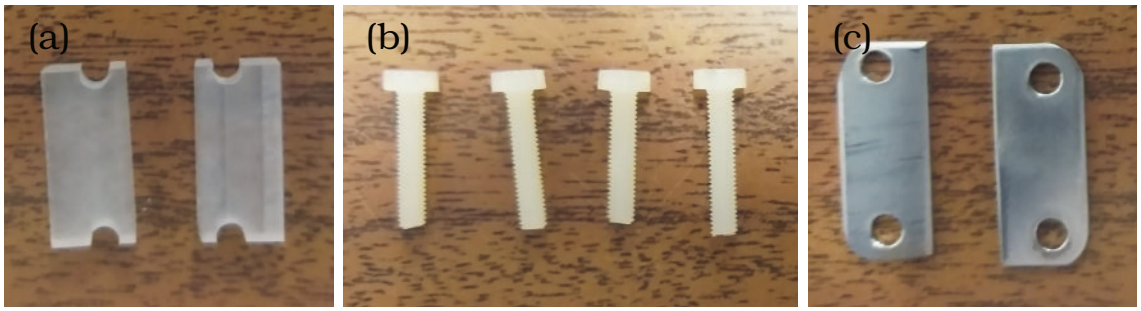

Figure 4.12: New pieces used to isolate the culture medium from the electrodes: (a) PMMA spacers; (b) Nylon screws; (c) Stainless steel plates.

For illustrative purposes, and as a means to better understand the assembly of this new configuration, this design is represented in Figure 4.13. As shown, the surfaces of the PMMA spacers are distanced from the internal walls of the bioreactor. The idea behind this was to avoid the medium level raising through capillarity action and ending up still in contact with the electrodes. To assemble a sample, in this case, a PLA/PEDOT electrospun scaffold, it is necessary to carefully place the spacer and the first conductive plate on top of each side of the sample, then to bend the sample using a clamp, placing the second plate above the bent sample, and finally to screw the nylon screws to the bottom of the chamber, stabilizing the spacer and the sample pressed between both conductive plates. In this case, the second plate grants electrical contact with the side of the sample that was directly exposed to VPP. Finally, the whole assembly is shown, closely resembling the original setup from outside.

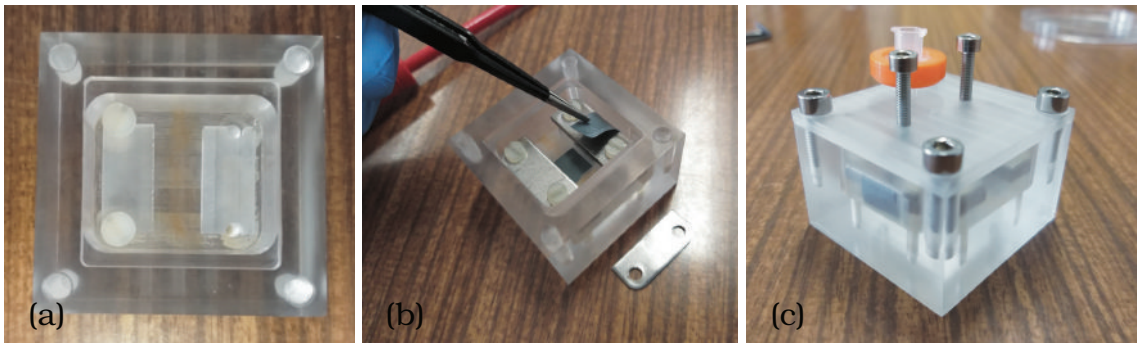

Figure 4.13: Assembly of the bioreactor with electrically insulating PMMA spacers: (a) The spacers were dimensioned to avoid contact with the chamber walls and are stabilized by the nylon screws; (b) PLA/PEDOT sample being assembled between two stainless steel plates; (c) Complete assembly. A sample is visible at the left wall passing behind the spacer and the first conductive plate, and the second plate above it.

This new setup ended up not being a good solution for the following reasons. When

it comes to assembly, it is more complicated when compared to the first setup described, and only works with electrospun scaffolds, or other malleable materials, since it is necessary to bend the material twice at a 90º angle, approximately. The sample shown also requires careful manipulation to avoid damage or ripping, during the assembly. More importantly, this assembly failed to achieve its desired effect. When estimating the appropriate working volume for each design, it was observed, for the direct coupling system, that a maximum volume of 600 µL was possible, before medium started to easily overflow to the top surface of the electrodes. However, when trying the same amount in the new design, an uneven medium dispersion was observed, towards the side and back of the spacers. To compensate for this effect, the working volume was increased to 1 mL, most of which flowed evenly to the back and sides of the spacers, contacting the electrodes through capillarity and leaving almost no volume in the desired area of culture, completely invalidating this approach. The described effects are visible in Figure 4.14. Therefore, this design was abandoned and all the ES tests were performed resorting to the direct coupling setup.

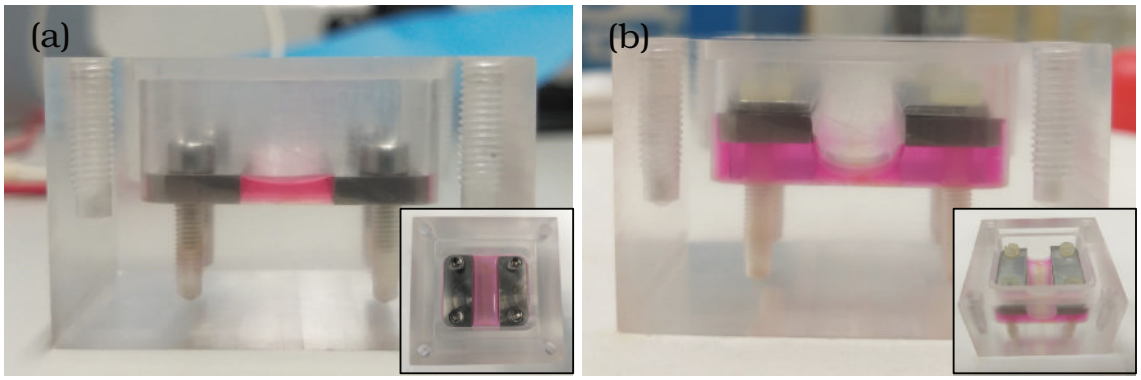

Figure 4.14: Determining the working volume for the bioreactor: (a) Direct coupling setup containing 500 µL of culture medium. An unpronounced meniscus is formed; (b) Unsuccessful attempt of insulating the medium from the electrodes. Using a working volume of 1 mL, the medium flowed from the desired area, and contact with the electrodes is not avoided.

This section was mainly focused on explaining the reasoning behind the chosen design, and the results of the prototype design, production and assembly. Although some topics concerning the function and usability of the bioreactor were already discussed, the results of sections 4.3.3, 4.6 and 4.7 provide a deeper insight into its features, by testing the bioreactor in different scenarios.

4.3 Fabrication of Conductive Scaffolds

The goal of this task was the production of a biocompatible scaffold with a conductive surface, suitable to be fixed on the bioreactor, and on which SH-SY5Y cells could be seeded and subjected to ES of various sorts. A wide variety of attempts were made,

namely by implementing different materials and fabrication techniques. The results from these attempts are described in detail below and led to the selection of one type of scaffold for *in vitro* testing.

The scaffolds for VPP were produced using PLA/FeTos solutions, meaning that the oxidant, required for the polymerization process, was already contained in the solution from which films and electrospun matrices were fabricated. By the time these experiments were performed, the system of solvents used in this solutions was being optimized by another member of the NEURiTES project. Pires et al. showed that PLA/PEDOT matrices, prepared using CHL and DMF as solvents of PLA and FeTos, respectively, achieved levels of conductivity in the range of what is reported in the literature for similar applications [103], including ES of cells.

In this connection, while the electrospinning process was being optimized [103], attempts were made to quickly produce a conductive surface for preliminary testing of the bioreactor. The original task of producing electruspun scaffolds was delayed and the suitability of the solutions used, thus far, for electrospinning, was further explored with other techniques of easier and faster fabrication.

4.3.1 Film Casting

As a starting point, four different initial concentrations of PLA were selected, using a ratio of PLA:FeTos of 2:1 (hereby referred to as group A). Each solution was poured onto an acetate sheet, and left to dry overnight. It is important to mention that there was no control over the time during which solutions of PLA/FeTos were subjected to magnetic stirring prior to film casting. As shown in Figure 4.15, PLA/FeTos films, with the exception of A6, presented a higher concentration of oxidant at their limits. Importantly, PLA control films were all malleable and resilient, in contrast with samples containing FeTos which were all brittle, making them unsuitable for assembly on the bioreactor, as they would easily break. Although not perceptible by the picture, the surface of films A6, A8 and A10, containing FeTos, was not smooth, presenting small rounded domains. A6 did not detach from the acetate sheet.

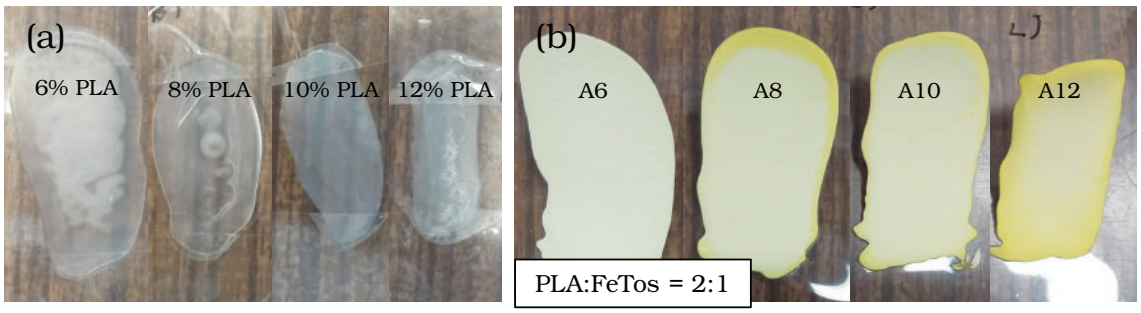

Figure 4.15: Films produced from (a) PLA and (b) PLA/FeTos solutions with a ratio of PLA to FeTos of 2:1. Four different initial concentrations of PLA were considered, namely 6% (sample A6), 8% (sample A8), 10% (sample A10) and 12% (sample A12) PLA.

Despite film brittleness, a small sample from each film of group A was subjected to VPP for 4 h at 70 °C. As visible in Figure 4.16 (a), all the samples turned blue, meaning that polymerization of EDOT occurred at their surfaces [104]. However, the distribution of PEDOT was heterogeneous. In general, the blue from the film surfaces was darker with increased PLA concentration, as films contained progressively more FeTos for the same PLA/FeTos ratio. Furthermore, the blue color was also darker in regions where a higher concentration of oxidant was present, prior to VPP. This is particularly visible in sample A12, in which darker yellow regions became darker blue regions as PEDOT was formed. These observations agree with the fact that EDOT polymerization takes place at the oxidant/monomer interface [99]. Moreover, VPP was also performed for only 2 h at the same temperature, in different samples of films A8, A10 and A12, which detached from the acetate sheet. In this case, all samples displayed a similar light blue color, which can be explained by less PEDOT formation on those samples. Film brittleness was similar before and after VPP.

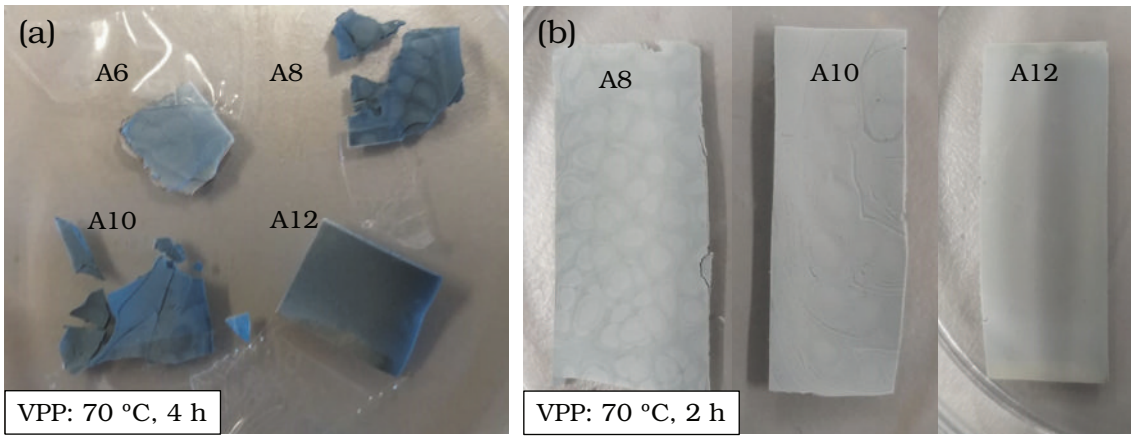

Figure 4.16: VPP of films from group A. Different samples were exposed to EDOT vapors for either (a) 4 h, or (b) 2 h, at 70 °C.

The brittleness in oxidant containing films was a major drawback and renders them unusable for our purpose. To address this concern, new films were produced with increasing ratio of PLA to FeTos, with the goal of reducing film brittleness. Accordingly, the following step consisted in increasing this ratio to 2.5 (group B), which ultimately, did not result in any improvements to film brittleness. These films are represented in Figure 4.17 and display a surface pattern similar to that of group A. Small domains are present in all samples and domain size appears to have increased with PLA concentration. Films B6 and B8 did not detach from the acetate sheet and were cut directly from the sheet for VPP. In contrast, films B10 and B12 detached from the sheet and exhibit similar brittleness to the films from group A.

Firstly, VPP was performed at 50 °C for 4 h, which rendered all films with a similar blue color, indicative of PEDOT formation. The borders of the domains were visibly darker. By increasing the VPP temperature to 70 °C and reducing, to 2 h, the time of

exposure to EDOT vapors, new samples from films B10 and B12 displayed a more homogeneous and darker blue color.

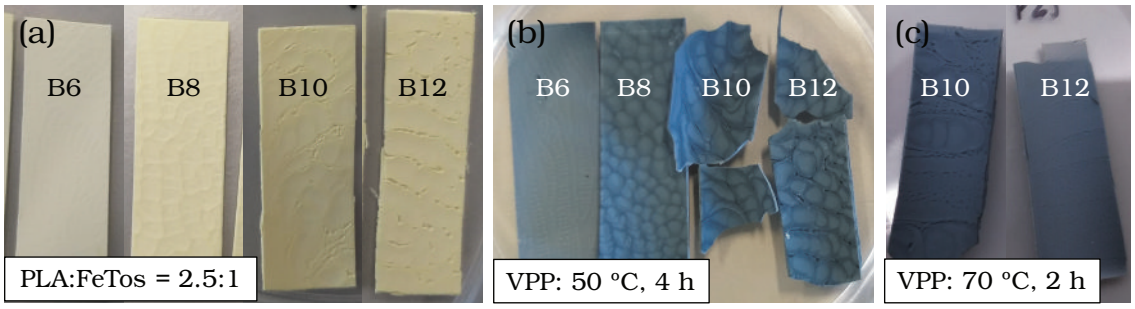

Figure 4.17: Films produced from PLA and PLA/FeTos solutions with a ratio of PLA to FeTos of 2.5:1. (a) PLA/FeTos films; (b) VPP results from 4 h of exposure to EDOT vapors, at 50 °C; (c) VPP results from 2 h of exposure to EDOT vapors, at 70 °C.

The ratio of PLA to FeTos was increased further to 3:1 (group C), with similar results to what was described so far, as displayed in Figure 4.18. Once again, only the films with the two higher concentrations of PLA, C10 and C12, detached from the acetate sheet. PEDOT was formed in both samples, as surfaces displayed a dark blue color, characteristic of this polymer, and film brittleness was still prevalent.

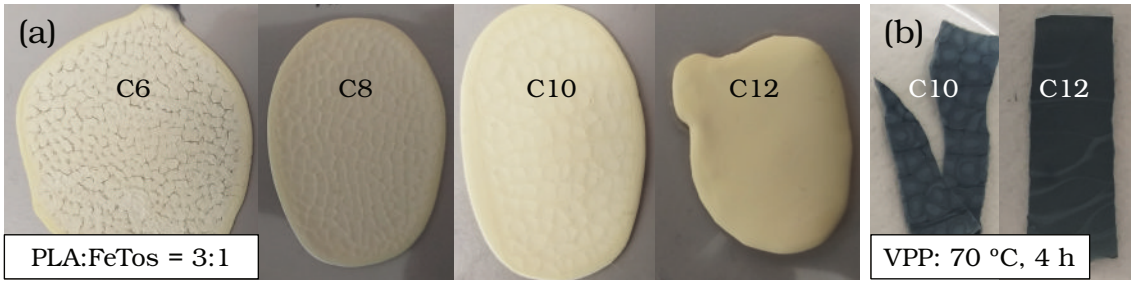

Figure 4.18: Films produced from PLA and PLA/FeTos solutions with a ratio of PLA to FeTos of 3:1. (a) PLA/FeTos films; (b) VPP results from 4 h of exposure to EDOT vapors, at 70 °C.

Two final ratios were tested, namely 12:1 (group E) and 20:1 (group F). Regarding group E, shown in Figure 4.19, films E6, E8 and E10 were not detachable and showed a surface pattern very akin to what was seen in films of the same PLA concentration and smaller PLA/FeTos ratios. E12, which detached from the acetate sheet by itself, showed a relatively smooth surface.

Importantly, a malleable and less brittle film was produced from the same PLA/FeTos solution as E10, by performing film casting inside a 37 °C stove. One hour after the solution was poured, the described malleable film had detached from the acetate sheet and displayed the characteristics described, constituting the first improvement over the tests performed thus far. Its surface exhibited larger domains, which were more evident after VPP. As shown in Figure 4.19 (b), the latter mentioned and the E12 films were

exposed to EDOT vapors, achieving a similar dark blue coloration. The domains from the E10 film produced at 37ºC showed a lighter coloration. In contrast to what was desired, after VPP, the latter became as rigid and brittle as the E12 film.

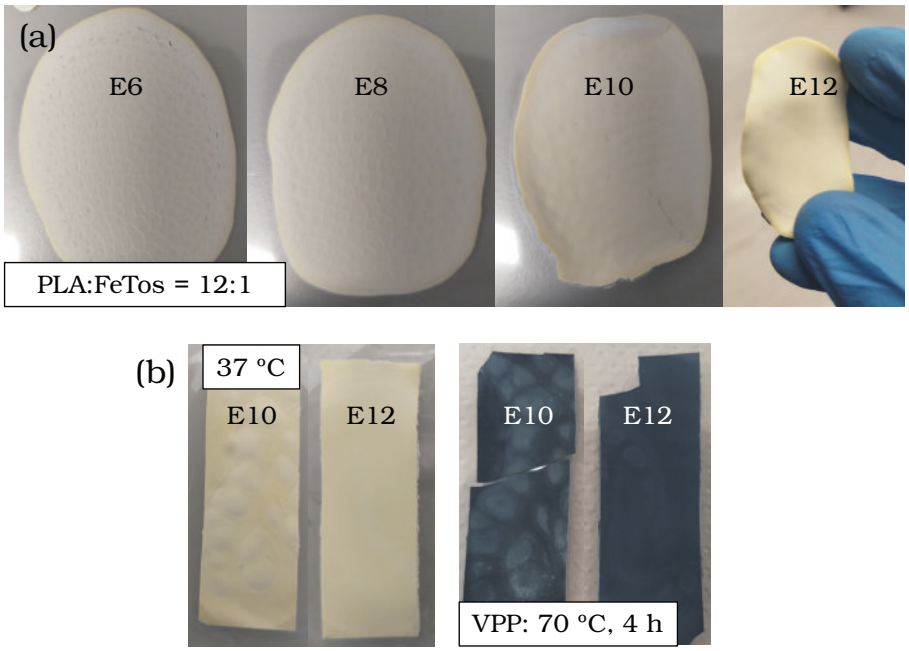

Figure 4.19: Films produced from PLA and PLA/FeTos solutions with a ratio of PLA to FeTos of 12:1. (a) PLA/FeTos films; (b) VPP results from 4 hour of exposure to EDOT vapors at 70 °C.

Lastly, for group F, the two lower concentrations of PLA were not considered and the films produced are displayed in Figure 4.20. Both films detached from the acetate sheet and presented some large domains. Overall, the surface of the films was smooth. When performing VPP of film samples at 70 °C for 4 h, the films did not show the expected dark blue color of PEDOT, as seen in previous films. Instead, the surface of the films displayed a light green coloration. Then, the duration of exposure to the EDOT vapors was increased to 6 h, which resulted in a more bluish color, yet still distinct from the typical PEDOT color. More importantly, these ratio did not introduce any significant upgrade regarding the reduction of film brittleness, comparing to the lower ratios tested.

In sum, the tests performed using film casting did not result in the fabrication of a suitable conductive film, as all the samples produced were brittle, breaking easily, even with careful manipulation. This method was, therefore, abandoned. A small number of tests was performed using the spin coating and the dip coating technique and are described in Appendix C.

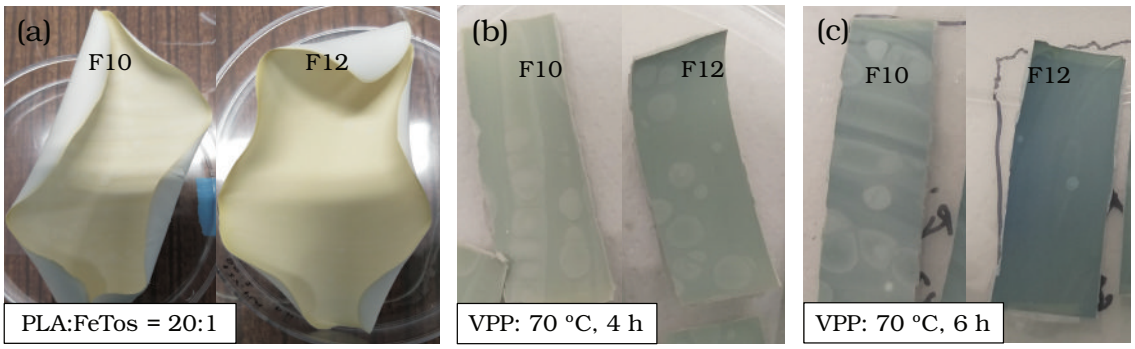

Figure 4.20: Films produced from PLA and PLA/FeTos solutions with a ratio of PLA to FeTos of 20:1. (a) PLA/FeTos films; (b) VPP results from 4 h of exposure to EDOT vapors, at 70 °C; (c) VPP results from 6 h of exposure to EDOT vapors, at 70 °C.

4.3.2 Electrospinning

As explained, film production was not successful. Thus, matrices optimized by Pires et al. [103] were reproduced using the solution represented in Figure 4.21 (c). Ambient conditions were 31.8% of relative humidity and 21 °C, and the deposition was stable, with no accumulation of solution at the tip of the needle. The fibers obtained were exposed to EDOT vapors for 4 h at 70 °C, and from that process, PEDOT was formed, indicated by the characteristic blue color of the matrices [104]. PEDOT formation appeared more homogeneous in matrices of Figure 4.22 (b) and was, therefore, chosen over (c) for future tests, namely the cytotoxicity assay, assessment of cell growth on the materials and the ES assay. SEM images from these fibers were obtained and are represented in Figure 4.23. The surface of the fibers appears similar, independently of the presence of PEDOT, however, for proper assessment of this aspect, images of higher resolution should be made. More importantly, the fibers presented a satisfactory level of alignment and a preferential direction is also observed.

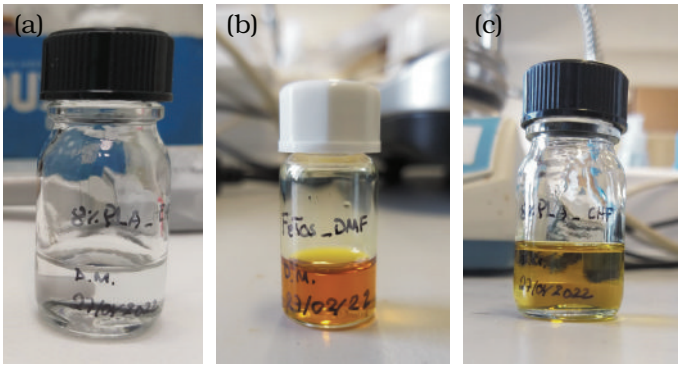

Figure 4.21: Solutions prepared for the electrospinning process: (a) 8% PLA solution in CHL; (b) FeTos solution in DMF; (c) PLA/FeTos solution prepared by mixing the former solutions for a ratio of polymer to oxidant of 2:1.

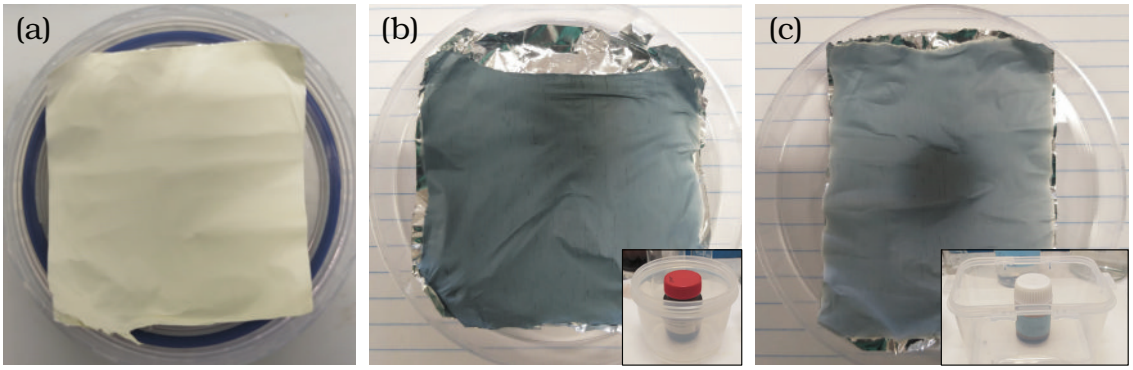

Figure 4.22: PLA/PEDOT scaffolds from VPP of (a) aligned PLA fibers containing FeTos. The chamber in which sample (b) was exposed to the EDOT vapors was smaller than the one used for sample (c).

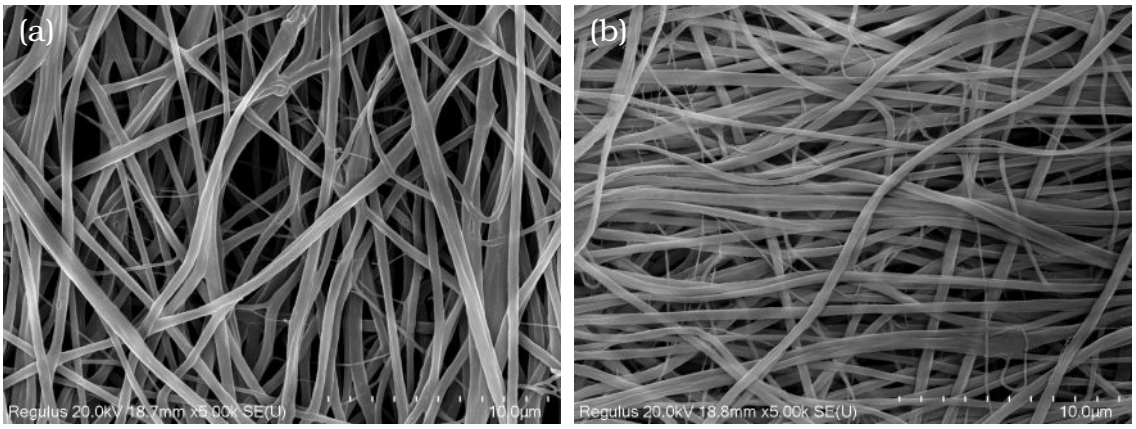

Figure 4.23: SEM images of the electrospun fibers produced: (a) PLA fibers; (b) PLA/PEDOT fibers.

4.3.3 Electrical Characterization

The method used by Pires et al. [103] to perform *IV* curves of PLA/PEDOT electrospun scaffolds consisted in manually inserting silver paint on two separate regions from the surface of the material, as a 2-point probe assembly. This poses some challenges depending on the material being used. In the case of electrospun materials, it is not the most adequate approach, since it is very challenging to restrict the painted region to a given regular electrode geometry and to avoid current conduction through painting infiltrated in the fibrous structure. For this dissertation, a 2-point probe system was also employed, however using the fixation system of the bioreactor as contact electrodes with the surface of the materials. In fact, this characterization procedure is performed under conditions close to those of electrical stimulation of the cells, allowing the characterization of the device used in this stimulation. In particular, it will allow analyzing the electrical currents involved in the stimulation process. This tests were very important and should be pursued further, as it is necessary to better characterize the electrical behavior of the

PEDOT covered electspun PLA fibers, with and without the presence of culture medium, foreseeing the application of currents in cell cultures performed on the bioreactor.

The *IV* curves were obtained for a range of applied voltages from -1 V to 1 V, since it is in alignment with what is used in the literature for ES of cells, and also because larger voltages were considered not safe for continuous application in tests performed with culture medium, in section 4.6. *IV* curves from samples of all three scaffolds from Figure 4.22, with and without culture medium, are presented below (Figure 4.25). The samples were prepared for assembly on the bioreactor as shown in Figure 4.24.

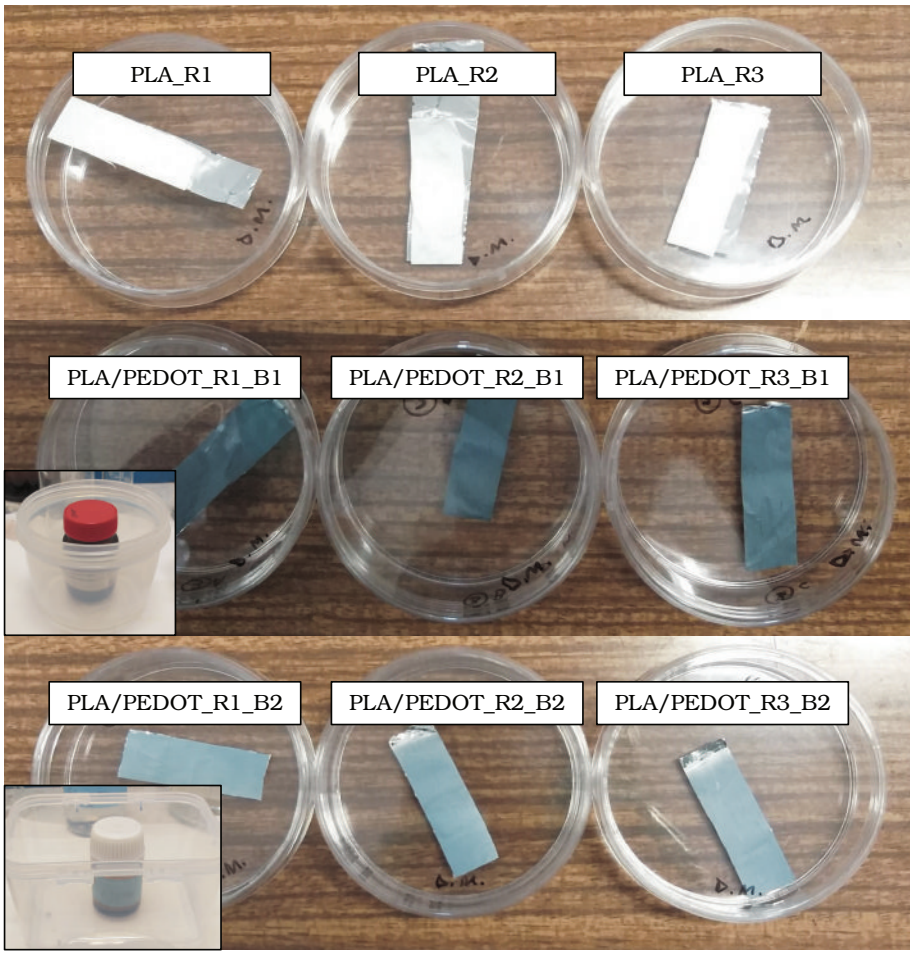

Figure 4.24: Samples of electrospun PLA fibers, with and without PEDOT, for which *IV* curves were obtained. Three replicates of each are considered (R1, R2 and R3) and, in the case of fibers containing PEDOT, the chamber in which VPP was performed is labeled as B1 (for the rounded chamber), and B2 (for the square chamber).

As expected, the samples that were not subjected to VPP, are not conductive, as the read values were very similar to a scenario were no sample was present. Contrarily, both scaffolds tested containing PEDOT presented some degree of conductivity. In all samples, a non linear relation is observed between the voltage applied and the current on the material, which means that these scaffolds do not follow Ohm's Law, and are,

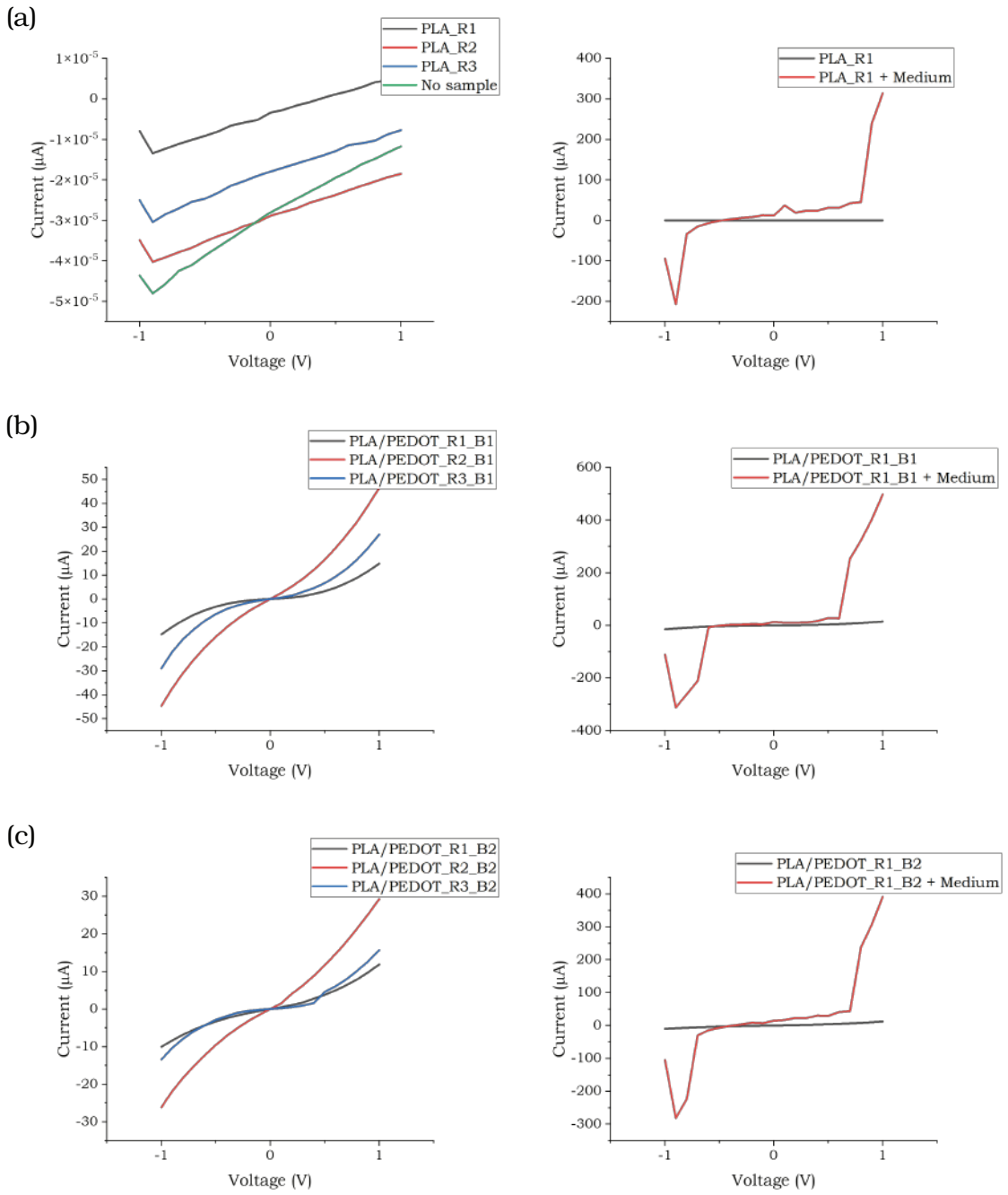

Figure 4.25: *IV* curves from the PLA electrospun fibers produced with and without PEDOT. In the left, the *IV* curves from three different replicates of the same scaffold are represented. The right side compares the values obtained from a dry sample and from that same sample containing culture medium.

therefore, considered non-ohmic conductors. The values of current were in the same range for PLA/PEDOT samples of both VPP chambers. These samples were shown to conduct currents of an order of magnitude of 1×10^{-5} A. The measures obtained with samples exposed to culture medium were non-linear and not conclusive. Overall, the values obtained using the bioreactor as a 2-point probe seem reasonable, but this system needs further validation, testing more samples and evaluating parameters that may affect the readings.

4.4 Cytotoxicity Assay

Resazurin is a non-fluorescent blue dye that is widely used as an indicator of cell viability. Once incubated with resazurin, viable mammalian cells which are metabolically active, will reduce resazurin to resorufin, a fluorescent pink compound. As such, by measuring the absorbance of a sample in which cells were incubated with resazurin for a certain period, it is possible to infer their metabolic activity through the change in color of the medium, and thus, obtain a percentage of viable cells, normalized to a negative control [105].

So, the results from the cytotocitity assay are presented as measures of cell viability after exposure of SH-SY5Y cell to two types of conditioned media, both at four different extract concentrations. The results, being normalized to the live-cell/negative control (C-), should be values between 0 and 1, with the absorbance of 1 being attributed to the control itself. Contrarily, the dead-cell/positive control (C+) should have a value close to zero. In sum, the less cytotoxic a material is, the closer the cell viability will be to 1.

In order to verify if controls were appropriate, as to ensure credible results, microscopy images of both the live-cell and the dead-cell controls were taken, and are presented in Figure 4.26. As observed, the live-cell control contains well adhered SH-SY5Y cells, some grown in clusters and others more separated from each other, at approximately 60-70% confluency. With respect to the dead-cell control, the image shows a large amount of non-adhered dead SH-SY5Y cells, in a ball like shape, with no visible live cells. As such, controls were considered suitable for the resazurin assay.

Overall, as detailed in Figure 4.27, results reveal that none of the extracts tested is cytotoxic, since cell viability values are close to 1, independently of the concentration tested. Also, as expected, the value for the viability of the dead-cell control is close to zero.

4.5 SH-SY5Y Growth on Materials

SH-SY5Y cells were grown in PLA and PLA/PEDOT aligned fibers, while exposed to the differentiation condition deemed most effective, 3% FBS + 10 µM RA. These cells were kept for a total of 13 days, during which morphological markers of differentiation were visible, including the extension of some longer neurites, following the preferential

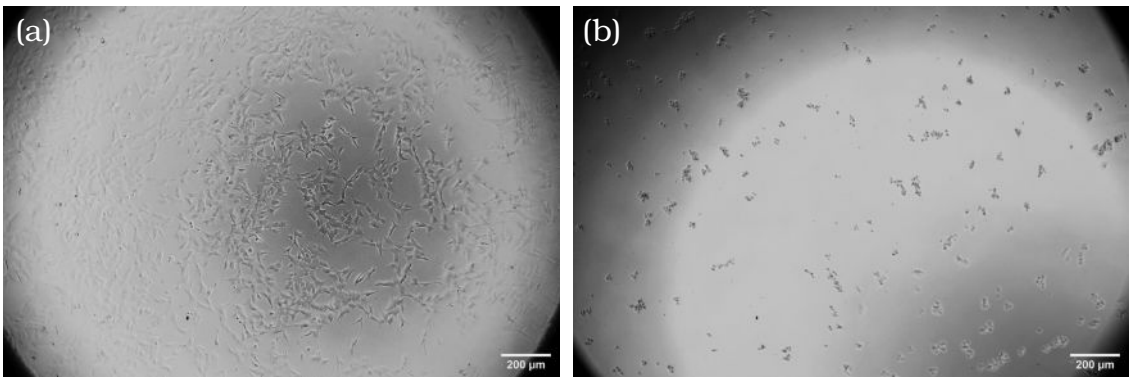

Figure 4.26: SH-SY5Y cell controls at the day of the resazurin assay: (a) Live-cell control (C-); (b) Dead-cell control (C+).

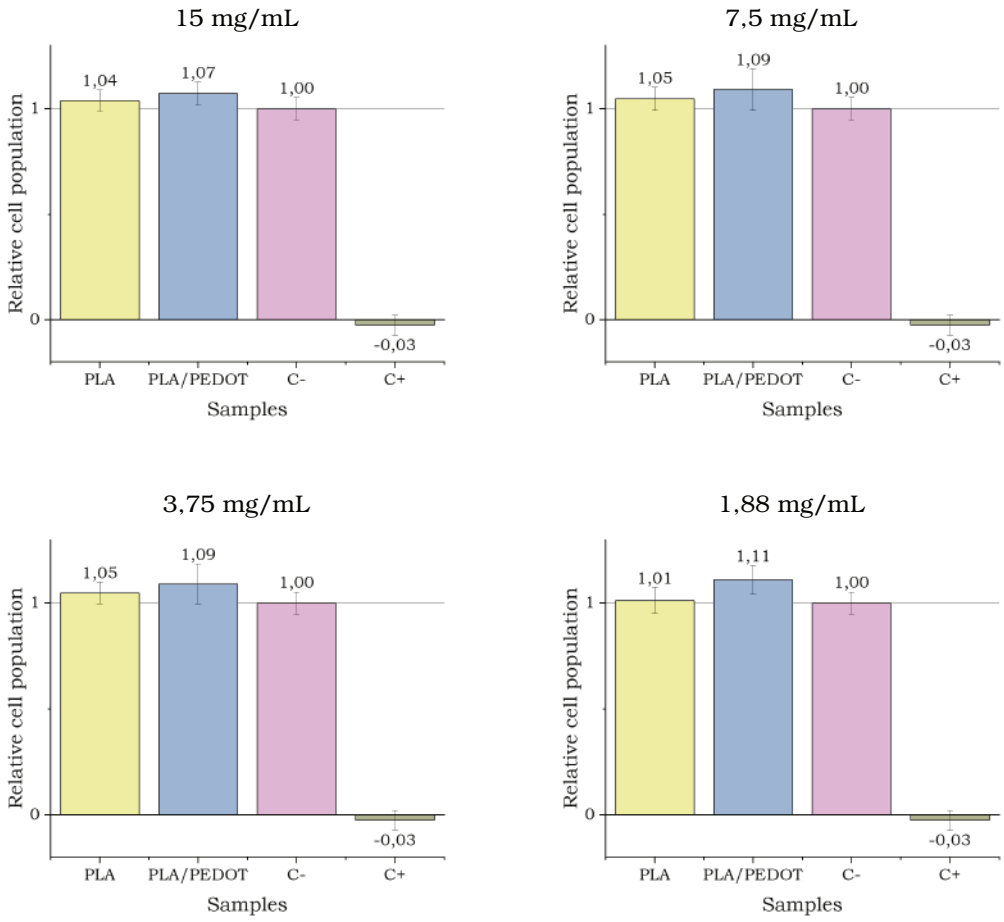

Figure 4.27: Viability of SH-SY5Y cells when exposed to PLA and PLA/PEDOT extracts, in four different concentrations. Results are normalized to the negative control (C-).

direction of fiber alignment, which successfully worked as a guidance cue for neuronal growth. The evolution of the SH-SY5Y cells in each material is represented in Figure 4.28.

The coverslip control presented a similar evolution compared to the correspondent condition at section 4.1. By day 5, meaning 4 days of exposure to RA, cells already exhibited a differentiated morphology, namely by showing extended neurites, establishing contact with nearby cells, resembling axons, in an area of relatively spaced cells. As the culture progressed, some areas of higher cell density were found and, as expected, a smaller number of cells extended neurites. At day 9, some long neurites were still visible. Finally, day 13 was also marked by a small population of cells with a polarized cell body and some longer neurites establishing connections to other cells, however a larger population of cells exhibiting a rounded cell body and small neuritic extensions was still present.

Overall, cells cultured in fibers appeared to be at a lower density, when compared to the coverslip control. As these fibers are considered non-cytotoxic, this effect has two possible explanations. On the one hand, cell adhesion to the fibers may not be ideal. However, adhesion tests were not conducted to further extrapolate on this observation. On the other hand, when obtaining the fluorescence images, it was observed that some cells seemed to be at different focusing planes, which is in accordance to the type of scaffold that is being studied. As fibers are superimposed to each other, is is natural for cells to adhere in fibers at different plane heights.

The growth of SH-SY5Y cells was similar in both PLA and PLA/PEDOT aligned fibers. From as early as day 5, a pattern is observed in which cells extended neurites with directionality, in contrast with the randomly extended neurites found in the coverslip control. This is a positive indication of topographical support associated with the presence of aligned fibers, as desired. In PLA/PEDOT fibers, this effect is not as clear due to poor image quality. Some small clusters were also present. At day 9, cells showed a similar distribution and pattern, and neurite lenght was not significantly increased. Finally, by day 13, directionality appeared even more marked, with a larger population of cells exhibiting neurites, growing in the direction of preferential fiber alignment, in both groups. Even in less polarized cells, their small projections are parallel to the longer neurites found close by. It was not clear which material led to more and longer neurites, nonetheless these results are in agreement with the findings from Pires et al. [103], in which differentiation in a preferential direction was found in similar matrices. In fact, the author found neurites in SH-SY5Y cells differentiated in similar conditions, that appear to be of a similar length. A larger sample is needed to execute a statistically relevant quantitative analysis of neurite length evolution and number of neurites extended by cell, on both materials.

4.6 Electrical Field Induced Medium Alterations

As already mentioned, even though direct coupling systems are the most common approach to deliver ES to cells in culture, there are some considerations needed to ensure

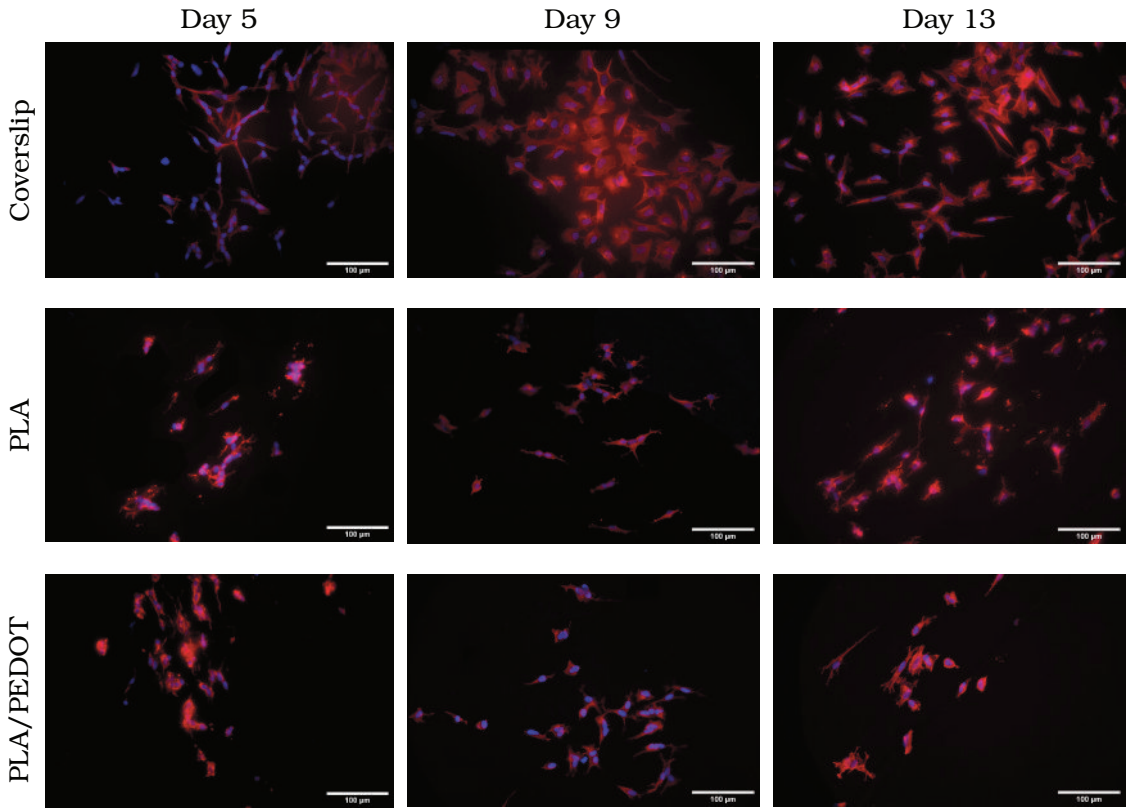

Figure 4.28: Fluorescence images of SH-SY5Y cell growth on the scaffolds at three different time points. Cell nuclei are marked in blue, whereas cytoskeletons appear in red.

cell safety, associated with the presence of electrodes in direct contact with the culture media, an electrolyte solution [9]. These are associated with electrochemical processes of charge injection that can occur at the electrode/electrolyte interface, while establishing a given potential difference between the electrodes [106].

There are two main charge transfer mechanisms taking place at the electrode/culture medium interface, upon the application of an electrical field between the two electrodes, namely Faradaic and non-Faradaic reactions. In Faradaic reactions, electrons are transferred between the electrode and the medium, promoting redox reactions in the electrolyte, while in non-Faradaic reactions, no electrons are transferred between the electrode and the medium. While the former is responsible for reduction and oxidation reactions in the electrolyte, the latter leads to a redistribution of charged compounds in the medium [106]. The knowledge of this reactions is of great importance in experimental planning, including, in this case, the design of a safe protocol for the ES of SH-SY5Y cells.

In this connection, different voltage gradients were established between the electrodes of the bioreactor, containing either water or low-serum DMEM and visible alterations were registered. The specific conditions that were tested, as well as remarks on what was observed, are specified in Table 4.1 and represented in Figure 4.29. These conditions were in the range of electrical fields found to induce neuronal differentiation of SH-SY5Y

cells, as detailed in Table 2.1 from the literature review.

In order to prevent water electrolysis, occurring at 1.2 V, Pires et al. chose to apply 1 V through a distance of 1 cm to a culture of SH-SY5Y cells [54]. Both these conditions were reproduced in water, and after 1 h of application, none seemed to produce any visible effects. As such, 2 V/cm was chosen to induce and visualize water electrolysis. In fact, in condition C, medium became yellowish, which is indicative of a drop in water pH, by the formation of acidic byproducts, due to water electrolysis [106]. Furthermore, an extra condition was tested, 5 V/cm, on the one hand, to get a sense of the progression of byproduct formation with increasing electrical fields, and on the other hand, to compare with results from a second set of conditions, in which equivalent voltages were applied at a certain frequency. As expected, this condition produced visible alterations, namely formation of yellowish species in the water, as well as formation of small bubbles in both electrodes. These results suggest that, in conditions C and D, the generated current was sufficient to induce electron transfer at the interface between the stainless steel electrodes and the electrolyte. In condition D, the bubbles are best explained as byproducts from the reduction and oxidation of water, at the cathode and at the anode, respectively, as detailed by Merril et al. [106]. Hydrogen is formed at the cathode and oxygen is formed at the anode.

These same fields were applied in medium supplemented with 5% FBS, as it was the condition with the highest serum content, from the ones being tested, in parallel, in section 4.1. Contrarily to what was observed in water, the application of a 1.2 V/cm electrical field led to a change in the color of the medium. The phenol red die present in the medium started to turn yellow, progressing from the positive electrode. This is, probably, associated with oxidation of water, taking place at the anode, which produces hydron species, meaning that the medium was more acidic in that region. Furthermore, there is clear adsorption of species to the surface of the positive electrode, which can be identified as negatively charged proteins from the culture medium, forced to the electrode, as the current generated was sufficient for charge redistribution. Conditions C' and D' showed the same effects, yet progressively more pronounced. In both, a clear yellow phase was quickly formed from the positive electrode, as well as foam originating from the negative electrode.

As observed, only a field of 1 V/cm did not produce any visible alteration in the low-serum medium. As such, only this condition was deemed suitable for use in the ES assay, as well as fields of a lower magnitude. However, there is also the option of using a function generator to produce a biphasic pulsed stimulus, which was tested in a similar fashion. These option has gained interest over the continuous application of a stimulus, constituting a safer approach overall [107]. The idea behind this is that, as current direction changes with a certain frequency, there will be a stimulus applied, which is intended to produce a physiological effect on cells, followed by a reversed stimulus of the same magnitude, which reverses some of the electrochemical processes, depending on the kinetics of each reaction. This concept is explained in more detailed elsewhere

Table 4.1: Results from 1 h of continuous electrical field application to water and low-serum DMEM using the bioreactor.

Condition	Medium	V (V)	EF (V/cm)	Remarks
A	Water	0.88	1	No visible alterations.
B	Water	1.06	1.2	No visible alterations.
C	Water	1.76	2	Water became yellowish.
D	Water	4.40	5	Gas formation occurred, visible in the form of bubbles in both electrodes; some yellowish species are visible.
A'	5% FBS DMEM	0.88	1	Medium is intact; some dirt detached from the electrode.
B'	5% FBS DMEM	1.06	1.2	Clear change of medium color from pink to yellowish, starting from the positive electrode; adsorption of unknown species to the positive electrode.
C'	5% FBS DMEM	1.76	2	Medium became progressively more yellow starting from the positive electrode; presence of two phases, yellow and pink, divided by a black interface; foam originated from the negative electrode.
D'	5% FBS DMEM	4.40	5	Similar to condition C', but it was more pronounced and progressed quicker.

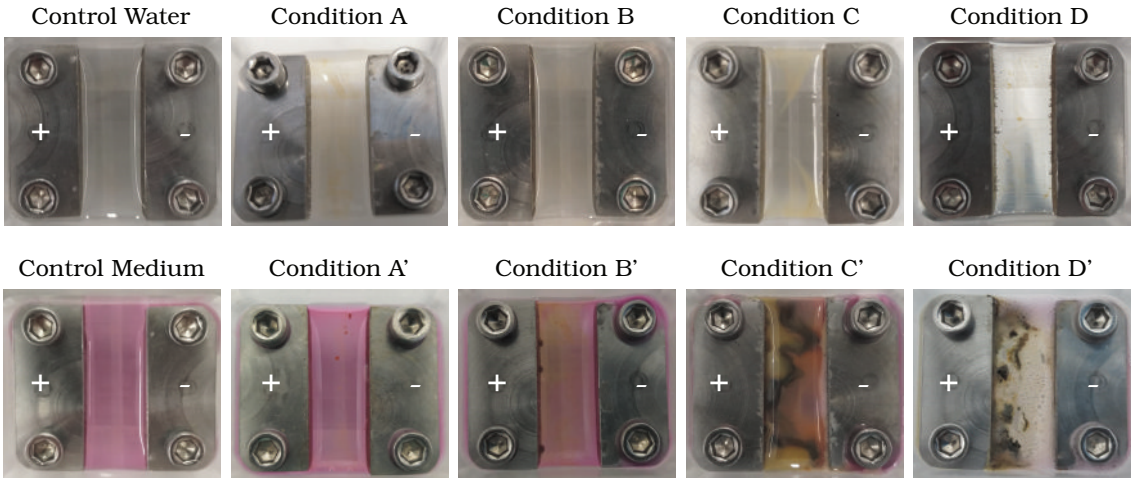

Figure 4.29: Visible alterations in water and low-serum DMEM from 1 h of continuous application of distinct voltage gradients between the electrodes.

[106]. In accordance to what was expected, the conditions detailed in Table 4.2 and represented in Figure 4.30, produced little to no visible alterations, in neither water or low-serum medium and were deemed safe for cell stimulation. Only condition H' is not recommended, since it presented a slight modification in medium color to a yellowish tone, indicative of medium acidification. Importantly, the peak-to-peak voltage values correspond to the values applied continuously in the already described experiments, but were delivered in pulses reversed at a frequency of 0.5 Hz. Finally, one important consideration is that, some of the images may be misleading, since some of the yellowish regions were, actually, marks left on the bottom of the PMMA well and not from the water/medium used. This was taken into account when writing the remarks.

Table 4.2: Results from 1 h of biphasic electrical field application to water and low-serum DMEM using the bioreactor.

Condition	Medium	V pk-pk (V)	EF (V/cm)	f (Hz)	Remarks
E	Water	0.88	± 0.5	0.5	No visible alterations.
F	Water	1.06	± 0.6	0.5	No visible alterations.
G	Water	1.76	± 1	0.5	No visible alterations.
H	Water	4.40	± 2.5	0.5	No visible alterations.
E'	5% FBS DMEM	0.88	± 0.5	0.5	No visible alterations.
F'	5% FBS DMEM	1.06	± 0.6	0.5	No visible alterations.
G'	5% FBS DMEM	1.76	± 1	0.5	No visible alterations.
H'	5% FBS DMEM	4.40	± 2.5	0.5	Medium turned slightly yellowish; this effect is more visible from the side.

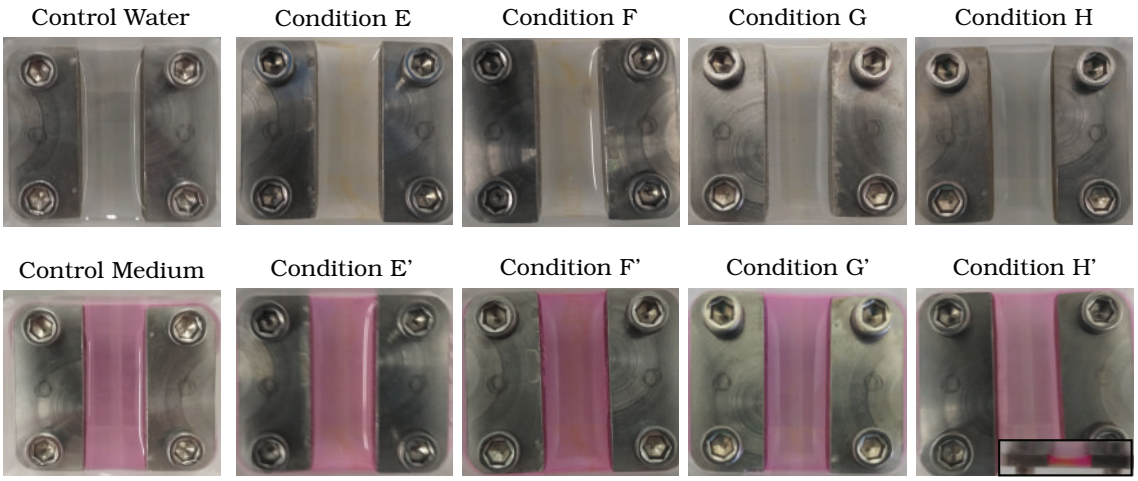

Figure 4.30: Results from 1 h of biphasic voltage application between the electrodes, using water and low-serum DMEM.

4.7 Electrical Stimulation Assay

In parallel with the culture from section 4.5, a single *in vitro* assay was performed, where SH-SY5Y cells, from the same suspension, were cultured in the bioreactor and subjected to multiple optimized differentiation agents, including ES, as an attempt to further induce neuronal differentiation. Specifically, these cells were grown in PLA/PEDOT aligned fibers, using DMEM supplemented with 3% FBS and 10 µM of RA, while an electrical field of 500 mV/cm was being established between the electrodes of the bioreactor, 1 h/day, for a total of 9 days. Generally, no significant improvements resulted from the addition of this particular ES, over the differentiation of cells without stimulation. A general view of the cells found in this assay is shown in Figure 4.31.

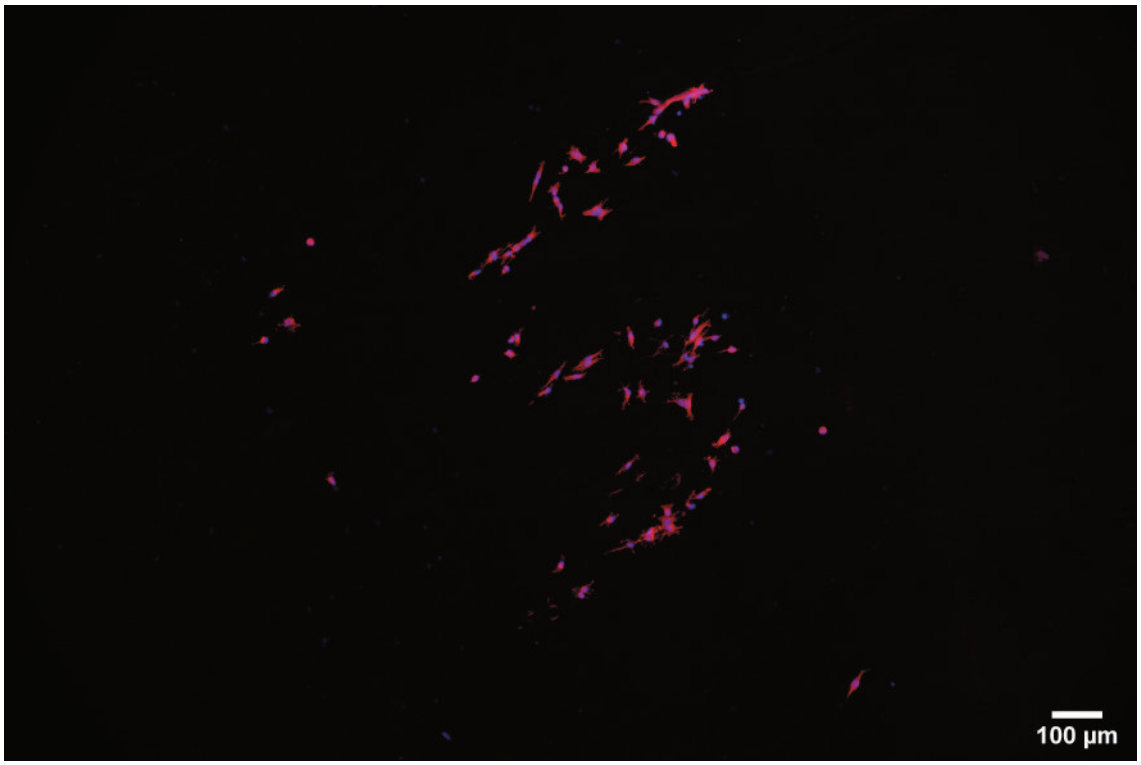

Figure 4.31: Fluorescence image of the general view of SH-SY5Y cells subjected to the ES protocol, using the bioreactor. Cell nuclei are marked in blue, whereas cytoskeletons appear in red.

Due to limited time, only one sample was studied with one ES condition. So, it was important to select a condition that would both, in theory, produce a visible improvement in cell differentiation and, at the same time, avoid the risk of significantly affecting cell viability. The chosen electrical field, met the criteria set in section 3.6, by which a continuous electrical field should not surpass 1 V/cm, tested for 1 h. The same duration of application of the stimulus was used in this assay. Furthermore, continuous ES have been successfully implemented for neuronal differentiation, with values of electrical field being commonly used at a range between 100 mV/cm and 100 mV/mm [8], [57], [58],

[60]. Importantly, a control without simulation was being simultaneously conducted in section 4.28, at three distinct time points. In accordance, it was established that the ES assay would consist in a 9 day culture.

The selected ES protocol was not particularly effective in promoting neuronal differentiation, comparing to what was observed in a similar sample without ES. Cell density was similar in both groups, and was adequate to understand the different cell morphologies present in each. Relative to neurite alignment, both groups showed cells with relatively short neurites, following a preferential direction of alignment. A few cells with longer neurites were observed in the ES group, as shown in Figure 4.32. However, there was still a population of cells that showed undifferentiated morphology, with short neurites and rounded cell bodies. This was not quantified and needs further analysis, namely by collecting a larger sample of both conditions.

Even though this particular ES failed to significantly enhance the level of neuronal differentiation of cells cultured in aligned fibers and low-serum medium containing RA, this assay is considered a proof of functionality and usability of the bioreactor. It has been shown that, by using the bioreactor produced, assembled as a direct coupling system, it is possible to perform culture and ES of SH-SY5Y cells. Importantly, a wide variety of conditions can be tested, by either using a power supply or a function generator, given possible medium alterations are previously assessed, which provides a large margin of parameters to be manipulated in future tests.

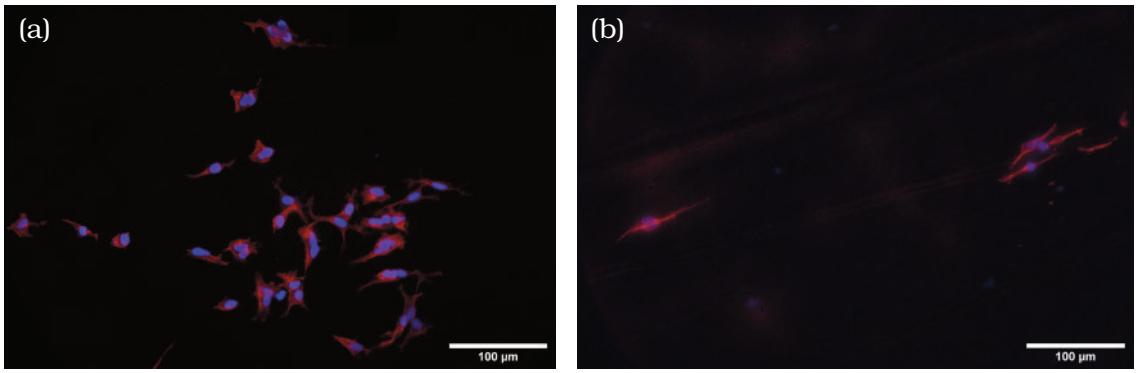

Figure 4.32: Fluorescence images comparing SH-SY5Y growth and differentiation in aligned fibers of PLA/PEDOT: (a) Without ES; (b) With ES.

5

Conclusions and Future Perspectives

In this final section, the major conclusions of each task of this dissertation are presented. The extent to which each of the goals proposed was fulfilled will be discussed, leading to an outline of suggestions of future work.

This dissertation was conducted in partnership with the NEURiTES project PTDC/CTM-COM/32606/2017. Altogether, the work developed contributed to the project, and to the field of neuronal TE, since it provides a new setup and experimental model to further explore the potential of external application of ES on the regeneration of neuronal cells and, ultimately, help develop treatment strategies to aid those suffering from lesions of the nervous system.

In retrospect, there are a lot of steps that could have been performed in a different manner, during the course of this dissertation. Many of them have a considerable margin for improvement and further exploration, namely through applying more systematic approaches to better characterize results.

5.1 Optimization of Differentiation Protocol

Using 1% FBS significantly affected cell viability for both concentrations of RA. In groups of both 3% an 5% FBS, morphological signs of differentiation were visible with only 2 days of exposure to RA, independently of its concentration. It was noted that, as clusters became less visible, a population of cells tended to present more pyramidal shaped and elongated bodies, some of which extending long neurites. In the following days of culture, the level of differentiation did not progress significantly, and all conditions were still marked by the presence of rounded undifferentiated cells. Due to the early presence of a slightly larger population of cells presenting neuritic extensions, 3% FBS + 10 µM RA was the medium chosen for neuronal differentiation in the *in vitro* tests conducted on the materials, both with and without stimulation.

This task needs further optimization in order to achieve a cell morphology more similar to what is presented in Figure A.1 (b). Future cultures should further assess the influence of DMSO concentration in the medium, as both 0.5% and 1% controls led to

significant cell death, yet cell viability in the differentiation medium was not affected to the same extent. Establishing the ideal initial cell density was also problematic, as 2×10^3 cells/cm^2 led to excessive proliferation in more clustered areas, which limits differentiation, yet with 1×10^3 cells/cm^2, cells were plated too sparsely, significantly reducing proliferation and increasing cell death, leaving very few cells for evaluation. So, a better balance between cell proliferation and cell death should be attempted, namely by using an intermediate density of 1.5×10^3 cells/cm^2. Another possible factor contributing to loss of neuronal characteristics is a high cell passage [91]. As a suggestion, this culture should be repeated using both concentrations of RA, and 3% and 5% FBS in DMEM, with SH-S5Y5 cells of a passage lower than 23, as used by Simões et al. [90].

5.2 Design and Assembly of the Bioreactor

The main goal of this dissertation, the development of a bioreactor for the ES of cells, was achieved. After several preliminary design attempts, a final one was achieved for a direct coupling system, the simplest and most used method in the literature [20]. Despite the method of stimulation being the same, the setup that was created is more robust, compared to approaches using cell culture plates or Petri dishes in a non-standardized manner [8], [20], [66].

Fixing the produced matrices to the bottom of the well worked as expected, by placing a sample under the internal electrodes. However, this assembly is not optimal since it leaves two 0.75 cm x 0.88 cm areas of culture uncovered by the sample. As a first approach to avoid the loss of cell suspension during *in vitro* assays, two *teflon* blocks could be used to cover those areas, leaving only an area of culture of 1 cm x 0.88 cm, which would be completely covered by the conductive scaffold, as desired. Fixing the electrodes exclusively through the pressure applied by the two M2 lid screws can also be attempted, which would also allow the placement of a larger sample under the electrodes, since the internal screws would not be used.

In general, the prototype produced closely resembles the design chosen and allows a versatile control of currents and parameters for ES of cells. As a first prototype, the bioreactor consists of a single well. In the future, once more ES conditions have been tested with this setup, it would be ideal to create a multi-well design, as is it very time consuming to conduct experiments one sample at a time, especially for longer cultures, like those performed during this dissertation. Furthermore, running the multiple wells simultaneously would be a more controlled experiment when it comes to ensuring the same conditions are met (same medium preparation, same cell suspension, among other aspects). In fact, a 6-well design was already analysed, but not produced yet, since further testing is needed in the existing chamber. This is represented in Figure 5.1, as an example of future work.

It is worth mentioning that the electrical connections can also be established with a personalized voltage or current provider. In the long term, in conjunction with the

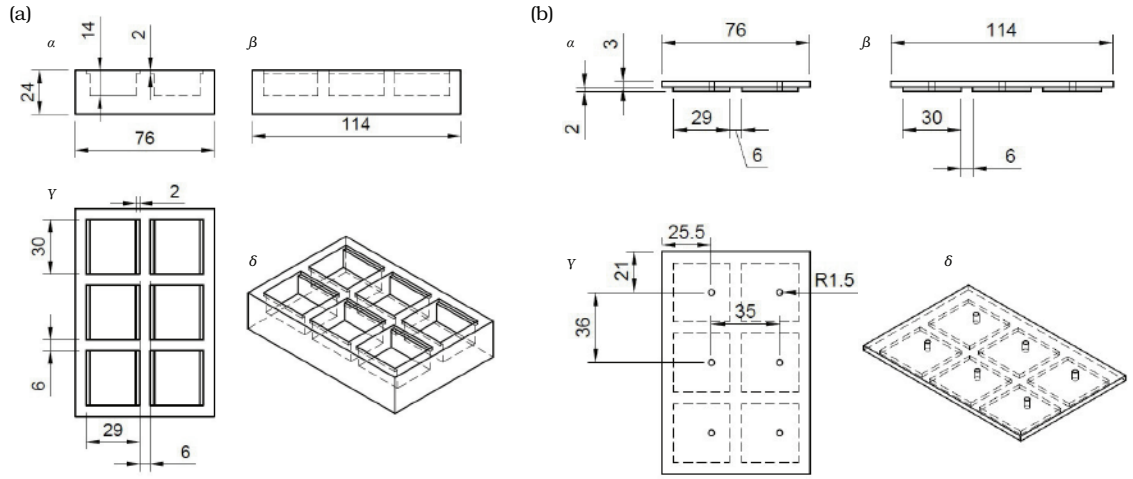

Figure 5.1: Dimensional drawing of the front (α), side (β), top (γ) and orthometric (δ) views from a proposed (a) 6-well stimulation system and its (b) lid. All dimensions are in mm.

6-well design, it would be interesting to expound on the idea of creating a low-weight, portable and programmable current/voltage provider. Some thought was already given to this possibility and some preliminary tests were performed using an Arduino Uno. One suggestion would be to assemble tension dividers in a breadboard, using a six-channel digital potentiometer, like the AD5206 model from Mouser Electronics [108], which can be controlled by programming an Arduino Uno [109].

5.3 Fabrication of Conductive Scaffolds

Conductive scaffolds were a subject of interest in this dissertation, given the nature of the stimulus being considered for achieving better neuronal differentiation, which is ES. A variety of attempts were made for obtaining a conductive film, which in general, failed due to film brittleness, which made the films obtained unsuitable for assembly in the bioreactor. Furthermore, increasing the PLA to FeTos ratio did not reduce film brittleness. SEM images revealed that the electrospinning technique was successfully employed in the production of aligned PLA fibers. These were produced from a solution incorporating the oxidant required for polymerization of EDOT vapors on the fibers. VPP was performed, resulting in PEDOT formation on the electrospun scaffolds, whose electrical behavior was assessed in a preliminary manner. The bioreactor was used as a 2-point probe, for obtaining *IV* curves of the materials produced. In the PLA/PEDOT scaffolds, the currents measured were of the order of magnitude of 1×10^5 A. The measurements performed on samples containing culture medium were not conclusive. The characterization of the electrical behavior of PLA/PEDOT fibers needs further exploration and is a crucial step for understanding their suitability for ES of cells. Cyclic voltametry of these samples is widely recommended in future work.

5.4 SH-SY5Y Growth on Materials

Fluorescence morphological imaging of SH-SY5Y cells grown and differentiated on aligned PLA and PLA/PEDOT fibers at three different time points showed visible RA-induced neuritic extensions. These grew according to the preferential direction of fiber alignment, which worked as a topographical guidance cue. This effect was similar in fibers with and without PEDOT.

Future perspectives encompass collecting a significantly large sample so that a quantitative analysis of neurite length can be performed and therefore, establish a control for the ES assay, for which the same analysis is recommended. Besides length, it can also be interesting to investigate the number of neurites extended by each cell. ImageJ [101] provides a plugin, NeuronJ, specifically built for neurite tracing and analysis, which could be explored in further assays. Moreover, it would also be of great value to quantify specific neuronal gene expression of SH-SY5Y cells, cultured with and without ES, using RT-PCR for β-III tubulin, MAP2 and synaptophysin, among others [82].

5.5 Electrical Field Induced Medium Alterations

Different electrical fields were tested on the bioreactor, containing only low-serum DMEM to understand the range of ES conditions that could be applied without the risk of compromising the original medium composition, either by changing medium pH, through water electrolysis, or by formation of toxic byproducts from electrode corrosion. It was concluded that, for the ES assay, the continuous application of electrical fields over 1 V/cm for 1 hour, should be avoided. Furthermore, biphasic stimulation was deemed a safer choice, since periodic inversions in current direction contribute to reverse some electrochemical reactions in the media. The medium only seemed to became more acidic for ± 2.5 V/cm, 0.5 Hz, which was still much less damaging, comparing to a continuous application of 2 V/cm, for 1 hour.

To gain greater insight for the design of future ES protocols, this type of test should be continued. More conditions should be tested, namely different AC frequencies applied for longer periods of time.

5.6 Electrical Stimulation Assay

Finally, an ES protocol was performed on SH-SY5Y cells cultured on PLA/PEDOT aligned fibers, fixed on the bioreactor, while exposed to 3% FBS + 10 µM RA medium. These cells, subjected to 500 mV/cm, 1 h/day, for 9 days, displayed a similar population of cells extending neurites, compared to the unstimulated control, and showed preferential alignment following fiber direction. Although cell morphology shows some signs of differentiation, it was not significantly enhanced by the presence of this particular ES.

As only one sample and a single condition was tested, it is necessary to keep conducting similar research on this setup. It is also important to better characterize the stimulus being applied in real time, namely by monitoring the input and output stimulus using an oscilloscope. A wide variety of protocols encompassing ES should and can now be tested by other members of the NEURiTES project. Most questions are still unanswered, and the mechanisms by which ES improves neuronal regeneration remain unclear. Nevertheless, we believe that great insight can be achieved through the application of external ES *in vitro*. For that, a bioreactor was designed, assembled and tested, successfully addressing the main goal of this dissertation and contributing to the field of neuronal TE.

Bibliography

[1] J. M. Lourenço, *The NOVAthesis LaTeX Template User's Manual*, NOVA University Lisbon, 2021. [Online]. Available: https://github.com/joaomlourenco/novathesis/raw/master/template.pdf.

[2] M. Nadi and R. Midha, "61 - management of peripheral nerve injuries", in *Principles of Neurological Surgery (Fourth Edition)*, R. G. Ellenbogen, L. N. Sekhar, N. D. Kitchen, and H. B. da Silva, Eds., Fourth Edition, Philadelphia: Elsevier, 2018, 832–841.e2, ISBN: 978-0-323-43140-8. [Online]. Available: https://www.sciencedirect.com/science/article/pii/B9780323431408000615 (visited on 08/26/2021).

[3] M. E. Vargas and B. A. Barres, "Why is wallerian degeneration in the cns so slow?", *Annual Review of Neuroscience*, vol. 30, no. 1, pp. 153–179, 2007. [Online]. Available: https://doi.org/10.1146/annurev.neuro.30.051606.094354 (visited on 08/25/2021).

[4] A. Faroni, S. A. Mobasseri, P. J. Kingham, and A. J. Reid, "Peripheral nerve regeneration: Experimental strategies and future perspectives", *Advanced Drug Delivery Reviews*, vol. 82, pp. 160–167, 2015. [Online]. Available: http://dx.doi.org/10.1016/j.addr.2014.11.010 (visited on 08/25/2021).

[5] "Tissue Engineering of the Nervous System", in *Tissue Engineering*, Academic Press, 2014, pp. 583–625, ISBN: 9780124201453. [Online]. Available: https://www.elsevier.com/books/tissue-engineering/blitterswijk/978-0-12-420145-3.

[6] A. N. Koppes, A. L. Nordberg, G. M. Paolillo, *et al.*, "Electrical stimulation of schwann cells promotes sustained increases in neurite outgrowth", *Tissue Engineering - Part A*, vol. 20, no. 3-4, pp. 494–506, 2014. [Online]. Available: https://pubmed.ncbi.nlm.nih.gov/24063574/ (visited on 01/24/2021).

[7] J. M. Cregg, M. A. DePaul, A. R. Filous, B. T. Lang, A. Tran, and J. Silver, "Functional regeneration beyond the glial scar", vol. 253, pp. 197–207, 2014. [Online].

Available: http://dx.doi.org/10.1016/j.expneurol.2013.12.024 (visited on 02/25/2021).

[8] L. Ghasemi-Mobarakeh, M. P. Prabhakaran, M. Morshed, M. H. Nasr-Esfahani, and S. Ramakrishna, "Electrical stimulation of nerve cells using conductive nanofibrous scaffolds for nerve tissue engineering", *Tissue Engineering - Part A*, vol. 15, no. 11, pp. 3605–3619, 2009. [Online]. Available: https://www.liebertpub.com/doi/10.1089/ten.TEA.2008.0689?url_ver=Z39.88-2003&rfr_id=ori%5C%3Arid%5C%3Acrossref.org&rfr_dat=cr_pub++0pubmed (visited on 01/20/2021).

[9] C. Chen, X. Bai, Y. Ding, and I. S. Lee, "Electrical stimulation as a novel tool for regulating cell behavior in tissue engineering", *Biomaterials Research*, vol. 23, no. 1, pp. 1–12, 2019. [Online]. Available: https://biomaterialsres.biomedcentral.com/articles/10.1186/s40824-019-0176-8 (visited on 12/21/2020).

[10] M. Chappell and S. Payne, "The Action Potential", *Biosystems and Biorobotics*, vol. 24, no. July 2007, pp. 35–45, 2020. [Online]. Available: https://www.researchgate.net/publication/6316219_The_action_potential (visited on 02/16/2021).

[11] L. P. da Silva, S. C. Kundu, R. L. Reis, and V. M. Correlo, "Electric Phenomenon: A Disregarded Tool in Tissue Engineering and Regenerative Medicine", *Trends in Biotechnology*, vol. 38, no. 1, pp. 24–49, 2020. [Online]. Available: https://doi.org/10.1016/j.tibtech.2019.07.002 (visited on 03/08/2021).

[12] M. Levin, "Molecular bioelectricity: How endogenous voltage potentials control cell behavior and instruct pattern regulation in vivo", *Molecular Biology of the Cell*, vol. 25, no. 24, pp. 3835–3850, 2014. [Online]. Available: https://www.ncbi.nlm.nih.gov/pmc/articles/PMC4244194/ (visited on 01/30/2021).

[13] *NEURiTES | great*. [Online]. Available: https://sites.fct.unl.pt/great/pages/neurites (visited on 01/30/2021).

[14] G. M. Xiong, A. T. Do, J. K. Wang, C. L. Yeoh, K. S. Yeo, and C. Choong, "Development of a miniaturized stimulation device for electrical stimulation of cells", *Journal of Biological Engineering*, vol. 9, no. 1, p. 14, 2015. [Online]. Available: http://www.jbioleng.org/content/9/1/14 (visited on 02/10/2021).

[15] C. E. Schmidt, V. R. Shastri, J. P. Vacanti, and R. Langer, "Stimulation of neurite outgrowth using an electrically conducting polymer", *Proceedings of the National Academy of Sciences of the United States of America*, vol. 94, no. 17, pp. 8948–8953, 1997. [Online]. Available: https://www.pnas.org/content/94/17/8948 (visited on 01/18/2021).

[16] N. Tandon, C. Cannizzaro, P. H. G. Chao, *et al.*, "Electrical stimulation systems for cardiac tissue engineering", *Nature Protocols*, vol. 4, no. 2, pp. 155–173, 2009. [Online]. Available: https://www.nature.com/articles/nprot.2008.183 (visited on 01/22/2021).

[17] R. Banan Sadeghian, M. Ebrahimi, and S. Salehi, "Electrical stimulation of micro-engineered skeletal muscle tissue: Effect of stimulus parameters on myotube contractility and maturation", *Journal of Tissue Engineering and Regenerative Medicine*, vol. 12, no. 4, pp. 912–922, 2018. [Online]. Available: https://pubmed.ncbi.nlm.nih.gov/28622706/ (visited on 02/08/2021).

[18] C. J. Bettinger, J. P. Bruggeman, A. Misra, J. T. Borenstein, and R. Langer, "Biocompatibility of biodegradable semiconducting melanin films for nerve tissue engineering", *Biomaterials*, vol. 30, no. 17, pp. 3050–3057, 2009. [Online]. Available: https://pubmed.ncbi.nlm.nih.gov/19286252/ (visited on 02/07/2021).

[19] M. Hronik-Tupaj, W. L. Rice, M. Cronin-Golomb, D. L. Kaplan, and I. Georgakoudi, "Osteoblastic differentiation and stress response of human mesenchymal stem cells exposed to alternating current electric fields", *BioMedical Engineering Online*, vol. 10, 2011. [Online]. Available: http://www.biomedical-engineering-online.com/content/10/1/9 (visited on 01/04/2022).

[20] R. Balint, N. J. Cassidy, and S. H. Cartmell, "Electrical stimulation: A novel tool for tissue engineering", *Tissue Engineering - Part B: Reviews*, vol. 19, no. 1, pp. 48–57, 2013. [Online]. Available: https://pubmed.ncbi.nlm.nih.gov/22873689/ (visited on 01/17/2021).

[21] R. Zhu, Z. Sun, C. Li, S. Ramakrishna, K. Chiu, and L. He, "Electrical stimulation affects neural stem cell fate and function in vitro", vol. 319, 2019. [Online]. Available: https://doi.org/10.1016/j.expneurol.2019.112963 (visited on 03/07/2021).

[22] N. Golafshan, M. Kharaziha, M. Fathi, B. L. Larson, G. Giatsidis, and N. Masoumi, "Anisotropic architecture and electrical stimulation enhance neuron cell behaviour on a tough graphene embedded PVA: Alginate fibrous scaffold", *RSC Advances*, vol. 8, no. 12, pp. 6381–6389, 2018. [Online]. Available: https://pubs.rsc.org/fa/content/articlelanding/2018/ra/c7ra13136d#!divAbstract (visited on 10/04/2021).

[23] A. Babaie, B. Bakhshandeh, A. Abedi, *et al.*, "Synergistic effects of conductive PVA/PEDOT electrospun scaffolds and electrical stimulation for more effective neural tissue engineering", *European Polymer Journal*, vol. 140, p. 110 051, 2020. [Online]. Available: https://www.sciencedirect.com/science/article/abs/pii/S0014305720317651 (visited on 12/08/2021).

[24] M. Chudickova, P. Bruza, A. Zajicova, *et al.*, "Targeted neural differentiation of murine mesenchymal stem cells by a protocol simulating the inflammatory site of neural injury", *Journal of Tissue Engineering and Regenerative Medicine*, vol. 11, no. 5, pp. 1588–1597, 2017. [Online]. Available: https://pubmed.ncbi.nlm.nih.gov/26118945/ (visited on 12/21/2020).

[25] L. Jin, B. Hu, Z. Li, *et al.*, "Synergistic Effects of Electrical Stimulation and Aligned Nanofibrous Microenvironment on Growth Behavior of Mesenchymal Stem Cells", *ACS Applied Materials and Interfaces*, vol. 10, no. 22, pp. 18 543–18 550, 2018. [Online]. Available: https://pubs.acs.org/doi/pdf/10.1021/acsami.8b04136 (visited on 01/11/2022).

[26] K.-A. Kim, K. Ja, S. Lee, and S. Kim, "Biphasic Electrical Currents Stimulation Promotes both Proliferation and Differentiation of Fetal Neural Stem Cells", *PLoS ONE*, vol. 6, no. 4, p. 18 738, 2011. [Online]. Available: https://journals.plos.org/plosone/article?id=10.1371/journal.pone.0018738 (visited on 02/12/2021).

[27] I. S. Kim, J. K. Song, Y. L. Zhang, *et al.*, "Biphasic electric current stimulates proliferation and induces VEGF production in osteoblasts", *Biochimica et Biophysica Acta - Molecular Cell Research*, vol. 1763, no. 9, pp. 907–916, 2006. [Online]. Available: https://pubmed.ncbi.nlm.nih.gov/16930744/ (visited on 02/11/2021).

[28] B. Ercan and T. J. Webster, "The effect of biphasic electrical stimulation on osteoblast function at anodized nanotubular titanium surfaces", *Biomaterials*, vol. 31, no. 13, pp. 3684–3693, 2010. [Online]. Available: https://pubmed.ncbi.nlm.nih.gov/20149926/ (visited on 01/07/2022).

[29] M. Hartig, U. Joos, and H. P. Wiesmann, "Capacitively coupled electric fields accelerate proliferation of osteoblast-like primary cells and increase bone extracellular matrix formation in vitro", *European Biophysics Journal*, vol. 29, no. 7, pp. 499–506, 2000. [Online]. Available: https://pubmed.ncbi.nlm.nih.gov/11156291/ (visited on 01/07/2022).

[30] C. P. Huang, X. M. Chen, and Z. Q. Chen, "Osteocyte: The impresario in the electrical stimulation for bone fracture healing", *Medical Hypotheses*, vol. 70, no. 2, pp. 287–290, 2008. [Online]. Available: https://www.sciencedirect.com/science/article/abs/pii/S0306987707003970 (visited on 01/07/2022).

[31] H. Zhuang, W. Wang, R. M. Seldes, A. D. Tahernia, H. Fan, and C. T. Brighton, "Electrical stimulation induces the level of TGF-β1 mRNA in osteoblastic cells by a mechanism involving calcium/calmodulin pathway", *Biochemical and Biophysical Research Communications*, vol. 237, no. 2, pp. 225–229, 1997. [Online]. Available: https://www.sciencedirect.com/science/article/abs/pii/S0006291X97971187 (visited on 01/07/2022).

[32] D. A. Savitz and E. E. Calle, "Leukemia and occupational exposure to electromagnetic fields: Review of epidemiologic surveys", *Journal of Occupational Medicine*, vol. 29, no. 1, pp. 47–51, 1987. [Online]. Available: http://www.jstor.org/stable/45007520 (visited on 01/08/2022).

[33] T. Bodamyali, B. Bhatt, F. J. Hughes, *et al.*, "Pulsed electromagnetic fields simultaneously induce osteogenesis and upregulate transcription of bone morphogenetic proteins 2 and 4 in rat osteoblasts in vitro", *Biochemical and Biophysical Research Communications*, vol. 250, no. 2, pp. 458–461, 1998. [Online]. Available: https://www.sciencedirect.com/science/article/pii/S0006291X98992439?via%5C%3Dihub (visited on 01/08/2022).

[34] R. Gaetani, M. Ledda, L. Barile, *et al.*, "Differentiation of human adult cardiac stem cells exposed to extremely low-frequency electromagnetic fields", *Cardiovascular Research*, vol. 82, no. 3, pp. 411–420, 2009. [Online]. Available: https://academic.oup.com/cardiovascres/article/82/3/411/475221 (visited on 01/08/2022).

[35] C. L. Ross and B. S. Harrison, "Effect of pulsed electromagnetic field on inflammatory pathway markers in RAW 264.7 murine macrophages", *Journal of Inflammation Research*, vol. 6, no. 1, pp. 45–51, 2013. [Online]. Available: https://www.ncbi.nlm.nih.gov/pmc/articles/PMC3617815/ (visited on 01/08/2022).

[36] W. H. Hei, S. H. Byun, J. S. Kim, *et al.*, "Effects of electromagnetic field (PEMF) exposure at different frequency and duration on the peripheral nerve regeneration: in vitro and in vivo study", *International Journal of Neuroscience*, vol. 126, no. 8, pp. 739–748, 2016. [Online]. Available: https://pubmed.ncbi.nlm.nih.gov/26010211/ (visited on 02/11/2021).

[37] Y. Cheng, Y. Dai, X. Zhu, *et al.*, "Extremely low-frequency electromagnetic fields enhance the proliferation and differentiation of neural progenitor cells cultured from ischemic brains", *NeuroReport*, vol. 26, no. 15, pp. 896–902, 2015. [Online]. Available: https://pubmed.ncbi.nlm.nih.gov/26339991/ (visited on 11/03/2021).

[38] Y. L. He, D. D. Liu, Y. J. Fang, X. Q. Zhan, J. J. Yao, and Y. A. Mei, "Exposure to Extremely Low-Frequency Electromagnetic Fields Modulates Na+ Currents in Rat Cerebellar Granule Cells through Increase of AA/PGE2 and EP Receptor-Mediated cAMP/PKA Pathway", *PLoS ONE*, vol. 8, no. 1, p. 54 376, 2013. [Online]. Available: https://journals.plos.org/plosone/article?id=10.1371/journal.pone.0054376 (visited on 01/08/2022).

[39] R. Piacentini, C. Ripoli, D. Mezzogori, G. B. Azzena, and C. Grassi, "Extremely low-frequency electromagnetic fields promote in vitro neurogenesis via upregulation of Cav1-channel activity", *Journal of Cellular Physiology*, vol. 215, no. 1,

pp. 129–139, 2008. [Online]. Available: https://onlinelibrary.wiley.com/doi/full/10.1002/jcp.21293 (visited on 01/08/2022).

[40] L. Ghasemi-Mobarakeh, M. P. Prabhakaran, M. Morshed, *et al.*, "Application of conductive polymers, scaffolds and electrical stimulation for nerve tissue engineering", *Journal of Tissue Engineering and Regenerative Medicine*, vol. 5, no. 4, e17–e35, 2011. [Online]. Available: https://onlinelibrary.wiley.com/doi/10.1002/term.383 (visited on 01/20/2021).

[41] G. Thrivikraman, S. K. Boda, and B. Basu, "Unraveling the mechanistic effects of electric field stimulation towards directing stem cell fate and function: A tissue engineering perspective", *Biomaterials*, vol. 150, pp. 60–86, 2018. [Online]. Available: https://www.sciencedirect.com/science/article/abs/pii/S0142961217306300?via%5C%3Dihub (visited on 02/10/2021).

[42] C. A. Ariza, A. T. Fleury, C. J. Tormos, *et al.*, "The Influence of Electric Fields on Hippocampal Neural Progenitor Cells", *Stem Cell Reviews and Reports*, vol. 6, no. 4, pp. 585–600, 2010. [Online]. Available: https://link.springer.com/article/10.1007/s12015-010-9171-0 (visited on 09/21/2021).

[43] R. Babona-Pilipos, I. A. Droujinine, M. R. Popovic, and C. M. Morshead, "Adult subependymal neural precursors, but not differentiated cells, undergo rapid cathodal migration in the presence of direct current electric fields", *PLoS ONE*, vol. 6, no. 8, 2011. [Online]. Available: https://www.ncbi.nlm.nih.gov/pmc/articles/PMC3166127/ (visited on 01/11/2022).

[44] R. Babona-Pilipos, A. Pritchard-Oh, M. R. Popovic, and C. M. Morshead, "Biphasic monopolar electrical stimulation induces rapid and directed galvanotaxis in adult subependymal neural precursors", *Stem Cell Research and Therapy*, vol. 6, no. 1, pp. 1–14, 2015. [Online]. Available: https://stemcellres.biomedcentral.com/articles/10.1186/s13287-015-0049-6 (visited on 01/07/2022).

[45] R. Balint, N. J. Cassidy, and S. H. Cartmell, "Conductive polymers: Towards a smart biomaterial for tissue engineering", *Acta Biomaterialia*, vol. 10, no. 6, pp. 2341–2353, 2014. [Online]. Available: https://www.sciencedirect.com/science/article/pii/S1742706114000671 (visited on 01/18/2021).

[46] X. X. Wang, G. F. Yu, J. Zhang, M. Yu, S. Ramakrishna, and Y. Z. Long, "Conductive polymer ultrafine fibers via electrospinning: Preparation, physical properties and applications", *Progress in Materials Science*, vol. 115, p. 100 704, 2021. [Online]. Available: https://www.sciencedirect.com/science/article/abs/pii/S0079642520300682 (visited on 01/29/2021).

[47] B. Guo and P. X. Ma, "Conducting Polymers for Tissue Engineering", *Biomacromolecules*, vol. 19, no. 6, pp. 1764–1782, 2018. [Online]. Available: https://www.ncbi.nlm.nih.gov/pmc/articles/PMC6211800/ (visited on 02/05/2021).

[48] H. Xu, J. M. Holzwarth, Y. Yan, *et al.*, "Conductive PPY/PDLLA conduit for peripheral nerve regeneration", *Biomaterials*, vol. 35, no. 1, pp. 225–235, 2014. [Online]. Available: https://pubmed.ncbi.nlm.nih.gov/24138830/ (visited on 02/14/2021).

[49] H. Nekounam, S. Gholizadeh, Z. Allahyari, *et al.*, "Electroconductive scaffolds for tissue regeneration: Current opportunities, pitfalls, and potential solutions", *Materials Research Bulletin*, vol. 134, no. January 2020, p. 111 083, 2021. [Online]. Available: https://doi.org/10.1016/j.materresbull.2020.111083 (visited on 01/18/2021).

[50] R. Boni, A. Ali, A. Shavandi, and A. N. Clarkson, "Current and novel polymeric biomaterials for neural tissue engineering", vol. 25, no. 1, pp. 1–21, 2018. [Online]. Available: https://doi.org/10.1186/s12929-018-0491-8 (visited on 03/07/2021).

[51] L. Fan, Y. Xiong, Z. Fu, *et al.*, "Polyaniline promotes peripheral nerve regeneration by enhancement of the brain-derived neurotrophic factor and ciliary neurotrophic factor expression and activation of the ERK1/2/MAPK signaling pathway", *Molecular Medicine Reports*, vol. 16, no. 5, pp. 7534–7540, 2017. [Online]. Available: https://pubmed.ncbi.nlm.nih.gov/28944860/ (visited on 02/15/2021).

[52] G. Thrivikraman, G. Madras, and B. Basu, "Intermittent electrical stimuli for guidance of human mesenchymal stem cell lineage commitment towards neural-like cells on electroconductive substrates", *Biomaterials*, vol. 35, no. 24, pp. 6219–6235, 2014. [Online]. Available: https://pubmed.ncbi.nlm.nih.gov/24816362/ (visited on 02/14/2021).

[53] M. H. Bolin, K. Svennersten, X. Wang, *et al.*, "Nano-fiber scaffold electrodes based on PEDOT for cell stimulation", *Sensors and Actuators, B: Chemical*, vol. 142, no. 2, pp. 451–456, 2009. [Online]. Available: https://www.sciencedirect.com/science/article/abs/pii/S0925400509004018 (visited on 02/06/2021).

[54] F. Pires, Q. Ferreira, C. A. Rodrigues, J. Morgado, and F. C. Ferreira, "Neural stem cell differentiation by electrical stimulation using a cross-linked PEDOT substrate: Expanding the use of biocompatible conjugated conductive polymers for neural tissue engineering", *Biochimica et Biophysica Acta - General Subjects*, vol. 1850, no. 6, pp. 1158–1168, 2015. [Online]. Available: https://www.sciencedirect.com/science/article/abs/pii/S0304416515000409 (visited on 12/21/2020).

[55] N. C. Tsai, J. W. She, J. G. Wu, P. Chen, Y. S. Hsiao, and J. Yu, "Poly(3,4-ethylenedioxythiophene) Polymer Composite Bioelectrodes with Designed Chemical and Topographical Cues to Manipulate the Behavior of PC12 Neuronal Cells", *Advanced Materials Interfaces*, vol. 6, no. 5, pp. 1–11, 2019. [Online]. Available: https://onlinelibrary.wiley.com/doi/abs/10.1002/admi.201801576 (visited on 12/21/2020).

[56] Y. Sun, Q. Quan, H. Meng, *et al.*, "Enhanced Neurite Outgrowth on a Multiblock Conductive Nerve Scaffold with Self-Powered Electrical Stimulation", *Advanced Healthcare Materials*, vol. 8, no. 10, pp. 1–11, 2019. [Online]. Available: https://onlinelibrary.wiley.com/doi/abs/10.1002/adhm.201900127 (visited on 02/22/2021).

[57] J. Huang, X. Hu, L. Lu, Z. Ye, Q. Zhang, and Z. Luo, "Electrical regulation of Schwann cells using conductive polypyrrole/chitosan polymers", *Journal of Biomedical Materials Research - Part A*, vol. 93, no. 1, pp. 164–174, 2010. [Online]. Available: https://onlinelibrary.wiley.com/doi/10.1002/jbm.a.32511 (visited on 09/30/2021).

[58] X. Zhou, A. Yang, Z. Huang, G. Yin, X. Pu, and J. Jin, "Enhancement of neurite adhesion, alignment and elongation on conductive polypyrrole-poly(lactide acid) fibers with cell-derived extracellular matrix", *Colloids and Surfaces B: Biointerfaces*, vol. 149, pp. 217–225, 2017. [Online]. Available: http://dx.doi.org/10.1016/j.colsurfb.2016.10.014 (visited on 09/07/2021).

[59] L. Tian, M. P. Prabhakaran, J. Hu, M. Chen, F. Besenbacher, and S. Ramakrishna, "Synergistic effect of topography, surface chemistry and conductivity of the electrospun nanofibrous scaffold on cellular response of PC12 cells", *Colloids and Surfaces B: Biointerfaces*, vol. 145, pp. 420–429, 2016. [Online]. Available: http://dx.doi.org/10.1016/j.colsurfb.2016.05.032 (visited on 09/07/2021).

[60] J. Song, B. Sun, S. Liu, *et al.*, "Polymerizing pyrrole coated poly (l-lactic acid-co-ϵ-caprolactone) (PLCL) conductive nanofibrous conduit combined with electric stimulation for long-range peripheral nerve regeneration", *Frontiers in Molecular Neuroscience*, vol. 9, no. NOV2016, pp. 1–13, 2016. [Online]. Available: https://www.frontiersin.org/articles/10.3389/fnmol.2016.00117/full (visited on 09/07/2021).

[61] L. Sordini, F. F. Garrudo, C. Rodrigues, *et al.*, "Effect of electrical stimulation conditions on neural stem cells differentiation on crosslinked PEDOT:PSS films", *Frontiers in Bioengineering and Biotechnology*, vol. 9, 2021. [Online]. Available: https://www.frontiersin.org/articles/10.3389/fbioe.2021.591838/full (visited on 02/21/2021).

[62] C. Fu, S. Pan, Y. Ma, W. Kong, Z. Qi, and X. Yang, "Effect of electrical stimulation combined with graphene-oxide-based membranes on neural stem cell proliferation and differentiation", *Artificial Cells, Nanomedicine and Biotechnology*, vol. 47, no. 1, pp. 1867–1876, 2019. [Online]. Available: https://www.tandfonline.com/doi/full/10.1080/21691401.2019.1613422 (visited on 02/11/2021).

[63] W. Zhu, T. Ye, S. J. Lee, *et al.*, "Enhanced neural stem cell functions in conductive annealed carbon nanofibrous scaffolds with electrical stimulation", *Nanomedicine:*

Nanotechnology, Biology, and Medicine, vol. 14, no. 7, pp. 2485–2494, 2018. [Online]. Available: https://www.sciencedirect.com/science/article/abs/pii/S1549963417300850 (visited on 02/11/2021).

[64] L. He, Z. Sun, J. Li, *et al.*, "Electrical stimulation at nanoscale topography boosts neural stem cell neurogenesis through the enhancement of autophagy signaling", *Biomaterials*, vol. 268, p. 120 585, 2021. [Online]. Available: https://doi.org/10.1016/j.biomaterials.2020.120585 (visited on 03/08/2021).

[65] E. M. Steel, J. Y. Azar, and H. G. Sundararaghavan, "Electrospun hyaluronic acid-carbon nanotube nanofibers for neural engineering", *Materialia*, vol. 9, p. 100 581, 2020. [Online]. Available: https://www.sciencedirect.com/science/article/abs/pii/S2589152919303771 (visited on 03/08/2021).

[66] S. Wu, Y. Qi, W. Shi, M. Kuss, S. Chen, and B. Duan, "Electrospun conductive nanofiber yarns for accelerating mesenchymal stem cells differentiation and maturation into Schwann cell-like cells under a combination of electrical stimulation and chemical induction", *Acta Biomaterialia*, 2020. [Online]. Available: https://www.sciencedirect.com/science/article/abs/pii/S1742706120306966 (visited on 10/09/2021).

[67] N. W. S. Kam, E. Jan, and N. A. Kotov, "Electrical stimulation of neural stem cells mediated by humanized carbon nanotube composite made with extracellular matrix protein", *Nano Letters*, vol. 9, no. 1, pp. 273–278, 2009. [Online]. Available: https://pubs.acs.org/doi/10.1021/nl802859a (visited on 01/21/2021).

[68] C. Chen, S. Ruan, X. Bai, C. Lin, C. Xie, and I. S. Lee, "Patterned iridium oxide film as neural electrode interface: Biocompatibility and improved neurite outgrowth with electrical stimulation", *Materials Science and Engineering C*, vol. 103, 2019. [Online]. Available: https://doi.org/10.1016/j.msec.2019.109865 (visited on 02/22/2021).

[69] A. Rahmani, S. Nadri, H. S. Kazemi, Y. Mortazavi, and M. Sojoodi, "Conductive electrospun scaffolds with electrical stimulation for neural differentiation of conjunctiva mesenchymal stem cells", *Artificial Organs*, vol. 43, no. 8, pp. 780–790, 2019. [Online]. Available: https://onlinelibrary.wiley.com/doi/10.1111/aor.13425 (visited on 01/22/2021).

[70] L. J. Kobelt, A. E. Wilkinson, A. M. McCormick, R. K. Willits, and N. D. Leipzig, "Short Duration Electrical Stimulation to Enhance Neurite Outgrowth and Maturation of Adult Neural Stem Progenitor Cells", *Annals of Biomedical Engineering*, vol. 42, no. 10, pp. 2164–2176, 2014. [Online]. Available: https://link.springer.com/article/10.1007%5C%2Fs10439-014-1058-9 (visited on 09/06/2021).

[71] M. N. Peter, A. Warnecke, U. Reich, *et al.*, "Influence of In Vitro Electrical Stimulation on Survival of Spiral Ganglion Neurons", *Neurotoxicity Research*, 2019. [Online]. Available: https://link.springer.com/article/10.1007%5C%2Fs12640-019-00017-x (visited on 02/22/2021).

[72] N. Tandon, E. Cimetta, A. Taubman, *et al.*, "Biomimetic electrical stimulation platform for neural differentiation of retinal progenitor cells", *Proceedings of the Annual International Conference of the IEEE Engineering in Medicine and Biology Society, EMBS*, pp. 5666–5669, 2013. [Online]. Available: https://www.ncbi.nlm.nih.gov/pmc/articles/PMC4476523/ (visited on 11/16/2021).

[73] H. Zhao, A. Steiger, M. Nohner, and H. Ye, "Specific intensity direct current (DC) electric field improves neural stem cell migration and enhances differentiation towards βIII-tubulin+ neurons", *PLoS ONE*, vol. 10, no. 6, pp. 1–22, 2015. DOI: 10.1371/journal.pone.0129625. [Online]. Available: https://journals.plos.org/plosone/article?id=10.1371/journal.pone.0129625 (visited on 01/07/2022).

[74] Y. J. Chang, C. M. Hsu, C. H. Lin, M. S. C. Lu, and L. Chen, "Electrical stimulation promotes nerve growth factor-induced neurite outgrowth and signaling", *Biochimica et Biophysica Acta - General Subjects*, vol. 1830, no. 8, pp. 4130–4136, 2013. [Online]. Available: https://www.sciencedirect.com/science/article/abs/pii/S0304416513001359?via%5C%3Dihub (visited on 01/18/2021).

[75] E. Tomaskovic-Crook, Q. Gu, S. N. A. Rahim, G. G. Wallace, and J. M. Crook, "Conducting Polymer Mediated Electrical Stimulation Induces Multilineage Differentiation with Robust Neuronal Fate Determination of Human Induced Pluripotent Stem Cells", *Cells*, vol. 9, no. 3, p. 658, 2020. [Online]. Available: https://www.mdpi.com/2073-4409/9/3/658 (visited on 02/21/2021).

[76] H. F. Chang, Y. S. Lee, T. K. Tang, and J. Y. Cheng, "Pulsed DC electric field-induced differentiation of cortical neural precursor cells", *PLoS ONE*, vol. 11, no. 6, pp. 1–17, 2016. [Online]. Available: https://journals.plos.org/plosone/article?id=10.1371/journal.pone.0158133 (visited on 01/07/2022).

[77] M. S. Graves, T. Hassell, B. L. Beier, G. O. Albors, and P. P. Irazoqui, "Electrically mediated neuronal guidance with applied alternating current electric fields", *Annals of Biomedical Engineering*, vol. 39, no. 6, pp. 1759–1767, 2011. [Online]. Available: https://link.springer.com/article/10.1007%5C%2Fs10439-011-0259-8 (visited on 01/06/2021).

[78] A. C. Mendonça, C. H. Barbieri, and N. Mazzer, "Directly applied low intensity direct electric current enhances peripheral nerve regeneration in rats", *Journal of Neuroscience Methods*, vol. 129, no. 2, pp. 183–190, 2003. [Online]. Available: https://www.sciencedirect.com/science/article/abs/pii/S0165027003002073?via%5C%3Dihub (visited on 02/08/2021).

[79] Y. Shapira, V. Sammons, J. Forden, *et al.*, "Brief Electrical Stimulation Promotes Nerve Regeneration following Experimental In-Continuity Nerve Injury", *Clinical Neurosurgery*, vol. 85, no. 1, pp. 156–163, 2019. [Online]. Available: https://academic.oup.com/neurosurgery/article/85/1/156/5035748 (visited on 02/08/2021).

[80] D. Becker, D. S. Gary, E. S. Rosenzweig, W. M. Grill, and J. W. McDonald, "Functional electrical stimulation helps replenish progenitor cells in the injured spinal cord of adult rats", *Experimental Neurology*, vol. 222, no. 2, pp. 211–218, 2010. [Online]. Available: https://reader.elsevier.com/reader/sd/pii/S0014488609005317?token=70A1F601C413D10260D6CB9F29003DCC7CD5063B04502ABB382649ECFBD355CF0DE0CD18994668297AE86BD1DB2A56E2 (visited on 02/06/2021).

[81] J. Du, G. Zhen, H. Chen, *et al.*, "Optimal electrical stimulation boosts stem cell therapy in nerve regeneration", *Biomaterials*, vol. 181, pp. 347–359, 2018. [Online]. Available: https://doi.org/10.1016/j.biomaterials.2018.07.015 (visited on 03/07/2021).

[82] J. Kovalevich and D. Langford, "Considerations for the Use of SH - SY5Y Neuroblastoma Cells in Neurobiology", in *Neuronal Cell Culture: Methods and Protocols*, New York City, USA: Humana Press, 2013, pp. 9–21. [Online]. Available: http://link.springer.com/10.1007/978-1-62703-640-5 (visited on 09/27/2021).

[83] J. L. Biedler, L. Helson, and B. A. Spengler, "Morphology and Growth, Tumorigenicity, and Cytogenetics of Human Neuroblastoma Cells in Continuous Culture", *Cancer Research*, vol. 33, no. 11, pp. 2643–2652, 1973. [Online]. Available: https://cancerres.aacrjournals.org/content/33/11/2643.long (visited on 11/25/2021).

[84] J. L. Biedler and M. Schachner, "Multiple Neurotransmitter Synthesis by Human Neuroblastoma Cell Lines and Clones", *Cancer Research*, vol. 38, no. November 1972, pp. 3751–3757, 1978. [Online]. Available: https://cancerres.aacrjournals.org/content/38/11_Part_1/3751.long (visited on 11/30/2021).

[85] S. Dwane, E. Durack, and P. A. Kiely, "Optimising parameters for the differentiation of SH-SY5Y cells to study cell adhesion and cell migration", *BMC Research Notes*, vol. 6, no. 1, 2013. DOI: 10.1186/1756-0500-6-366. [Online]. Available: http://www.biomedcentral.com/1756-0500/6/366 (visited on 11/25/2021).

[86] J. R. Murillo, L. Goto-Silva, A. Sánchez, F. C. Nogueira, G. B. Domont, and M. Junqueira, "Quantitative proteomic analysis identifies proteins and pathways related to neuronal development in differentiated SH-SY5Y neuroblastoma cells", *EuPA Open Proteomics*, vol. 16, no. March, pp. 1–11, 2017. [Online]. Available: http://dx.doi.org/10.1016/j.euprot.2017.06.001 (visited on 11/30/2021).

[87] M. Encinas, M. Iglesias, Y. Liu, *et al.*, "Sequential treatment of SH-SY5Y cells with retinoic acid and brain-derived neurotrophic factor gives rise to fully differentiated, neurotrophic factor-dependent, human neuron-like cells", *Journal of Neurochemistry*, vol. 75, no. 3, pp. 991–1003, 2000. [Online]. Available: https://onlinelibrary.wiley.com/doi/epdf/10.1046/j.1471-4159.2000.0750991.x (visited on 11/30/2021).

[88] U. S. Singh, J. Pan, Y. L. Kao, S. Joshi, K. L. Young, and K. M. Baker, "Tissue transglutaminase mediates activation of RhoA and MAP kinase pathways during retinoic acid-induced neuronal differentiation of SH-SY5Y cells", *Journal of Biological Chemistry*, vol. 278, no. 1, pp. 391–399, 2003. [Online]. Available: http://dx.doi.org/10.1074/jbc.M206361200 (visited on 12/06/2021).

[89] Y. T. Cheung, W. K. W. Lau, M. S. Yu, *et al.*, "Effects of all-trans-retinoic acid on human SH-SY5Y neuroblastoma as in vitro model in neurotoxicity research", *NeuroToxicology*, vol. 30, no. 1, pp. 127–135, Jan. 2009. [Online]. Available: https://pubmed.ncbi.nlm.nih.gov/19056420/ (visited on 12/13/2021).

[90] R. F. Simões, R. Ferrão, M. R. Silva, *et al.*, "Refinement of a differentiation protocol using neuroblastoma SH-SY5Y cells for use in neurotoxicology research", *Food and Chemical Toxicology*, vol. 149, p. 111 967, 2021. [Online]. Available: https://doi.org/10.1016/j.fct.2021.111967 (visited on 12/13/2021).

[91] *SH-SY5Y Cell Line human Neuroblast from neural tissue., 94030304 | Sigma-Aldrich*. [Online]. Available: https://www.sigmaaldrich.com/catalog/product/sigma/cb_94030304?lang=pt&region=PT&gclid=CjOKCQiA1KiBBhCcARIsAPWqoSrNVN2edxYjSsO2fOu_1IKCuXy2rkKhs6t4pOcz5wGq6ed_FMOvnTkaAtrmEALw_wcB (visited on 02/16/2021).

[92] F. M. Lopes, R. Schröder, M. L. C. d. F. Júnior, *et al.*, "Comparison between proliferative and neuron-like SH-SY5Y cells as an in vitro model for Parkinson disease studies", *Brain Research*, vol. 1337, pp. 85–94, 2010. [Online]. Available: https://reader.elsevier.com/reader/sd/pii/S0006899310007651?token=3B0491C342AEE40E5EFB101EA6F47EA0F0D46D10CA3CA1B1E036E80275A2458B0519A9B4327C5A013C149F78F446909F&originRegion=eu-west-1&originCreation=20210415132818 (visited on 12/13/2021).

[93] Sigma, "all trans-RETINOIC ACID", Sigma Prod . No . R 2625, 1996.

[94] J. Galvao, B. Davis, M. Tilley, E. Normando, M. R. Duchen, and M. F. Cordeiro, "Unexpected low-dose toxicity of the universal solvent DMSO", *FASEB Journal*, vol. 28, no. 3, pp. 1317–1330, 2014. [Online]. Available: https://faseb.onlinelibrary.wiley.com/doi/full/10.1096/fj.13-235440 (visited on 12/12/2021).

[95] Autodesk, *Fusion 360 | 3D CAD, CAM, CAE & PCB Cloud-Based Software | Autodesk*, 2021. [Online]. Available: https://www.autodesk.co.uk/products/fusion-360/overview%20https://www.autodesk.com/products/fusion-360/overview?term=1-YEAR (visited on 12/06/2021).

[96] K. T. L. Trinh, D. A. Thai, W. R. Chae, and N. Y. Lee, "Rapid Fabrication of Poly(methyl methacrylate) Devices for Lab-ona-Chip Applications Using Acetic Acid and UV Treatment", *ACS Omega*, vol. 5, no. 28, pp. 17 396–17 404, 2020. [Online]. Available: https://dx.doi.org/10.1021/acsomega.0c01770 (visited on 12/07/2021).

[97] J. C. Edelmann, L. Jones, R. Peyronnet, L. Lu, P. Kohl, and U. Ravens, "A bioreactor to apply multimodal physical stimuli to cultured cells", *Methods in Molecular Biology*, vol. 1502, pp. 21–33, 2016. [Online]. Available: https://spiral.imperial.ac.uk/handle/10044/1/39082 (visited on 12/07/2021).

[98] Corbion, "Product Data Sheet LUMINY®L175", 6/0974, 2019.

[99] A. T. Lawal and G. G. Wallace, "Vapour phase polymerisation of conducting and non-conducting polymers: A review", *Talanta*, vol. 119, pp. 133–143, 2014. [Online]. Available: http://dx.doi.org/10.1016/j.talanta.2013.10.023 (visited on 12/19/2021).

[100] "Vacuum vapour phase polymerization of high conductivity PEDOT: Role of PEG-PPG-PEG, the origin of water, and choice of oxidant", *Polymer*, vol. 53, no. 11, pp. 2146–2151, 2012. [Online]. Available: http://dx.doi.org/10.1016/j.polymer.2012.03.028 (visited on 06/27/2022).

[101] *ImageJ*. [Online]. Available: https://imagej.nih.gov/ij/ (visited on 03/22/2022).

[102] T. Kume, Y. Kawato, F. Osakada, *et al.*, "Dibutyryl cyclic AMP induces differentiation of human neuroblastoma SH-SY5Y cells into a noradrenergic phenotype", *Neuroscience Letters*, vol. 443, no. 3, pp. 199–203, 2008. [Online]. Available: https://www.sciencedirect.com/science/article/pii/S0304394008010483 (visited on 02/22/2022).

[103] L. S. Pires, "Production of PEDOT-coated scaffolds by vapor phase polymerization for neural regeneration", M.S thesis, NOVA SST, Almada, PT, 2021.

[104] D. Levasseur, I. Mjejri, T. Rolland, and A. Rougier, "Color tuning by oxide addition in PEDOT:PSS-based electrochromic devices", *Polymers*, vol. 11, no. 1, pp. 1–12, 2019. [Online]. Available: https://www.mdpi.com/2073-4360/11/1/179 (visited on 04/14/2022).

[105] K. Präbst, H. Engelhardt, S. Ringgeler, and H. Hübner, "Basic colorimetric proliferation assays: MTT, WST, and resazurin", in *Methods in Molecular Biology*, vol. 1601, Humana Press, New York, NY, 2017, ch.1, pp. 1–17. [Online]. Available: https://link.springer.com/protocol/10.1007/978-1-4939-6960-9_1.

[106] D. R. Merrill, M. Bikson, and J. G. Jefferys, "Electrical stimulation of excitable tissue: Design of efficacious and safe protocols", *Journal of Neuroscience Methods*, vol. 141, no. 2, pp. 171–198, 2005. [Online]. Available: https://www.sciencedirect.com/science/article/abs/pii/S0165027004003826?via%5C%3Dihub (visited on 03/27/2022).

[107] I. Rocha, G. Cerqueira, F. Varella Penteado, and S. I. Córdoba de Torresi, "Electrical Stimulation and Conductive Polymers as a Powerful Toolbox for Tailoring Cell Behaviour in vitro", *Frontiers in Medical Technology*, vol. 3, p. 33, 2021. [Online]. Available: https://www.frontiersin.org/articles/10.3389/fmedt.2021.670274/full (visited on 11/14/2021).

[108] *ADUM121N1WBRZ Analog Devices | Mouser Portugal*. [Online]. Available: https://pt.mouser.com/ProductDetail/Analog-Devices/AD5206BRZ50?qs=NmRFExCfTkEbUsK%5C%252BbjRGtg%5C%3D%5C%3D (visited on 03/29/2022).

[109] *Digital Potentiometer Control | Arduino Documentation | Arduino Documentation*. [Online]. Available: https://docs.arduino.cc/tutorials/communication/DigitalPotControl (visited on 03/29/2022).

[110] G. López-Carballo, L. Moreno, S. Masiá, P. Pérez, and D. Barettino, "Activation of the phosphatidylinositol 3-kinase/Akt signaling pathway by retinoic acid is required for neural differentiation of SH-SY5Y human neuroblastoma cells", *Journal of Biological Chemistry*, vol. 277, no. 28, pp. 25 297–25 304, 2002, ISSN: 00219258. [Online]. Available: https://www.sciencedirect.com/science/article/pii/S0021925819664872 (visited on 02/22/2022).

[111] R. Constantinescu, A. T. Constantinescu, H. Reichmann, and B. Janetzky, "Neuronal differentiation and long-term culture of the human neuroblastoma line SH-SY5Y BT - Neuropsychiatric Disorders An Integrative Approach", *J Neural Transm Suppl.*, vol. 72, pp. 17–28, 2007. [Online]. Available: https://pubmed.ncbi.nlm.nih.gov/17982873/ (visited on 02/22/2022).

[112] S. Påhlman, A. I. Ruusala, L. Abrahamsson, L. Odelstad, and K. Nilsson, "Kinetics and concentration effects of TPA-induced differentiation of cultured human neuroblastoma cells", *Cell Differentiation*, vol. 12, no. 3, pp. 165–170, 1983. [Online]. Available: https://www.sciencedirect.com/science/article/abs/pii/0045603983900064 (visited on 02/22/2022).

[113] S. Påhlman, L. Odelstad, E. Larsson, G. Grotte, and K. Nilsson, "Phenotypic changes of human neuroblastoma cells in culture induced by 12-O-tetradecanoyl-phorbol-13-acetate", *International Journal of Cancer*, vol. 28, no. 5, pp. 583–589, 1981. [Online]. Available: https://onlinelibrary.wiley.com/doi/abs/10.1002/ijc.2910280509?sid=nlm%5C%3Apubmed (visited on 02/22/2022).

[114] J. A. Korecka, R. E. van Kesteren, E. Blaas, *et al.*, "Phenotypic Characterization of Retinoic Acid Differentiated SH-SY5Y Cells by Transcriptional Profiling", *PLoS ONE*, vol. 8, no. 5, 2013. [Online]. Available: https://journals.plos.org/plosone/article?id=10.1371/journal.pone.0063862 (visited on 02/22/2022).

[115] S. Sánchez, C. Jiménez, A. C. Carrera, J. Diaz-Nido, J. Avila, and F. Wandosell, "A cAMP-activated pathway, including PKA and PI3K, regulates neuronal differentiation", *Neurochemistry International*, vol. 44, no. 4, pp. 231–242, 2004. [Online]. Available: https://www.sciencedirect.com/science/article/pii/S0197018603001505 (visited on 02/22/2022).

A

Literature Review: SH-SY5Y neuronal differentiation

This Appendix presents the approaches present in the literature for inducing proliferation (Table A.1) and differentiation (Table A.2) of the SH-SY5Y human neuroblastoma cell line as summarized tables.

The main differences between SH-SY5Y cells in an undifferentiated and a differentiated state are visible in Figure A.1. Undifferentiated cells tend to grow in clusters (white arrow). Cells in the center of the cluster do not present a well defined shaped, yet as the distance from the center of the cluster increases cells begin to exhibit short extensions pointing outwards (white arrowhead). In opposition, differentiated cells are more separated from each other and less clusters are visible, which facilitates the assessment of their morphology, depending on cell density. In this state, pyramidal-like cell bodies are prevalent (white arrowhead), as well as more and longer neurites [82].

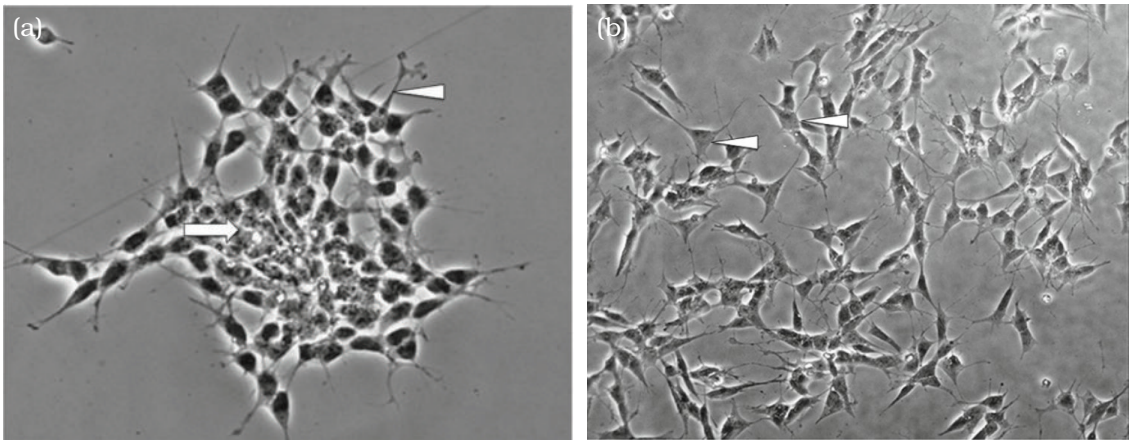

Figure A.1: SH-SY5Y neuroblastoma cell line: (a) Undifferentiated state; (b) Differentiated state. Adapted from [82].

Table A.1: Summary of the conditions used for culture and sub-culture of SH-SY5Y cells.

Culture conditions	Sub-culture conditions	Reference
Ham's F12/Eagle's Minimum Essential Medium (EMEM) (1:1, v/v) + glutamine (2 mM) + 1% v/v non-essential amino acids + 15% v/v FBS/fetal calf serum (FCS).	Cultures were split once 70-80% confluent. Cells were seeded at 1×10^3 - 1×10^4 cells/cm^2. 0.25% trypsin or trypsin/ethylenediaminetetraacetic acid (EDTA) was used. It is important to note that an increased number of passages has been associated with loss of neuronal characteristics.	[91]
DMEM/F12 (1:1, v/v) medium + 10% v/v FBS + 1% v/v penicillin/streptomycin filtered through a 0.22 µm pore filter apparatus. Cells should be cultured in a humidified, 5% CO_2, 37 °C incubator and growth medium refreshed every 4-7 days.	Kovalevich et al. provide a detailed subculture protocol (more information can be found in the original paper): Subculture should be performed once 80-90% confluence is reached. Cells should be rinsed once with sterile 1x phosphate buffered saline (PBS). Trypsin should then be added to the adherent cells until visibly detached from the culture flask. To neutralize tryspin, an equal volume of DMEM/F12 medium + 10% v/v FBS should be added to the culture flask. Cells should be plated at approximately 3×10^3 - 1×10^5 cells/cm^2.	[82]
Cells were cultured in a humidified, 5% CO_2, 37 °C incubator and only used until 23rd passage.	Simões et al. provide a detailed sub-culture protocol (more information can be found in the original paper): Cells were cultured or plated once 90-100% confluence was reached. Cells were washed once with 1x PBS. Later, 3 mL of 0.05% trypsin/EDTA were added to the culture flask, for 5 min at 5% CO_2, 37 °C. Following, 3 mL of cell culture medium + 10% v/v FBS were added. Cells were split into different tissue culture dishes.	[90]
SH-SY5Y cells were cultured in DMEM/F12 (1:1, v/v) + 10% v/v FBS + glutamine (2 mM) + gentamicin (0.28 mg/µL) + amphotericin B (250 µg), in a humidified, 5% CO_2, 37 °C incubator.	Medium was replaced every 3 days. Cells were sub-cultured once 90% confluence was reached. All treatments were performed when cells were 75% confluence.	[92]
Roswell Park Memorial Institute (RPMI) 1640 medium + 10% v/v FBS + gentamycin sulfate (0.15 mg/mL), at 37 °C with 5% CO_2. Medium was replaced every 3 days.	Cells were split before reaching confluence.	[110]

Table A.1 continued from previous page

Culture conditions	Sub-culture conditions	Reference
DMEM + L-glutamine + sodium piruvate + D-glucose (1000 mg/L) + amino acids to which were added 20% v/v heat inactivated FBS + penicillin (100 U/mL) + streptomycin (100 mg/mL) + Hepes (10 mM). SH-SY5Y cells were grown to confluence in T25 flasks in a humidified, 5% CO_2, 37 °C incubator.	Cells were split twice a week and seeded at 2.5×10^4 cells cm^2.	[111]
DMEM/F12 + 10% v/v heat inactivated FBS + penicillin (10 U/mL) + streptomycin (100 µg/mL). Cells were cultured in a humidified, 5% CO_2, 37 °C incubator.	Culture medium was changed every 3 days. This was maintained until appropriate confluency for differentiation or subculture was reached.	[86]
EMEM + 10% v/v FCS + penicillin (100 IU/mL) + streptomycin (50 µg/mL). Cells were cultured in a humidified, 5% CO_2, 37 °C incubator.	Medium was changed twice every week. Cells were passaged once confluent.	[112]
EMEM + 15% v/v FCS + penicillin (100 IU/mL) + streptomycin (50 µg/mL) + amphotericin B (1.25 µg/mL). Cells were cultured in a humidified, 5% CO_2, 37 °C incubator.	Medium was changed twice a week. Subcultures of confluent cultures were preceded by a 5 min treatment by 0.02% EDTA.	[113]
EMEM + non-essential amino acids (Eagle's formulation) + 15% v/v FBS + penicillin (100 IU/mL) + streptomycin (100 µg/mL).	-	[84]
DMEM + 10% v/v FBS + L-glutamine (10 mM) + penicillin/streptomycin (5 mg/mL).	-	[85]
10% complete medium (Minimal Essential Medium (MEM) + 10% v/v heat inactivated FBS + L-glutamine (2 mM) + penicillin (50 U/mL) + streptomycin (50 mg/mL)). Cells were cultured in a humidified, 5% CO_2, 37 °C incubator.	-	[89]
DMEM + L-glutamine (2 mM) + 15% v/v inactivated FCS. Cells were cultured in a humidified, 5% CO_2, 37 °C incubator. Cells were seeded at an initial density of 1×10^4 cells/cm^2 in culture dishes previously coated with 0.05 mg/mL collagen.	-	[87]
Cells were cultured with DMEM + 10% v/v FBS + 1% v/v penicillin + 1% v/v streptomycin in a humidified, 5% CO_2, 37 °C incubator. Cells were grown in the presence of 150 µg/mL G418 and 10% v/v FBS.	-	[88]

Table A.1 continued from previous page

Culture conditions	Sub-culture conditions	Reference
DMEM/F12 without L-glutamine + 0.5% v/v FCS + penicillin (100 U/mL) + streptomycin (0.1 mg/mL) for 8 days. Cells were grown in 96-well plates coated with poly-L-lysine (0.1 mg/mL) + growth factor reduced Matrigel Matrix (1 mg/mL) without phenol red, in a humidified, 5%CO_2, 37 °C incubator. 1×10^4 cells were plated.	-	[114]
DMEM + 10% v/v FBS + NaHCO3 (18 mM) + kanamycin (0.06 mg/mL). Cells were plated at a density of 4.2×10^4 cells/cm^2 and cultured in a humidified, 5% CO_2, 37 °C incubator. One day after plating, cells were incubated in Neurobasal medium + B-27 supplement + L-glutamine (500 µM).	-	[102]
DMEM + 10% v/v heat inactivated FCS + glutamine (2 mM) + penicillin/streptomycin.	-	[115]

Table A.2: Summary of the conditions found to induce neuronal differentiation of SH-SY5Y cells.

Differentiation Conditions	Reference
Kovalevich et al. provide a detailed differentiation protocol (more information can be found in the original paper): Grow cells from 24-48 h and then replace the growth medium with Neurobasal medium + B27 supplement + GlutaMAX^{TM} + 10 µM RA. Cells should be exposed to the differentiation medium for at least 3 to 5 days, refreshing the medium every 48 hour.	[82]
Treatment consisted in exposing cells to low-glucose culture medium + 1% v/v FBS + 1% v/v antibiotic-antimycotic + 10 µM RA for a total of 3 days. RA was dissolved in DMSO, prepared in stock solutions of 100 nM and added to the culture medium in the appropriate amount to achieve the selected concentration of 10 µM.	[90]
Neuronal differentiation treatment consisted in exposing cells to culture media supplemented with 1% v/v FBS + 10 µM RA, 24 h after cell seeding. Cells were treated for 4, 7 and 10 days and medium was changed every 3 days.	[92]
Highest levels of neurite outgrowth and longest neurites were observed in groups treated with 10 µM RA or 50 nM insulin-like growth factor 1 (IGF-1) for 72 h.	[85]
Growth medium was replaced by a low-serum medium with 3% v/v FBS + 10 µM RA, 48 h after seeding. Cells were exposed to differentiation medium for 7 days.	[89]
One day after cell seeding, cells were exposed to DMEM + 15% v/v FBS + 10 µM RA for 5 days. At the end of the 5 days, cells were washed with DMEM, and then exposed to 50 ng/ml BDNF for different periods of time.	[87]
Once 20% confluence was reached, cells were treated with medium supplemented with 3% v/v FBS + 5 µM RA for 1-4 days. Medium was changed every day.	[88]

Table A.2 continued from previous page

Differentiation Conditions	Reference
Treatments included exposing cells to either 1 µM RA or 100 nM 12-O-tetradecanoylphorbol-13-acetate (TPA) for different periods of time and a maximum of 48 h. This agents were dissolved in EtOH or DMSO.	[110]
The treatment consisted in 14 days of exposure to L-15 medium (Invitrogen) + 10% v/v FBS + 10 µM RA. Then, for 10 days, RA was removed and mitotic inhibitors were added to the media, namely 10 µM 5-fluoro-2'-deoxyuridine (FdUr), 10 µM uridine (Ur), and 1 µM cytosine arabinoside (araC). Following this 10 days, media was supplemented only with FdUr and Ur until the end of the culture (typically, there was a total of 16 days of treatment with mitotic inhibitors).	[111]
Cells were cultured in medium with 1 µM RA for 8 days.	[114]
Once 70% confluency was reached, cells were treated with 10 µM RA for 5 days, with medium being changed at day 2. At the end of the 5 days, cells were washed three times with DMEM/F12 and incubated with DMEM/F12 + GlutaMAX^{TM} + 100 U/mL penicillin + 100 µg/mL streptomycin + 50 ng/mL BDNF. Medium was replaced on days 8 and 11.	[86]
TPA was used as differentiation agent. The medium preparation was performed from a 1.6×10^{-3} M stock solution of TPA in EtOH. When diluted, the final concentration of EtOH did not exceed 0.1% v/v. Medium was changed twice a week.	[112]
To induce differentiation, TPA (1.6×10^{-8} M) + NGF (5 BU/mL) or only TPA (1.6×10^{-8} M), was added to the medium, which was changed twice a week.	[113]
Dibutyryl cAMP (0.1-10 mM), RA (1-10 µM), 8-Bromo-cAMP (0.1-3 mM) or butyrate (0.01-0.3 mM) was added to the medium for 3 days. Medium was changed every 48 h.	[102]
Growth medium was changed to Neurobasal medium + B-27 supplement + 1 mM dibutyryl cAMP. Cells were maintained for 24-96 h in the differentiation medium.	[115]

Furthermore, depending on the composition of the differentiation medium used, SH-SY5Y neuroblastoma cells will display a distinct neuronal phenotype. As such, the method selected for *in vitro* experiments should take into account the desired phenotype [82]. Table A.3 presents the predominant phenotype of differentiated SH-SY5Y cells, according to the differentiation agents used.

Table A.3: Predominant phenotypic display of SH-SY5Y cells depending on the exposure to a certain differentiation agent/combination of agents [82].

Differentiation Agent	Phenotype
RA	Cholinergic neurons
Phorbol Ester	Adrenergic neurons
Dibutyryl cAMP	Adrenergic neurons
RA + Phorbol Ester	Dopaminergic neurons

B

Protocols

B.1 Cell Culture

All the described procedures must be performed under aseptic technique.

B.1.1 SH-SY5Y Cell Thawing

1. Quickly thaw a cryovial in a 37 °C water bath until there is a small piece of ice left;
2. Wipe the vial with 70% ethanol and place it inside a biological safety cabinet;
3. Transfer the thawed cell suspension into a falcon and centrifuge for 5 minutes at 200 g;
4. Discard the supernatant and add 5 mL of fresh culture medium to the falcon;
5. Gently resuspend the cells and transfer them into a T25 flask;
6. Confirm the presence of cells in suspension on the microscope;
7. Incubate the cells in 37 °C/5% CO_2 conditions.

B.1.2 SH-SY5Y Cell Trypsinization

1. Aspirate culture medium from the T25 flask using a Pasteur pipette;
2. Gently wash the adhered cells with 5 mL of PBS;
3. Add 500 µL of trypsin (TrypLE^{TM} Express, Gibco) and gently swirl the T25 flask to ensure full coverage of the cell monolayer;
4. Incubate for 5 minutes;
5. Verify if the trypsinization process was successful by observing the T25 flask under microscope. If not, gently tap the sides of the T25 flask to help detach the cells;

6. Add 4.5 mL of DMEM low glucose with stable glutamine and sodium pyruvate to the T25 flask. Adding the cell culture medium will inactivate the trypsin;

7. Use a 5 mL pipette and a pipette aid to disperse the medium by pipetting over the bottom surface multiple times, maximizing cell recovery;

8. Transfer the cell suspension into a cell culture tube and perform protocol B.1.6;

9. Adjust the cell suspension to the desired density.

B.1.3 SH-SY5Y Cell Subculture

1. Execute protocol B.1.2;

2. Resuspend the cell suspension multiple times and transfer 0.5 mL to a new cell culture tube;

3. Add 4.5 mL of DMEM low glucose with stable glutamine and sodium pyruvate to the new tube;

4. Resuspend and transfer the 5 mL of the new cell suspension to the T25 flask;

5. Incubate the T25 flask in 37 °C/5% CO_2 conditions;

6. Discard what is left from the original cell suspension by mixing it with a disinfectant for biological safety. Otherwise, cryopreserve the remaining cells following protocol B.1.4.

B.1.4 Cryopreservation of SH-SY5Y Cells

1. Execute protocol B.1.2;

2. Centrifuge the cell suspension for 5 minutes at 200g;

3. Discard the supernatant carefully without disturbing the cell pellet;

4. Add 500 µL of DMSO and 4.5 ml of FBS to the cell pellet;

5. Gently resuspend multiple times using a pipette and a pipette aid;

6. Divide the cell suspension in cryovials by adding 1 mL to each cryovial and identify them properly with the name of the person performing the protocol, date, cell type, passage and number of cells;

7. Store the cryovials at −80 °C.

B.1.5 Changing Cell Culture Medium

1. Warm up fresh culture media at 37 °C in a water bath;

2. Prepare the biological safety cabinet with a waste pot containing some disinfectant;

3. Wipe the flask or well plate were cells are seeded with 70% ethanol and place it inside the cabinet. Repeat the process for the falcon containing the fresh and warmed up culture media;

4. Discard the old media from the flask or well plate using a Pasteur pipette or a micropipette, respectively;

5. Immediately transfer the adequate amount of the fresh pre-warmed media to the flask or well plate;

6. Incubate the cells in 37 °C/5% CO_2 conditions.

B.1.6 Cell Counting

1. Transfer between 50 and 100 µL of the cell suspension to an Eppendorf tube;

2. Add an equal amount of trypan blue stain (0.4%) to the previously mentioned Eppendorf tube and gently mix;

3. Clean the hemocytometer with 70% ethanol. Moisten the coverslip with a drop of water and affix it to the hemocytometer;

4. Very gently, fill the two counting chambers of the hemocytometer with the cell suspension (8-10 µL in each camera) and observe in an inverted phase contrast microscope with a 10X objective;

5. Set the focus to the grid lines and count the viable cells. Count at least 3 squares in each chamber. Only consider cells inside a square and on two of the grid lines delimiting the square. Keep the same counting system for every square considered;

6. Calculate the density of viable cells by following the formula where D is the viable cell density (cells/mL), N is the total number of viable cells counted, n is the number of squares considered for the counting, 2 is the dilution factor and 10^4 is the chamber factor:
$$D = \frac{N}{n} \times 2 \times 10^4$$

7. Clean the hemocytometer and the coverslip with distilled water and place them inside a proper glass container, immersed in 70% ethanol until the next use.

B.1.7 Preparation of Retinoic Acid Stock Solutions

1. Determine the volume of DMSO necessary for dissolving 100 mg of a RA powder (Sigma-Aldrich) achieving a concentration of 10 mM, given that the molar mass of RA is 300.44 g mol^{-1} [93];

2. Inside the biological safety cabinet, transfer the calculated volume into a cell culture tube;

3. Break the tip of the RA ampoule, and transfer the whole content of RA powder into the tube;

4. Gently mix until complete dissolution is achieved, obtaining a solution of RA in DMSO at the desired concentration of 10 mM;

5. Divide the total volume of the solution in 1 mL and 1.5 mL aliquotes and store at −20 °C;

6. If a lower concentration is desired, perform the necessary dilution of the 10 mM RA solution in the appropriate volume of DMSO.

B.1.8 Resazurin Assay

1. Prepare a (1:1) v/v solution of 0.04 g/mL and DMEM + 10% v/v FBS complete DMEM medium;

2. Replace the extract medium with the solution prepared in Step 1;

3. Incubate for 3 h;

4. Place the 96-well plate on the absorbance reader (Biotek ELX 8000UV);

5. Obtain the absorbance readings for 570 nm and 600 nm;

6. Subtract the average absorbance readings at 600 nm from the average absorbance readings at 570 nm (*Av* 570 - *Av* 600), for every extract concentration and control groups (C-, C+ and CM);

7. Obtain the converted resazurin index value by performing the following operation: (*Av* 570 - *Av* 600) - (*CM* 570 - *CM* 600);

8. Obtain cell viability by performing the quotient of converted resazurin index values by the converted resazurin index value of the negative control, C-.

B.1.9 Fluorescence Imaging

B.1.9.1 SH-SY5Y Cell Fixing

1. Wash the cells once with PBS^{++};
2. Fill the working volume of each well with 4% v/v paraformaldehyde (PFA) in PBS^{++};
3. Wait 15 min;
4. Wash twice with PBS^{++};
5. Store at 4 °C.

B.1.9.2 SH-SY5Y Cell Staining

1. Permeabilize the cells with 0.5% v/v Triton X-100 in PBS for 5 minute;
2. Wash once with PBS;
3. Stain the cytoskeleton with 50 µL of Acti – $stain^{TM}$ 555 Phalloidin in a 2000:1 ratio of PBS to phalloidin stock solution for 30 min;
4. Wash three times with PBS;
5. Stain the nucleus with 50 µL of 300 nM 4',6-diamidino-2-phenylindole (DAPI) in PBS for 5 min;
6. Wash once with PBS;
7. Pour one drop of antifade mounting medium from Booster on each sample.

B.1.10 Culture Plate Layouts

In this subsection, the layouts representative of the condition distribution on the well plates used in several tasks of this dissertation is displayed. The following images correspond to the conditions tested for the:

- Optimization of the differentiation protocol (Figure B.1);
- Resazurin assay (Figure B.2);
- Culture on the materials assay (Figure B.3).

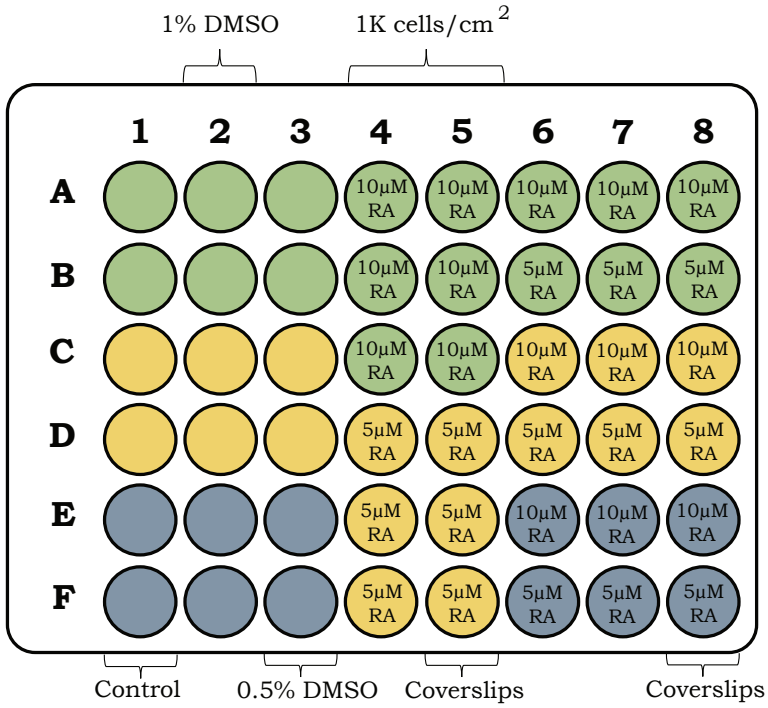

Figure B.1: Layout of the 48-well plate used for optimizing the differentiation protocol. The colors green, yellow and blue represent a concentration of 5%, 3% or 1% v/v FBS in DMEM, respectively. Columns 1-3 represent control groups and columns 4-8 represent the low-serum groups containing RA at the displayed concentrations.

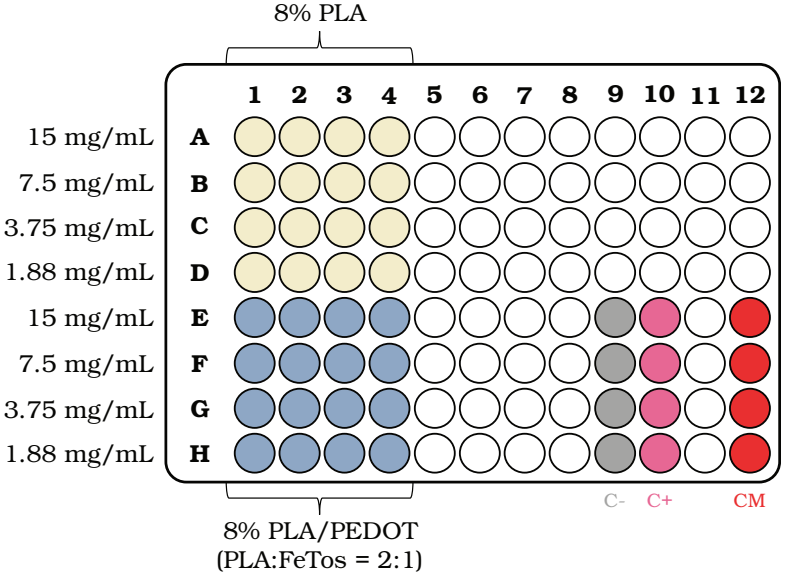

Figure B.2: Layout of the 96-well plate used for the resazurin assay. The four extract concentrations of each material tested are displayed, namely from PLA nanofibers (light yellow) and PLA nanofibers containing PEDOT (blue). Controls are also displayed: live-cell control, C- (gray), dead-cell control, C+ (pink) and the media control (red).

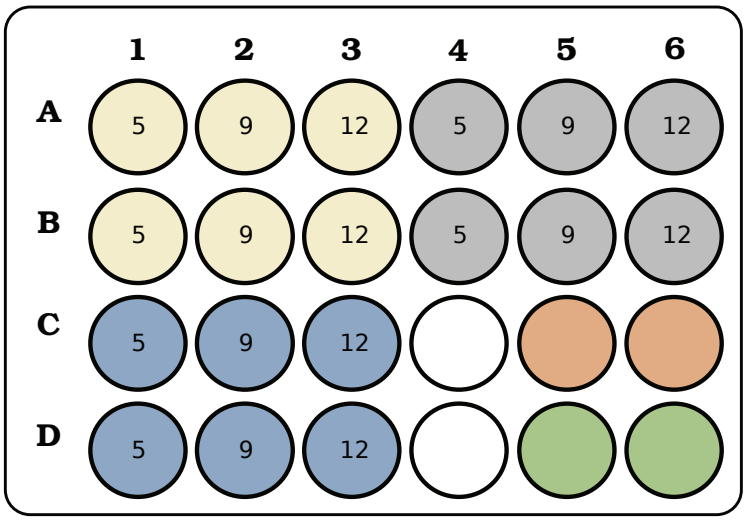

Figure B.3: Layout of the 24-well plate used for assessing the growth of SH-S5Y5 cells on materials. Cells were cultured onto PLA nanofibers (light yellow), PLA nanofibers containing PEDOT (blue) and converslips (gray), all secured in *teflons*. In the wells where a number is displayed, that number corresponds to the day of culture in which cells were fixed for fluorescence imaging. There are also control wells (orange) and control coverslips (green), without *teflons*.

C

Fabrication of Conductive Scaffolds: Additional Content

C.1 Spin Coating

In parallel with film casting, other techniques were briefly explored for the production of a conductive film. Firstly, the previously described PLA/FeTos solutions, with a ratio of PLA to FeTos of 2:1, were used for spin coating in two different surfaces: acetate sheets and coverslips. The results from these tests are displayed in Figure C.1.

Overall, this method allowed for quickly fabricating thin PLA films containing oxidant with a smooth surface, at naked eye. As PLA concentration increased, the films displayed a progressively yellowish color. This is expected, as more oxidant is present for a certain volume of solution, in order to maintain the ratio of PLA to FeTos, as PLA concentration increases. All films were malleable, yet not easily detachable from the surfaces, and showed poor elasticity. As future work, is would be interesting to perform VPP of the spin coated films, and attempt their detachment from the surfaces when performing the EtOH washes.

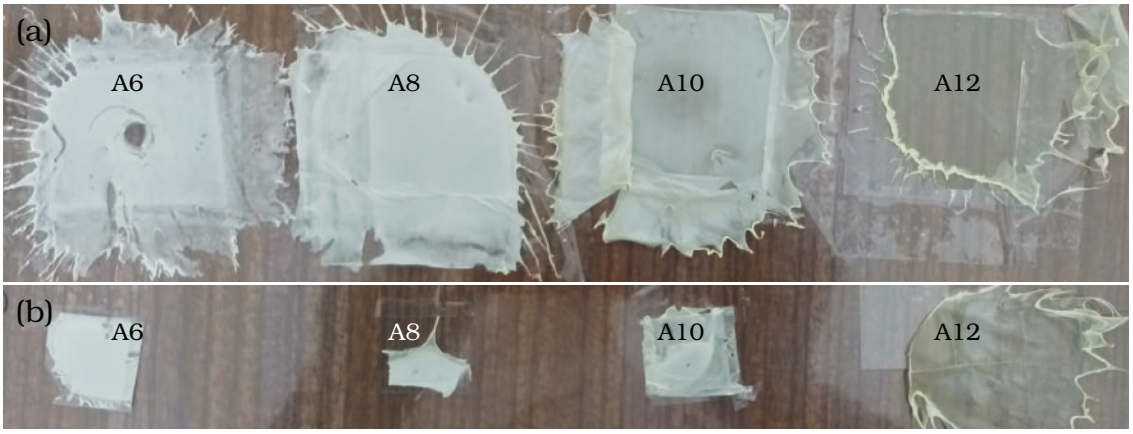

Figure C.1: Fabrication of thin films from PLA/FeTos solutions using a spin coating technique. (a) Spin coating on acetate sheets; (b) Spin coating on glass coverslips.

C.2 Dip Coating

Later, dip coating was used as an attempt to incorporate the oxidant, required for VPP of EDOT, in a PLA film. The goal was to create a conductive coat on the PLA film. However, as shown in Figure C.2, this method was unsuccessful in that, as the EtOH evaporated, the oxidant was not incorporated in the PLA film, leaving only oxidant powder agglomerates unevenly distributed on the film surface. No further attempts were made for dip coating.

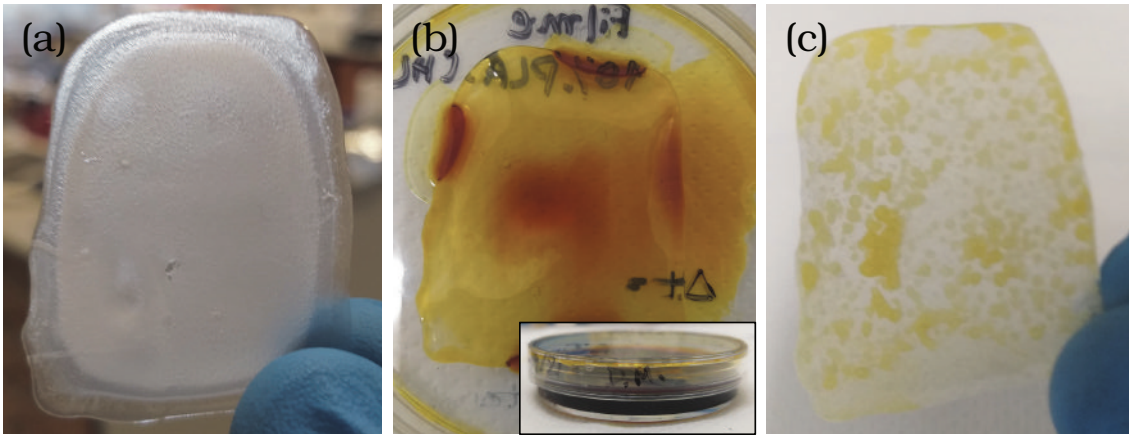

Figure C.2: Attempt for dip coating of a PLA film with a FeTos solution: (a) Film obtained by film casting of a 10% PLA solution in CHL; (b) Film immediately after being dipped on a 40% FeTos solution in EtOH; (c) Film after EtOH evaporation.

C.3 Electrospinning

Basic microscopic images were recorded from a coverslip with aligned electrospun fibers, collected during the deposition (Figure C.3).

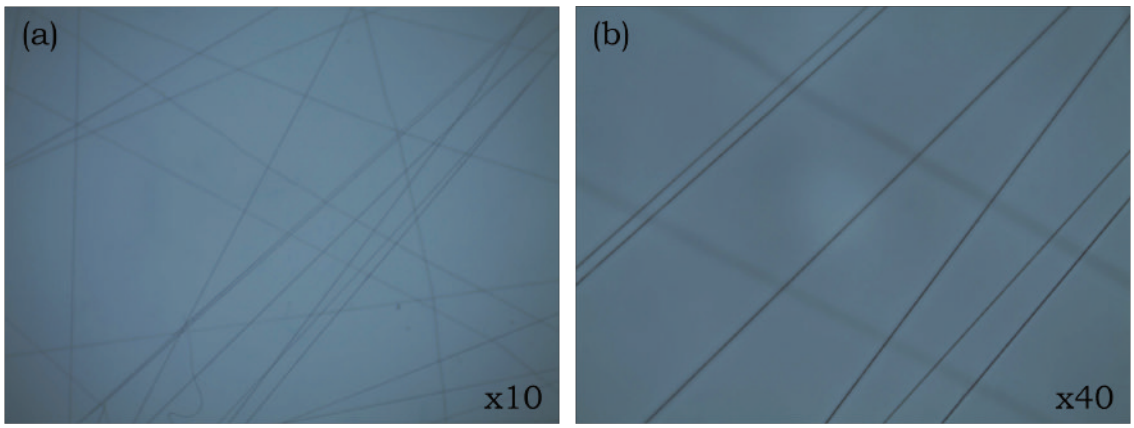

Figure C.3: Basic microscopic images from the deposition of PLA/FeTos fibers on a coverslip. These were obtained using both the (a) x10 and the (b) x40 objectives.